Alexandrium monilatum in the Lower Chesapeake Bay: Sediment Cyst Distribution and Potential Health Impacts on *Crassostrea virginica*

A Thesis

Presented to

The Faculty of the School of Marine Science

The College of William and Mary in Virginia

In Partial Fulfillment

of the Requirements for the Degree of

Master of Science

---

by

Sarah K. D. Pease

2016

APPROVAL SHEET

This thesis is submitted in partial fulfillment of

the requirements for the degree of

Master of Science

_____

Sarah K. D. Pease

Approved, by the Committee, August 2016

_____

Kimberly S. Reece, Ph.D.
Committee Co-Chairman/Co-Advisor

_____

Wolfgang K. Vogelbein, Ph.D.
Committee Co-Chairman/Co-Advisor

_____

Ryan B. Carnegie, Ph.D.

_____

Mark W. Luckenbach, Ph.D.

_____

Juliette L. Smith, Ph.D.

TABLE OF CONTENTS

Page

TABLE OF CONTENTS

(CONTINUED)

Page

ACKNOWLEDGMENTS

I want to extend a huge thank you to Kim Reece and Wolf Vogelbein for giving me the opportunity to work with them and learn from them for the past three years, and for giving me bragging rights among the graduate students for having photo evidence that my advisors were in the lab helping me at 10:00 pm. Thanks to Ryan Carnegie and Juliette Smith for answering my multitudes of questions, and for their hands-on involvement in my work. Thank you Mark Luckenbach, for the great stories and support. Of course, I owe everything to my loving parents and sister for their endless support, and encouragement to follow my dreams. A big thanks to my amazing roommates: Lydia Bienlien, Cindy Marin-Martinez, and Melissa Karp who have been there through the thick and thin of it all right from the start, and who have never ceased to amaze me with their kindness. Thanks to the "knowledge bank" that is: Gail Scott, Alanna MacIntyre, Rita Crockett, Carissa Gervasi, Patrice Mason, Bill Jones, Barb Rutan, Marta Sanderson, Corinne Audemard, and Laura Whitefleet-Smith, for all of the time and effort they have put in helping to teach me lab techniques and helping me get about my business. Thanks to Tom Harris for quizzing me when I least expected it. Thanks to Matt Skiljo, Rebecca LePrell, Keith Skiles, and Todd Egerton from the Virginia Dept. of Health for partnering with me and showing me how the State prepares for, and manages, harmful algal blooms. Thank you Tommy Leggett and Chessie Seafood for supplying the oysters for my research, and ABC for letting me house oysters on their racks for a while. Thanks to the

VIMS Analytical Services Laboratory for running nutrient and sediment sample analyses for this research. I am extremely grateful to Virginia Sea Grant: Troy Hartley, Susan Park, Sabine Rogers, Janet Krenn, and Sam Lake for their support, enthusiasm, and for including me in the “family”. Thanks to office-mates Randy Jones, Miguel Semedo, and Brendan Turley for keeping it real. A huge thank you to the undergraduates and volunteers who helped out with various pieces of this research: Leigha Stahl, Shannon Jones, Kristen Vogelbein, Emily Brown, Blake Ivey, Anna Lewis, and Sylvia Jones. Thanks to Don Anderson and his lab, especially Dave Kulis and Alexis Fischer, for their help and kind hosting of my visit to WHOI. I would like to thank the VIMS Office of Academic Studies, Southern Association of Marine Labs, National Shellfisheries Association, and National HAB Committee for supporting travel to conferences to present my research. Thanks to Mary Fabrizio, Mark Stratton, Cassidy Peterson, Julia Moriarty, and Danielle Tarpley for advice on statistics and all things “mud”. A big thanks to Tycho Van Hauwaert at the University of Ghent for sharing some of his thesis research results with me. Thank you to Linda Schaffner, Mike Ivey, Cathy Cake, Jen Hay, and Carol Birch for administrative support. Thank you to Jim Brister at the SRL for keeping things running smoothly. Thanks to Will Benton, Seth West, and Bob Polley in the IT Dept. for keeping my laptops working even after two fried hard drives. Thank you to the VIMS community as a whole for being so epically amazing! Lastly, a sincere thank you to my New Hampshire Dept. of Environmental Services colleagues who encouraged me to go back to school for my masters, and who inspired me and have helped support me in my career pursuits.

LIST OF TABLES

LIST OF FIGURES

Figure Page

LIST OF FIGURES

(CONTINUED)

Figure Page

ABSTRACT

The toxin-producing harmful algal bloom (HAB) species *Alexandrium monilatum* has long been associated with finfish and shellfish mortalities in the Gulf of Mexico. In the summer of 2007, *A. monilatum* re-emerged as a bloom-forming species in the Chesapeake Bay. Over the last decade, late summer blooms of *A. monilatum* have been expanding in range in the lower Chesapeake Bay and have reached record-high densities, particularly in the lower York River. This dinoflagellate species overwinters in the sediments as a resting cyst, and upon excystment under suitable environmental conditions produces blooms the following summer.

The research presented here includes the first mapping and quantification of resting cysts of *A. monilatum* in surface sediments in the Chesapeake Bay using quantitative real-time polymerase chain reaction (qPCR) assays. A systematic grid sampling design was employed to collect pre-bloom sediments in the southwestern portion of the Chesapeake Bay each year from 2014-2016. Cysts were widespread in the bottom sediments and sediment cyst density increased from 2014-2016, reaching as high as 90,000 cysts/cc in the York River channel. A multiple linear regression was used to model cyst density using environmental parameters. Sediment type was a strong predictor of cyst density, with higher cyst densities found at sites with more fine sediments (silts and clays).

Laboratory HAB toxicity bioassay methods were used to investigate potential adverse health impacts of *A. monilatum* on adult triploid eastern oysters, *Crassostrea virginica*. Oyster behavior and mortality were monitored and routine paraffin histology was performed to analyze tissue damage. Oysters did not exhibit mortality or tissue damage in a 48-hour fed toxicity bioassay. However, a 96-hour unfed toxicity bioassay led to 67% mortality, and erosion of the gill and mantle epithelial tissues in 94% of oysters exposed to *A. monilatum* (live cell or lysate). In the summer of 2015, oysters were deployed in the lower York River to assess effects of exposure before, during, and after a natural *A. monilatum* bloom. A subsample of six live oysters was collected weekly for two months and processed for histology. There was no mortality of deployed oysters, but minor epithelial erosion of the mantle was seen in half of the oysters sampled during the peak of the *A. monilatum* bloom from early to mid-August. Field and laboratory results showed that *C. virginica* did occasionally consume *A. monilatum*, and exposure of *C. virginica* to live *A. monilatum* or lysate could lead to epithelial erosion of external tissues and mortality.

It is clear from the findings of this research that *A. monilatum* has established itself in the York River region of the Chesapeake Bay and that at least under laboratory conditions, persistent exposure to *A. monilatum* (live or lysate) can have serious potential health impacts on adult oysters.

ALEXANDRIUM MONILATUM IN THE LOWER CHESAPEAKE BAY

GENERAL INTRODUCTION

Harmful algal blooms (HABs) are defined by a rapid increase in the density of one or a few distinct species of phytoplankton or macroalgae in the water column in a discrete location, and are associated with adverse aquatic animal or human health effects. A more colloquial term for these events is “red tide”, owing to the fact that these blooms often appear at the water’s surface as patches, or streaks, of reddish brown—although not all HAB events are visible (Shumway 1990). Health effects related to HABs are most commonly due to the depletion of dissolved oxygen in the water column upon decomposition of the bloom, or the production and release of toxins by the bloom-forming phytoplankton. HABs can lead to mass mortalities of marine organisms and other negative impacts such as toxin biomagnification through the food web. HAB toxins that impact human health are of special concern.

Several HAB species that impact human health produce potent toxins that can naturally bioaccumulate in shellfish meat during seasonal blooms (Shumway 1990). Consuming these toxin-contaminated shellfish can lead to serious illness or even death. Paralytic, amnesic, neurotoxic, and diarrhetic shellfish poisonings (PSP, ASP, NSP, and DSP, respectively) are a few of the serious human health concerns associated with HAB events in US coastal waterways (WHOI 2013), and play a large role in how the shellfish industry is managed to protect public health.

Of the thousands of phytoplankton species currently identified worldwide, almost one hundred species are known to be harmful (Landsberg 2002). Of the harmful species,

37 have been reported in the Chesapeake Bay (Marshall *et al*. 2008). In Virginia, HAB issues are addressed by the Virginia HAB Taskforce, a collaborative group of scientists and government officials who work to monitor and respond to HAB events. While no serious human health issues associated with HABs have been reported in Virginia to-date (K. Skiles, Virginia Department of Health, pers. comm.), it is essential that regionally-emerging bloom species be investigated and that the shellfish industry be aware of and prepared for any potential HAB issues. In recent years, several emerging toxin-producing HAB species, including *Alexandrium monilatum*, have been identified in Virginia waters (Marshall *et al.* 2008).

***Alexandrium monilatum* Background**

The species we now know as *A. monilatum* has a complicated taxonomic history. It was originally discovered in Offatts Bayou in Galveston, Texas during the mid-1930s. There were annual late-summer mass mortalities of marine organisms; the water would turn red or milky in color, "boil", and stink (Gunter 1942). These mysterious events continued for the next decade, turning the water red and luminescent. Connell and Cross (1950) hypothesized that these events were associated with algal blooms of an organism they identified at the time as belonging to the genus *Gonyaulax*. Howell (1953) determined that the organism blooming in Offatts Bayou was the same as a new species he had described from a bloom associated with a fish kill off of the east coast of Florida in 1951. Howell named this chain-forming, thecate dinoflagellate *Gonyaulax monilata*.

Years later in Venezuela, *G. monilata* was incorrectly identified as a novel species and given the name *Gessnerium mochimaensis* (Halim 1967). The species name was officially changed to *A. monilatum* by Balech in 1985 in his re-definition of the genus

Alexandrium Halim to incorporate members from the *Gonyaulax* genus that lacked the characteristic horns or spines typical of that genus. Major changes have since been made to the *Alexandrium* genus (Balech 1995; Rogers *et al*. 2006; John *et al*. 2014), but few phylogenetic analyses have included sequences from *A. monilatum* isolates. The most recent of these studies showed *A. monilatum* in the same clade as *A. satoanum*, *A. taylori*, and *A. pseudogoniaulax*, the clade being a sister group to the *A. tamarense* species complex that also includes *A. fundyense* and *A. catenella* (John *et al.* 2014). Interestingly, while the *A. tamarense* species complex is notorious for producing dangerous PSP toxins, *A. monilatum* and its close relatives are not known to produce significant quantities of these particular toxins (Balech 1995; Rogers *et al*. 2006).

The basic life cycle of *A. monilatum* consists of an asexual, chain-forming stage (Aldrich *et al*. 1967) which is followed by formation of individual gametes. These gametes can then fuse sexually to form a bioluminescent (Latz *et al.* 2008) life stage called a planozygote (Walker and Steidinger 1979). The planozygote later encysts, forming a hypnozygote that sinks and becomes incorporated in the bottom sediments until it is ready to excyst and start the cycle over again (Walker and Steidinger 1979).

The chain stage of the life cycle occurs during asexual division, while *A. monilatum* populations are in log growth phase, with longer chains often indicating rapidly growing populations (Aldrich *et al*. 1967). The length of the cell chains is thought to be limited by disturbance in the water, with more disturbances leading to shorter chains (Aldrich *et al*. 1967). In environmental samples it is not unusual to find the occasional chain of 60-80 cells. These chains of vegetative cells swim “vigorously” using flagella (Juhl 2005).

There are two types of cysts that can be formed by this dinoflagellate, the resting cyst, also known as the "hypnozygote", and the temporary cyst (Anderson *et al.* 1991). The hypnozygote is a typical life stage for many dinoflagellates that forms after sexual fusion of gametes and formation of the planozygote (a biflagellate, swimming stage; Walker and Steidinger 1979). Temporary cysts are formed in response to sudden unfavorable conditions, and are often seen in laboratory settings. These temporary cysts have thinner walls than true hypnozygotes (Anderson *et al.* 1991).

Hypnozygotes can rest in the sediments for months to many years, waiting for the cell to develop and for favorable environmental conditions (i.e. temperature), before excystment (Anderson *et al.* 1991). Under anoxic conditions hypnozygotes may not excyst, but instead may remain dormant (Anderson *et al.* 1991). *Alexandrium monilatum* cysts form "seed beds" in the sediments that can serve as a source for future blooms (Walker and Steidinger 1979); this makes assessment of cyst density and distribution in bottom sediments an important aspect for understanding bloom dynamics and distribution (Anderson *et al.* 1991).

Alexandrium monilatum is primarily an estuarine species, but occasionally blooms are found tens of kilometers offshore (Williams and Ingle 1972; Wardle *et al.* 1975). The species has been found as far offshore as 67.6 km and as deep as 23.8 m (Williams and Ingle 1972). Blooms of this species may appear in broad streaks across the water's surface or as reddish-brown water and can span tens of kilometers, lasting a few days to several weeks.

Blooms of *A. monilatum* have been recorded in all US states bordering the Gulf of Mexico (Connell and Cross 1950; Perry *et al.* 1979; Williams and Ingle 1972), off of the

Atlantic coast of Florida (Howell 1953), and in East Venezuela (Halim 1967), Costa Rica (Montero *et al*. 2008), and the Chesapeake Bay (MacKiernan 1968). There are a few poorly substantiated records of *A. monilatum* from other parts of the world, including a record from the southwestern coast of India (Sanilkumar *et al*. 2009), and another suggesting that *A. monilatum* was brought in ballast water to the Black Sea, where it bloomed in high densities in the early 1990s (Moncheva and Kamburska 2002). A full list of *A. monilatum* records can be found in Table 0.1.

Alexandrium monilatum has long been associated with finfish and invertebrate kills in the Gulf of Mexico (Connell and Cross 1950; Wardle *et al*. 1975). More recent laboratory work has shown that *A. monilatum* produces the lipophilic toxin "goniodomin A" (Hsia *et al*. 2006), which interferes with the structure and function of actin (Furukawa *et al*. 1993; Matsunaga *et al*. 1999). However, the potential for *A. monilatum* and its toxins to impact human health through natural exposure is currently unknown.

In 2007, the Chesapeake Bay witnessed its first bloom of *A. monilatum* since the mid-1960s (MacKiernan 1968; Marshall *et al.* 2008). With its recent re-emergence, the spatial distribution of *A. monilatum* has appeared to increase, and blooms of this HAB species have occurred almost annually in the southern Chesapeake Bay (Marshall and Egerton 2009, 2013). During these blooms, there have been mortalities of veined rapa whelks (*Rapana venosa;* Harding *et al*. 2009) and cownose rays (*Rhinoptera bonasus;* R. Fisher, Virginia Institute of Marine Science, pers. comm.), as well as anecdotal reports of mortalities of larval and adult eastern oysters, *Crassostrea virginica*. Preliminary laboratory exposures with *A. monilatum* have produced mortality in larval oysters and gill pathology in adult oysters (Reece *et al*. 2012). The potential threat to fishery and

aquaculture resources—as well as to human consumers of these resources—is an issue which requires attention.

To effectively manage *A. monilatum* risks in Virginia, a better understanding of the spatial and temporal distribution of this HAB species and its impacts on *C. virginica* health are required. Little is known about the behavior of *A. monilatum* in the Chesapeake Bay, the extent of its ability to affect local *C. virginica*, or the potential for oysters that have been exposed to this re-emerging HAB to pose a risk to human health. To get a better sense of the scope of the *A. monilatum* issue, and to address some of the associated oyster health concerns, an interdisciplinary research approach was used, involving molecular genetics, histopathology, and ecotoxicology. The goals of my research were to determine whether *A. monilatum* has established itself in the York River region of the Chesapeake Bay by assessing bottom sediment cyst distributions and densities, and to determine the potential impacts of *A. monilatum* and its toxins on the health of adult oysters through toxicity bioassays with a Chesapeake Bay *A. monilatum* isolate and local *C. virginica.*

LITERATURE CITED

Aldrich DV, Ray SM, Wilson WB. 1967. *Gonyaulax monilata*: Population growth and development of toxicity in cultures. *J Protozool,* 14:639–649.

Anderson DM, Fukuyo Y, Matsuoka K. 1991. Cyst methodologies. In: Manual on Harmful Marine Microalgae. p. 165–189.

Balech E. 1985. The genus *Alexandrium* or *Gonyaulax* of the Tamarensis group. In: Proceedings of the Third International Conference on Toxic Dinoflagellates, St. Andrews, New Brunswick, Canada, June 8-12, 1985. p. 33–38.

Balech E. 1995. The genus *Alexandrium* Halim (Dinoflagellata). Cork (Ireland): Sherkin Island Marine Station. 151 p.

Connell C, Cross J. 1950. Mass mortality of fish associated with the protozoan *Gonyaulax* in the Gulf of Mexico. *Science*, 112:359–363.

Ferraz-Reyes E, Reyes-Vasquez G, De Oliveros AL. 1985. Dinoflagellates of the genera *Gonyaulax* and *Protogonyaulax* in the Gulf of Cariaco, Venezuela. In: Proceedings of the Third International Conference on Toxic Dinoflagellates, St. Andrews, New Brunswick, Canada, June 8-12, 1985. p. 69–72.

Furukawa K, Sakai K, Watanabe S, Maruyama K, Murakami M, Yamaguchi K, Ohizumi Y. 1993. Goniodomin A induces modulation of actomyosin ATPase activity mediated through conformational change of actin. *J Biol Chem,* 268:26026–26031.

Gates JA, Wilson WB. 1960. The toxicity of *Gonyaulax monilata* Howell to *Mugil cephalus*. *Limnol Oceanogr*, 5(2):171–174.

Gunter G. 1942. Offatts Bayou, a locality with recurrent summer mortality of marine organisms. *American Midl Naturalist*, 28(3):631–633.

Halim Y. 1967. Dinoflagellates of the South-East Caribbean Sea (East-Venezuela). *Int Rev der gesamten Hydrobiol,* 52:701–755.

Harding JM, Mann R, Moeller P, Hsia MS, Road FJ, Carolina S. 2009. Mortality of the veined rapa whelk, *Rapana venosa*, in relation to a bloom of *Alexandrium monilatum* in the York River, United States. *J Shellfish Res*, 28(2):363-367.

Howell JF. 1953. *Gonyaulax monilata*, sp. nov., the causative dinoflagellate of a red tide on the East coast of Florida in August-September, 1951. *Trans Am Microsc Soc,* 72:153–156.

Hsia MH, Morton SL, Smith LL, Beauchesne KR, Huncik KM, Moeller PDR. 2006. Production of goniodomin A by the planktonic, chain-forming dinoflagellate *Alexandrium monilatum* (Howell) Balech isolated from the Gulf Coast of the United States. *Harmful Algae*, 5:290-299.

John U, Litaker RW, Montresor M, Murray S, Brosnahan ML, Anderson DM. 2014. Formal revision of the *Alexandrium tamarense* species complex (Dinophyceae) taxonomy: the introduction of five species with emphasis on molecular-based (rDNA) classification. *Protist,* 165:779–804.

Juhl AR. 2005. Growth rates and elemental composition of *Alexandrium monilatum*, a red-tide dinoflagellate. *Harmful Algae*, 4:287–295.

Landsberg JH. 2002. The effects of harmful algal blooms on aquatic organisms. *Rev Fish Sci*, 10(2):113–390.

Latz MI, Bovard M, VanDelinder V, Segre E, Rohr J, Groisman A. 2008. Bioluminescent response of individual dinoflagellate cells to hydrodynamic stress measured with millisecond resolution in a microfluidic device. *J Exp Biol,* 211:2865–75.

MacKiernan G. 1968. Seasonal distribution of dinoflagellates in the lower York River, Virginia [Thesis]. College of William & Mary. 104 p.

Marshall HG, Egerton TA, Johnson R, Semcheski M, Bowman N, Mansfield N. 2008. Re-occurring harmful algal blooms in the tidal waters of Virginia, USA. Ocean Sciences Meeting; March 2-7, 2008; Orlando, Florida.

Marshall HG, Egerton TA. 2009. Phytoplankton blooms: their occurrence and composition within Virginia's tidal tributaries. *Va J Sci*, 60(3):149–164.

Marshall HG, Egerton TA. 2013. Assessing seasonal relationships between chlorophyll *a* concentrations to phytoplankton composition, biomass, and abundance, emphasizing the bloom producing algae (HAB and others) within the James, Elizabeth, and Lafayette rivers in Virginia. Final report submitted to Virginia Department of Environmental Quality.

Matsunaga K, Nakatani K, Murakami M, Yamaguchi K, Ohizumi Y. 1999. Powerful activation of skeletal muscle actomyosin ATPase by goniodomin A is highly sensitive to troponin/tropomyosin complex. *J Pharm Exp Ther*, 291(3):1121–1126.

May SP, Burkholder JM, Shumway SE, Hegaret H, Wikfors GH, Frank D. 2010. Effects of the toxic dinoflagellate *Alexandrium monilatum* on survival, grazing and behavioral response of three ecologically important bivalve molluscs. *Harmful Algae*, 9:281-293.

Moncheva SP, Kamburska LT. 2002. Plankton stowaways in the Black Sea – impacts on biodiversity and ecosystem health. In: Alien marine organisms introduced by ships in the Mediterranean and Black seas – Istanbul, 6-9 November 2002. CIESM workshop monographs; 20. 1726-5886.

Montero MV, Bustamante EF, Guzmán JC, Vargas JC. 2008. Harmful blooms by noxious dinoflagellates in the Pacific coast of Costa Rica. *Hidrobiológica*, 18:suppl.1.

Norris DR. 1983. The occurrence of a toxic dinoflagellate in the Indian River system. *Fla Sci,* 46:150–153.

Owen KC, Norris DR. 1982. Benthic resting cysts of *Gonyaulax monilata* Howell and their relationship to red tides in the Indian River, Florida. *Fla Sci,* 45:227–233.

Perry HM, Stuck KC, Howse HD. 1979. First record of a bloom of *Gonyaulax monilata* in coastal waters of Mississippi. *Gulf Res Rep,* 6(3):313–316.

Reece KS, Vogelbein WK, Carnegie RB. 2012. Assessing the impacts of emerging harmful algal bloom species on shellfish restoration and aquaculture in Chesapeake Bay. Final report submitted to VA Sea Grant. Award #NA10OAR4170085.

Rogers JE, Leblond JD, Moncreiff CA. 2006. Phylogenetic relationship of *Alexandrium monilatum* (Dinophyceae) to other *Alexandrium* species based on 18S ribosomal RNA gene sequences. *Harmful Algae,* 5:275–280.

Sanilkumar MG, Padmakumar KB, Menon NR, Joseph KJ, Sanjeevan VN, Saramma AV. 2009. Algal blooms along the coastal waters of southwest India during 2005-08. *J Mar Biol Ass India,* 51:69–74.

Shumway SE. 1990. A review of the effects of algal blooms on shellfish and aquaculture. *J World Aquac Soc*, 21(2):65-104.

Víquez R, Hargraves PE. 1995. Annual cycle of potentially harmful dinoflagellates in the Golfo de Nicoya, Costa Rica. *Bull Mar Sci,* 57:467–475.

Walker LM, Steidinger KA. 1979. Sexual reproduction in the toxic dinoflagellate *Gonyaulax monilata. J Phycol,* 15:312–315.

Wardle WJ, Ray SM, Aldrich AS. 1975. Mortality of marine organisms associated with offshore summer blooms of the toxic dinoflagellate *Gonyaulax monilata* Howell at Galveston, Texas. In: LoCicero VR, editor. Proceedings of the First International Conference on Toxic Dinoflagellate Blooms. Wakefield (MA): Science and Technology Foundation. p. 257-263.

[WHOI] Woods Hole Oceanographic Institute. 2013 May 15. Harmful Algae. <http://www.whoi.edu/redtide/home>. Accessed 2014 January 30.

Williams J, Ingle RM. 1972. Ecological notes on *Gonyaulax monilata* (Dinophyceae) blooms along the West coast of Florida. *Mar Res Lab Fla Dept Nat Resour,* 1:1–12.

TABLE 0.1.

Historical record of *Alexandrium monilatum* adapted and updated from May *et al*. 2010. ND=no data. *Unsubstantiated records.

Location	Date	Bloom, >999 cells/mL (Y/N)	Reported mortality	Maximum bloom density (cells/mL)	Salinity	Temperature (°C)	Reference
Offatts Bayou, Galveston, TX	July-September 1949	Y	Finfish, shrimp	ND	ND	ND	Connell and Cross (1950)
Indian and Banana Rivers and City Pier, Sarasota, FL	August-September 1951	Y	Finfish	ND	18-32	30-34	Howell (1953)
Offatts Bayou, Galveston, TX	September 1955	Y	Finfish	1,000	ND	ND	Gates and Wilson (1960)
Mochima Bay, Venezuela	October-November 1962	N	ND	ND	ND	ND	Halim (1967)
Galveston, TX	ND	ND	ND	ND	ND	ND	Marvin (1964) cited in Juhl (2005)
Anna Maria Island to Cape Romano, FL	August-September 1966	Y	Finfish, crabs, lobsters, shellfish	1,335	27.8-36.1	29-34	Williams and Ingle (1972)
York River, VA	September 1966	Y	ND	ND	23.3-24.2	20.7-25.2	MacKiernan (1968)
York River, VA	August-September 1967	N	ND	ND	19.9-20.7	19.8-25.8	MacKiernan (1968)
Galveston, TX	August 1971-1972	Y	Finfish, crustaceans, molluscs, echinoderms, annelids, coelenterates	1,880	32-34	29-32	Wardle *et al*. (1975)
Indian and Banana Rivers, FL	July 1977	Y	No mortalities	1,700	30.5-32.0	29.5-32.0	Norris (1983)
Indian and Banana Rivers, FL	September 1977	Y	Finfish	ND	ND	ND	Norris (1983)

Location	Date	Bloom, >999 cells/mL (Y/N)	Reported mortality	Maximum bloom density (cells/mL)	Salinity	Temperature (°C)	Reference
Pensacola Bay, FL	August 1979	Y	No shellfish mortalities	5,700	ND	ND	Walker (unpublished) cited in Owen and Norris (1982)
Mobile Bay, AL	August 1979	Y	Finfish	ND	ND	ND	Perry *et al.* (1979)
Indian and Banana Rivers, FL	September 1979	N	ND	ND	16-21	24.5-30.0	Norris (1983)
Louisiana Coast	ND	ND	ND	ND	ND	ND	Perry (1980) cited in Juhl (2005)
Mississippi Coast and Sound	ND	Y	ND	1,650	ND	ND	Perry and McLelland (1981) cited in Juhl (2005)
Gulf of Cariaco, Venezuela	January-February and April-May 1984; January 1985	N	ND	ND	ND	ND	Ferraz-Reyes *et al.* (1985)
Gulf of Nicoya, Costa Rica	1985	N	ND	ND	ND	26-31	Víquez and Hargraves (1995)
Coastal MS	1998	Y	Zooplankton, ichthyoplankton	ND	ND	ND	ICES (1999) cited in May *et al.* (2010)
***Black Sea**	1990s	Y	ND	2,700	ND	ND	Moncheva *et al.* (2002)
Mississippi Sound	September 2000	N	ND	ND	35	28	Juhl (2005)
York River, VA	September 2007	Y	Veined rapa whelks	40,000	22.4-22.8	27-28	Harding *et al.* (2009)
***Southwest Coast of India**	2005-2008	N	ND	ND	ND	25-29	Sanilkumar *et al.* (2009)

CHAPTER 1:

DETECTING *ALEXANDRIUM MONILATUM* CYSTS IN THE LOWER CHESAPEAKE BAY

ABSTRACT

Late summer blooms of the toxin-producing harmful algal bloom (HAB) species *Alexandrium monilatum* in the Chesapeake Bay have been expanding in range and cell density over the last decade. This dinoflagellate species overwinters in the sediments as a resting cyst before excysting to produce blooms the following summer. This study provided the first mapping and quantification of resting cysts of *A. monilatum* in surface sediments in the Chesapeake Bay using quantitative real-time polymerase chain reaction (qPCR) assays. A systematic grid sampling design was employed to collect pre-bloom sediments in the York River region of the Chesapeake Bay each year from 2014-2016. Evidence for the existence of resting cysts of *A. monilatum* was based on DNA extracted from sediment samples and quantified using species-specific qPCR molecular methods. *Alexandrium monilatum* cysts are widespread in the bottom sediments of the southwestern portion of the Chesapeake Bay and cyst density has increased from 2014-2016. Cysts were present (>0 cysts/cc) at all sampled sites in all years, reaching densities as high as 90,000 cysts/cc at one site in the York River channel. A multiple linear regression was used to model cyst density using environmental parameters (i.e. sediment type and salinity). Sediment type was a good predictor of cyst density, with higher cyst densities found at sites with higher percentages of fine grain sediments (silts and clays). *Alexandrium monilatum* has clearly established itself in the York River region of the Chesapeake Bay as a recurring harmful algal bloom species which overwinters in cyst-form in the bottom sediments.

INTRODUCTION

The range and frequency of reported harmful algal blooms (HABs) has been increasing worldwide (as reviewed in: Landsberg 2002; Heisler *et al.* 2008). These noxious or toxic bloom events are associated with adverse aquatic animal or human health effects, and result from a rapid proliferation of one or a few distinct species of phytoplankton or macroalgae in an area. The HAB species *Alexandrium monilatum* (historically known as *Gonyaulax monilata*) is a chain-forming, thecate dinoflagellate originally described by Howell (1953) from a bloom associated with a fish kill off of the east coast of Florida. This species has long been associated with finfish and invertebrate kills in the Gulf of Mexico (Connell and Cross 1950; Wardle *et al*. 1975), and has been shown to produce the toxin goniodomin A (Hsia *et al*. 2006).

In 2007, the York River in the lower Chesapeake Bay witnessed its first bloom of *A. monilatum* since the mid-1960s (MacKiernan 1968). Since its re-emergence in the Bay, *A. monilatum* has bloomed almost annually, with the bloom season occurring between August and September (Marshall and Egerton 2009, 2013). Research animals held in flow-through systems receiving York River water at the Virginia Institute of Marine Science (VIMS) during the 2007 bloom were inadvertently exposed to this toxin-producing species. This led to the mortality of an entire rapa whelk colony (*Rapana venosa*; n>200; Harding *et al*. 2009), and a number of cownose rays (*Rhinoptera bonasus*; R. Fisher, VIMS, pers. comm.). Blooms in recent years have been suspected of contributing to occasional unexplained mortalities of larvae and spat of the eastern oyster,

Crassostrea virginica. There have been anecdotal reports of adult oyster and blue crab mortalities during these blooms as well.

In Virginia, *A. monilatum* blooms appear to originate near the mouth of the York River; however, the spatial distribution of *A. monilatum* in the region has expanded (Dauer *et al.* 2010). Blooms of *A. monilatum* have occurred in 6 of the last 9 years (67%; K. Reece, VIMS, unpublished data), during which time bloom concentrations recorded in the York River have reached densities a full order of magnitude (>5X) higher than any *A. monilatum* blooms reported globally (Perry *et al.* 1979). Bloom patches in the Bay quantified by quantitative real-time polymerase chain reaction (qPCR) standardized to 2007 York River *A. monilatum* bloom isolates grown in culture, have indicated densities >200,000 cells/mL (K. Reece, VIMS, unpublished data). Locally, these blooms are associated with intense bioluminescence (MacKiernan 1968).

Many dinoflagellate species form cysts; for some species, N or P depletion in the water induces sexuality and leads to cyst formation (Anderson *et al*. 1991). *Alexandrium monilatum* overwinters in the cyst, or "hypnozygote", stage until environmental conditions (i.e. temperature; Anderson *et al.* 1991) are right for the life cycle to begin again with germination and excysting of the cell (Walker and Steidinger 1979). Hypnozygotes of other dinoflagellate species can rest in the sediments from months to many years before excysting (Anderson *et al.* 1991). Under anoxic conditions, hypnozygotes often do not excyst, but instead remain dormant (Anderson *et al.* 1991). Turbation of anoxic sediments, either biological or mechanical, could bring cysts stored in these anoxic layers up to the oxic layers of the sediments. If these cysts are still viable,

they may excyst in oxic conditions, potentially providing an opportunity for old, previously-buried cysts to cause "new" blooms.

Like other *Alexandrium* species, including *A. fundyense* in the Gulf of Maine (Anderson *et al.* 1991), *A. monilatum* cysts form "seed beds" in the sediments that can serve as a source for future blooms (Walker and Steidinger 1979). Assessment of cyst density and distribution in bottom sediments is an important aspect of understanding bloom dynamics and distribution (Anderson *et al.* 1991), and surveying cyst distribution has become a routine practice in forecasting red tides caused by *A. fundyense* in the Gulf of Maine (Anderson *et al.* 2005).

Multiple methods exist to quantify cysts in sediments, each method with its own advantages and limitations. In the Gulf of Maine, the primary method used for quantifying *A. fundyense* cysts is the primulin staining method (Anderson *et al.* 1991, 2005; McGillicuddy *et al.* 2014). This primulin visual counting method, originally developed by Yamaguchi *et al.* (1995), has become a "gold standard" method for cyst quantification and has been applied successfully to other cyst species (Tobin and Horner 2011). Other methods of cyst quantification include visual counts using light microscopy without staining (White and Lewis 1982; Anderson and Keafer 1985; Lacasse *et al.* 2013; Gracia *et al.* 2013; Triki *et al.* 2014; Van Hauwaert 2016), species-specific qPCR assays (Erdner *et al.* 2010), and species-specific fluorescence *in situ* hybridization (FISH; Hattenrath-Lehmann *et al.* 2016).

Two studies have been published on *A. monilatum* cyst distribution to date. The first, a presence/absence study in the Indian River in Florida that used basic light microscopy to identify cysts, found *A. monilatum* cysts at 13 of 37 sites sampled (Owen

and Norris 1982). The authors of that study found correlations between *A. monilatum* cyst presence and sites where, 1) there was low water circulation, 2) blooms had occurred, or 3) shellfish had been imported from bloom waters. Sediment grain size however, showed no clear correlation to cyst presence. A recent study by Van Hauwaert (2016) quantified *Alexandrium* spp. cysts from Chesapeake Bay surface sediment samples using light microscopy, finding a high abundance of *Alexandrium* spp. cysts, particularly near the mouth of the York River. Van Hauwaert (2016) was not able to distinguish between cyst species within the *Alexandrium* genus however, and noted that *Alexandrium* cyst counts were conflated with cysts from a few other genera (i.e. *Scrippsiella* and *Prorocentrum*).

Little is known about *A. monilatum*'s ecological dynamics in the Chesapeake Bay beyond that the Bay experiences record-high bloom densities (K. Reece, VIMS, unpublished data), and that the range of these blooms has expanded in recent years (Dauer *et al.* 2010). To more effectively manage potential animal and human health risks attributable to re-emergence of this species in the lower Chesapeake Bay, a better understanding of the spatial and temporal distribution of *A. monilatum* is needed. As blooms are ephemeral and short-lived, this is best accomplished by examining the distribution and abundance of the resting cysts in bottom sediments. The primary objective of this study was to determine whether *A. monilatum* has established itself in the York River region of the Chesapeake Bay by mapping and quantifying cyst density of bottom sediments. I pursued this objective using newly developed, high-throughput, species-specific qPCR assay methods developed to facilitate cyst enumeration.

METHODS

Study Area

Chesapeake Bay is located along the East Coast of the US with a single inlet that opens to the Atlantic Ocean. A systematic grid sampling design was devised for the southwestern portion of the Chesapeake Bay using ArcMap 10.3.0 (ESRI, Redlands, CA). The main study area (25x40-km) incorporated Mobjack Bay and its tributaries, the York, Back, and Poquoson Rivers, as well as a portion of the Bay's mainstem (Fig.1.1). Sampling occurred in three consecutive years (2014-2016), and was performed between mid-May and late July. This time frame ("pre-bloom") is well after when *A. monilatum* would have encysted and sunk into the sediments, and is before the majority of cysts would be expected to excyst and germinate. Water depths at sampled sites ranged from 0.5-13.3 m. The main study area was expanded in 2015 to investigate a wider range of cyst distribution, and in 2016, only a portion of the main study area was sampled.

Sediment Sample Collection and Storage

Sites were located by GPS (Garmin eTrex® 20x, Lenexa, KS), and the coordinates corresponding to the location of each grab sample were recorded, along with time and a depth reading from the vessel's depth gauge. General surface water quality data (temperature, dissolved oxygen, salinity) were collected using a YSI 650 MDS (YSI Inc., Yellow Springs, OH), with separate readings of these parameters recorded for each replicate grab. Surface sediments were collected using a standard Ponar® grab (Wildco, Yulee, FL) from selected sites. To target the most recent cysts, a sample was taken from each grab from approximately the top centimeter of sediment; oxic sediments were lighter in color and helped indicate the top surface (Lacasse *et al.* 2012). Approximately

50 g of sediment was collected, put into a Ziploc bag, 50-mL Falcon tube, or 250-mL plastic bottle, and stored in the dark on ice until it could be returned to the lab. Sediments were stored in the dark at 3° C for up to 29 days before processing. Sediment density was calculated and recorded for each sample based on the mass of a given volume of sediment.

2014 Pre-bloom sampling

A grid covering the 25x40-km main study area, with its origin at 37.41863°N 76.28082°W established 20 sampling sites (A-T, see Fig. 1.1). Adjacent sites on the grid were 5000 m apart from one another. These "5000-m sites" were sampled in triplicate to evaluate within-site variability, with three separate benthic grabs performed in succession at each site (n=60). Sampling was performed from June 27-July 22, 2014, with each site sampled once within that time frame. Water depths at these sites ranged from 0.6-12.9 m, with an average of 6.0±3.9 s.d. m. Surface temperature ranged from 25.7-28.0° C, with an average of 26.7±0.6 s.d.° C. Surface salinity ranged from 14.3-20.7, with an average of 18.7±1.7 s.d..

To assess variation in cyst distribution and density at a scale smaller than 5000 m, a 500-m grid was created over the lower portion of the York River (Fig. 1.2). This grid spanned the area between the Coleman Bridge in Yorktown and the Bay, where *A. monilatum* blooms have been known to occur (MacKiernan 1968; Harding *et al.* 2009; Marshall and Egerton 2009; Dauer *et al.* 2010). Squares created by the grid were 500 m^2. If all four corners of the square were at a depth accessible to our Ponar® grab (approximately 1.2-12.2 m) the square was assigned a number. Using this depth stratum, 54 potential sampling squares were defined, and of those, seven non-overlapping squares

were randomly selected for sampling. One grab was performed at each of the four corners of each selected square (n=28). Sampling was performed from June 27-June 30, 2014, with each square sampled once within that time frame. Water depths at these sites ranged from 1.6-12.9 m, with an average of 5.6±3.4 s.d. m. Surface temperature ranged from 26.6-28.3° C, with an average of 27.5±0.6 s.d.° C. Surface salinity ranged from 16.1-17.5, with an average of 16.8±0.4 s.d..

Concurrent 100-mL surface water samples were collected for each replicate grab, at every site, to confirm the absence of vegetative cells of *A. monilatum* in overlying waters. These samples were kept cool and in the dark until they could be filtered through 3-µm Nitex filters. Filters were stored frozen at -20° C until ready for DNA extraction (see **DNA Extraction**).

2015 Pre-bloom sampling

In 2015, the 20 original 5000-m grid sites (A-T) were revisited. Three new 5000-m sites were added (Fig. 1.1) to extend the grid with the intention of capturing the extent of the *A. monilatum* cyst distribution based on 2014 results. These new sites were located further up the York River (YR1), outside of New Point Comfort in the mainstem of the Bay (PC1), and south of Back River in the mainstem of the Bay (U). All 23 of these "5000-m sites" were sampled in triplicate, with three separate grabs performed in succession at each site (n=69). Sampling was performed from May 19-28, 2015, with each site sampled once within that time frame. Water depths at these sites ranged from 1.5-13.3 m, with an average of 6.0±3.9 s.d. m. Surface temperature ranged from 20.6-24.4° C, with an average of 22.1±0.8 s.d.° C. Surface salinity ranged from 15.7-21.9, with an average of 19.3±1.3 s.d..

2016 Pre-bloom sampling

To compare quantification methods, a subset of ten sites from the original 5000-m grid were selected in the third year of the field study (C, E, G, H, L, M, P, Q, S, T; Fig. 1.1). Based on previous results, these sites were expected to represent a range of cyst densities, locations, and sediment types. Sites were sampled in triplicate, with three separate grabs performed in succession at each site (n=30). Samples were collected and stored as described above and were later homogenized by stirring, before being split and run in parallel with the 2014 "dry" and 2015 "wet" extraction methods, and visual quantification methods (see **Sediment Homogenization** and **Visual Quantification**). Sampling was performed from May 19-June 1, 2016, with each site sampled once within that time frame. Water depths at these sites ranged from 0.5-12.2 m, with an average of 6.1±4.4 s.d. m. Surface temperature ranged from 17.9-26.2° C, with an average of 20.6±2.3 s.d.° C. Surface salinity ranged from 14.6-19.2, with an average of 17.1±1.2 s.d..

Sediment Grain Size

Additional sediment samples (26-41 g) were collected from the 10 sites sampled in 2016 from the same triplicate grabs described above (see **2016 Pre-bloom sampling**) to investigate potential correlations between sediment cyst density and grain size. Samples were collected in pre-weighed Whirl-Pak bags and stored at 3° C until processed. Sediment grain size analysis was performed by the VIMS Analytical Services Laboratory. Sediment from each site was classified using the system designed by Shepard (1954), as modified by Schlee (1973). "% Coarse" was calculated by combining % gravel and % sand. "% Fine" was calculated by combining % silt and % clay. For statistical

analyses, sampling sites were categorized into the basic sediment types of "coarse" or "fine" based on which sediment grain size was dominant at the site (>50%).

Sediment Homogenization

Two methods of sediment homogenization prior to DNA extraction were utilized, a "dry" method and a "wet" method. The "dry" method consisted of stirring the sediments to homogenize them in the sample container prior to weighing out the 0.25 g required for using the PowerLyzer PowerSoil DNA Isolation kit protocol (MO BIO, Carlsbad, CA). This "dry" method was used for all 2014 samples. The "wet" method was developed in response to concerns that sediments were not being thoroughly homogenized by basic stirring, and consisted of adding artificial sea water (ASW, salinity 20; Instant Ocean, Blacksburg, VA) to dilute the sample to 4/5 sediment, following suggestions found in Anderson *et al.*'s *Cyst Methodologies* (1991). This slurry was then vigorously vortexed for 5 seconds, and 200 µL was quickly transferred to the PowerLyzer PowerSoil DNA Isolation kit bead tubes. The volume of slurry used was calculated to approximate 0.25 g of sample, based on the average sediment density (1.6±0.3 s.d. g/mL for 2015 pre-bloom samples), and accounting for the 4/5 dilution, conservatively rounding up to 200 µL. The exact mass of sediment extracted was calculated using the density of the sample:

$$Y = xvD$$

where, Y = grams of sediment sample extracted, x = sediment: slurry dilution factor (4/5 for this study), v = volume of slurry (mL) added to bead tube (0.2 mL in this study), and D = measured density of the sediment sample (g/mL). This "wet" method was used for all 2015 samples. For both methods, the exact amount of sediment (g) used for the DNA

extraction was recorded. In 2016, all samples were processed using both extraction methods; this was accomplished by stirring and removing the 0.25 g of sediment for the "dry" method, re-weighing the sample, diluting it to 4/5 sediment with ASW, and removing the 200 µL of slurry for the "wet" method; the remainder of the diluted sample was reserved for comparison with visual quantification methods and was stored in the dark at 3° C (see **Visual Quantification**).

DNA Extraction

The PowerLyzer PowerSoil DNA Extraction kit was used to extract DNA from sediment samples according to the manufacturer's instructions. Bead beating was carried out as recommended for clay soils, 45 s at 4000 RPM using the FastPrep™-24 (MP Biomedicals, Solon, OH). Extracted DNA was eluted once with 100 µL of the kit's elution reagent, and eluted DNA was stored at -20° C until qPCR analysis could be performed.

For the 2014 water samples, DNA was extracted from the frozen filters according to the manufacturer's instructions for the QIAamp Fast DNA Stool Mini kit (Qiagen, Germantown, MD). The optional, higher-heat, 95° C water bath was used to lyse cells after adding InhibitEX. Extracted DNA was eluted twice with 100 µL of the kit's elution reagent, and eluted DNA was stored at -20° C until qPCR analyses could be performed.

Standard Curve Development

Cultured York River *A. monilatum* isolates from the 2007 bloom, collected during log growth phase, were used as standard material for qPCR. Cell counts of the culture, performed using light microscopy, were used to determine a volume of culture to be filtered onto a 3-µm Nitex filter to represent a 100-mL sample with 4000-5000 cells/mL

(400,000-500,000 cells). These filters were stored at -20° C until ready for DNA extraction (as described above for the 2014 water samples).

Quantitative Real-time PCR

A pair of primers targeting the 18S ribosomal RNA gene was used for qPCR (Eurofins MWG Operon, Louisville, KY): a species-specific forward primer (VA DEQ 2014) designed based on an *A. monilatum* sequence deposited in NCBI's GenBank by Rogers *et al*. in 2006 (Accession # AY883005.1), and a reverse primer designed to target Alveolates (K. Reece, VIMS, unpublished data).

Primer set used (5'-3'):	
	Am-SSU-174F CAATCAAACCTGACTCTTGTGGG
	Am-SSU-409R GCCTGCTGCCTTCCTTAGATGTGGT

Reaction volumes of 10 µL included 5.00 µL of 1.00 µM Fast SYBR® Green Master Mix (ThermoFisher Scientific, Waltham, MA), 0.90 µL at 0.90 µM of forward primer Am-SSU-174F and reverse primer Am-SSU-409R, 2.20 µL of dH_2O, and 1.00 µL of DNA template. Cycling conditions consisted of 1 cycle at 95° C for 20 s, followed by 40 cycles of 95° C for 3 s, 60° C for 30s, 75.5° C for 30 s, followed by 1 cycle of 95° C for 15 s, 60° C for 1 min, 95° C for 15 s, and 60° C for 15 s, followed by melt curve analysis. Six standards were included on each plate, representing a 10-fold serial dilution of an extracted standard ranging from 4×10^{-3} to 4×10^{3} cells/mL, or 5×10^{-3} to 5×10^{3} cells/mL depending on the extracted standard. The range of detection based on the standard curve was 4-4000 or 5-5000 cells/mL, depending on the extracted standard. Each reaction was run in triplicate using a 7500 Fast Real-Time PCR System (Applied Biosystems®, Foster City, CA), with the software determining the threshold cycle values

(C_t) and providing interpolated values for cells/mL for each reaction based on the standard curve. The average of the interpolated cells/mL values from the triplicate reactions was transformed if necessary and used for statistical analyses. In order to perform numeric analysis, negative qPCR results (i.e. when no fluorescence was detected and the system recorded the sample quantity as "undetermined") were recorded as "0 cysts/cc" for sediments or "0 cells/mL" for water.

Due to differences in the extraction method of the sediment and water samples, sediment results needed to be transformed from cells/mL to cysts/cc using the following equation:

$$Z = fV_s d\left(\frac{D}{Y}\right)$$

where, Z = sediment cyst density in cysts/cc, f = fraction of standard volume that is extracted (1/5 for this study – refer to QIAamp Fast DNA Stool Mini kit protocol), V_s = total volume of culture (mL) filtered to make standard (100 mL in this study), d = Qty output from qPCR software (cells/mL), D = measured density of the sediment sample (g/mL), and Y = grams of sediment sample extracted. Latitude and longitude were used to map sediment cyst densities in ArcMap.

The method lower detection limit (DL) for sediment values was determined by finding the range of values equivalent to 4 or 5 cells/mL (depending on the standard used) in sediment using the full range of sample densities and sample masses extracted. The DL varied per sample with sediment density and actual mass of the sediment sample processed in the extraction, so a range of DLs was produced for each sampling year: in 2014 the lower DL ranged from 322-664 cysts/cc (mean 491±88 s.d. cysts/cc), in 2015 the lower DL was 500±0 s.d. cysts/cc, and in 2016 the lower DL ranged from 466-930

cysts/cc (mean 619±148 s.d. cysts/cc) for the "dry" extraction method and from 398-625 cysts/cc (mean 611±54 s.d. cysts/cc) for the "wet" extraction method. The overall mean lower DL across all sediment samples in all years was 527±97 s.d. cysts/cc. Given that the lower DL for all standard curves was four orders of magnitude lower than the upper DL, we estimated from the overall mean lower DL that the overall upper mean DL for cysts in this study would have been around 527,000±97,000 s.d. cysts/cc.

Statistical Analyses

The mean cyst density was calculated for each set of triplicate grabs within a site, and for each sampled square from the 2014 fine scale sampling. The minimum, maximum, mean, and standard deviation were calculated in each year for depth, temperature, salinity, and *A. monilatum* cyst density.

Statistical tests were run in R Studio (2015) using R version 3.3.0. All tests used a significance level (α) of 0.05. A simple linear regression and a Wilcoxon signed rank test were used to compare the "dry" and "wet" extraction methods for qPCR results from 2016. ANOVAs were used to test for differences between 500-m squares, and between 5000-m sites. Variance (s^2) was calculated using the equation:

$$s^2 = \frac{1}{n-1}\sum_{i=1}^{n}(x_i - \bar{x})^2$$

where, n = number of samples, x_i = cyst density for sample i, and $\bar{x}$ = mean cyst density.

To determine which environmental factors might play a role in cyst distribution and density, the data from the ten sites that were consistently sampled each year were explored using multiple linear regression. Cyst density was $\log_{10}$-transformed to normalize the data set. Scatterplots and correlation tests were used to explore

relationships between environmental parameters and cyst density. Depth, sediment type, year, and salinity were tested as predictors of cyst density. Temperature and dissolved oxygen (DO) were not used as predictors under the assumption that water surface measurements of temperature and DO at the time of sediment sampling were not likely to be good predictors of bottom sediment cyst density. Continuous predictors (depth, salinity) were centered and scaled to reduce effects of collinearity. Variance inflation factor (VIF) was calculated to assess collinearity of predictors. Graphical analyses were used to assess the presence of confounded predictors. A number of possible linear models were written and tested for fit using Akaike's Information Criterion corrected for finite sample sizes (AICc). The best fit model was chosen using backward selection with AIC_c. Least squares means of maximum cyst density were calculated for each sampling year to compare changes in cyst density between sampling years using pairwise contrasts.

Visual Quantification

In 2016, efforts were made to compare qPCR methods to visual quantification methods for enumerating cysts, using samples split in the lab for parallel processing. After sub-samples were removed for both "dry" and "wet" extraction methods for qPCR, the remaining diluted sediment was processed for primulin staining analysis based on methods modified from (Erdner *et al*. 2010), and for FISH staining based on methods modified from (Hattenrath-Lehmann *et al*. 2016). Results from these preliminary attempts to use primulin staining on *A. monilatum* cysts were unsatisfactory, and were not included in this study, however, a portion of all 2016 samples has been preserved for future primulin and FISH staining analyses. Additional commentary and the full protocol

for 2016 sediment sample processing with all quantification methods can be found in the Appendix.

RESULTS

Quantitative Real-time PCR

qPCR quantification of *A. monilatum* from 2014 pre-bloom benthic sediment grabs showed that the species is prevalent throughout the southwestern portion of the Chesapeake Bay (Tables 1.1 and 1.2, Figs. 1.3 and 1.4). Of the 48 sites sampled, 45 sites had at least one sample with a cyst density above the lower detection limit (DL; mean DL=491±88 s.d. cysts/cc). The highest cyst density recorded in 2014 was 12,717 cysts/cc at site M (depth ~12 m), located in the channel of the York River where it enters Chesapeake Bay. The lowest average cyst density recorded in 2014 was 40±46 s.d. cysts/cc at site P (depth ~1.8 m), a shallow site located south of the York River channel near Plum Tree Island. All 88 water samples were below the water sample DL (4 cells/mL), although 8 of these samples registered low fluorescence, with the qPCR system detecting quantities below the DL, indicating they were >0 cells/mL.

Results from 2015 sediment sampling again showed widespread occurrence of *A. monilatum* cysts, but at higher concentrations than seen in 2014 (Table 1.3, Fig. 1.5). New sampling sites PC1 and YR1 showed that *A. monilatum* cysts occurred in sediments northward into the main stem of the Bay, and further up the York River. New site U samples were all below the 2015 sediment cyst DL (mean DL=500±0 s.d. cysts/cc), although two of those were >0 cysts/cc. Sample YR1-1 (collected on May 19, 2015) was omitted from the dataset because the winch for the Ponar® grab broke after retrieving the sample, and the set of three replicate grabs could not be completed in one day. Triplicate grab sampling was completed at site YR1 on May 26, 2015. Of the 23 sites sampled, 21 sites had at least one sample with a cyst density above the lower DL. The highest cyst

density recorded in 2015 was 91,118 cysts/cc at site Q (depth ~10 m), located in the channel of the York River, far into the mainstem of Chesapeake Bay. The lowest average cyst density recorded in 2015 was 140±242 s.d. cysts/cc at site H (depth ~1.9 m), located near the mouth of Mobjack Bay.

Results from 2016 sediment sampling again showed wide distribution and dense concentrations of *A. monilatum* cysts throughout the study area (Table 1.4, Fig. 1.6). Of the 10 sites sampled, all had at least one sample with a cyst density above the DL (mean DL=619±148 s.d. cysts/cc). The highest cyst density recorded in 2016 was 62,673 cysts/cc at site L (depth ~18 m), located in the channel at the mouth of the York River. The lowest average cyst density recorded in 2016 was 545±944 s.d. cysts/cc at site H (depth ~2.5 m), located near the mouth of Mobjack Bay.

Sampling Scale

Variation in cyst density was high enough between the four corners of a 500-m square such that no difference could be detected between the seven squares tested (Table 1.5, Fig. 1.7; between squares $F=1.283$, $p=0.307$).

At a larger spatial scale, differences in cyst density were detected between 5000-m sites ($F=2.832$, $p=0.00276$). To normalize the data for this ANOVA, cyst density was $\log_{10}$-transformed, and the cyst density of sample H-3 was changed from 0 to 10 cysts/cc. Variances for 8 of the 20 sites were higher within, rather than between sites (Table 1.6, Fig. 1.8).

Method Comparison

In 2016, cyst quantification was performed using two different methods, the “dry” and “wet” extraction methods. Using the maximum cyst density of the triplicate grabs for

each of the ten sites, the Wilcoxon signed rank test showed no difference between the two extraction methods (V=31, p=0.7695). A simple linear regression was fit to these data: $y=1.0462x-2090$, $R^2 = 0.9588$ ($F=210.6$, $p=4.98x10^{-7}$) where, y is cyst density using the "wet" method, and x is the "dry" method (Fig. 1.9). The 95% confidence interval for the slope of the regression was 0.880-1.213. The linear regression equation was used to transform 2015 cyst density data to match the "dry" method used in 2014 and 2016, all further mentions of cyst density, represent densities transformed to, or acquired using, the "dry" extraction method.

There was a better fit to the model using the maximum cyst density of the replicate grab samples than the average; this was likely due in part to the fact that the average incorporated values that were extrapolated from the qPCR standard curve and were below the lower DL. Maximum cyst density values were more accurate and rarely fell below the detectable range (5 of 53 values); for this reason, maximum values were used for downstream statistical analysis.

Sediment Grain Size

Grain size analysis results from the VIMS Analytical Services Laboratory for the 10 sites sampled in 2016 can be found in Table 1.7. Grain size data were compared with the maximum cyst density from the triplicate grabs made at each site. Percent gravel, sand, silt, and clay were all tested for correlations to "dry" method cyst densities using Pearson's product-moment correlation. Gravel did not correlate with maximum cyst density (cor=-0.344, t=-1.0362, p=0.3304), and sand had a negative correlation (cor=-0.707, t=-2.8242, p=0.02235), while silt and clay both had a positive correlation with maximum cyst density (cor=0.801, t=3.7798, p=0.00539; cor=0.695, t=2.731, p=0.0258,

respectively). Maximum cyst density increased with increasing percent silt or clay, and decreased with increasing percent sand.

Percent gravel and sand were combined to represent % coarse, while percent silt and clay were combined to represent % fine sediments. Figure 1.10 shows that samples with low cyst densities came from sites with low % fine sediments, and samples with higher cyst densities came from sites with higher % fine sediments (cor=0.767, t=3.3799, p=0.009643). There were no sites sampled that had intermediate % fine sediments, suggesting that these data could be split into a categorical predictor of basic "sediment type"; sites with >50% fine were assigned to the "fine" category (n=6), and all others were assigned to the "coarse" category (n=4; Table 1.7; Fig. 1.10). All cyst densities for the fine sediments were higher, and the ranges larger, than for the coarse sediments, regardless of extraction method (Fig. 1.11). The ranges of values between methods for the fine sediments were more similar than between methods for the coarse sediments. The "wet" extraction method showed less variation than the "dry" method for coarse sediments.

Environmental Factors

Depth, sediment type, year, and surface measurements of water temperature and salinity data were explored to determine which environmental factors could be used to model cyst density. Cyst density data were normalized using a $\log_{10}$ transformation. No collinearity was found between predictors. Sediment type (coarse or fine) was only determined for ten sampling sites, so modeling data was restricted to data from these sites, which were sampled in all three years (2014-2016, n=30). Sediment type was assumed to remain stable during these years; this assumption was supported by gross

visual descriptions of sediment type recorded during 2014 sample collection. Year was highly correlated with cyst density (cor=0.56, $p<0.01$), with cyst density increasing with year. Year was negatively correlated with temperature (cor=-0.83, $p<0.001$) and salinity (cor=-0.41, $p<0.05$). Depth and sediment type were correlated (cor=0.77, $p<0.0001$), with more fine sediments at increasing depth. All deep sites were "fine" sites and all but one of the shallow sites were "coarse" sites. Due to the confounding of these two predictors, the weaker predictor of cyst density, depth, was left out of the model.

A multiple linear regression was calculated to predict maximum log cyst densities based on year, sediment type, and salinity. Underlying assumptions of the model were evaluated to validate the optimal model, including plotting residuals versus fitted values to evaluate homogeneity of variance. Backward selection using the Akaike Information Criterion corrected for finite sample sizes (AICc) revealed the best fit model to be:

$$\log_{10} D = 2.8172 + 0.8582\, Y_{15} + 0.9646\, Y_{16} + 0.8673\, G - 0.2233\, S + 0.4451\, G * S$$

$$F_{(5,24)} = 21.07,\ p = 4.563 \times 10^{-8},\ \text{with an } R^2 \text{ of } 0.7758$$

where, D = *A. monilatum* cyst density (cysts/cc), Y_{15} = year 2015 (coded as 1 = 2015, 0 = not 2015), Y_{16} = year 2016 (coded as 1 = 2016, 0 = not 2016), G = sediment type (coded as 1 = fine, 0 = coarse), and S = salinity. Year, sediment type, and the interaction between sediment type and salinity were significant predictors in the model (Table 1.8). The interaction was retained in the model and implied that the effect of salinity on cyst density depended on sediment type; coarse sediments showed a decrease in cyst density as salinity increased, while fine sediments showed little change in cyst density as salinity increased (Fig. 1.12). Accounting for variability due to sediment type and salinity, year has a significant impact on maximum log cyst density, with a significant increase in cyst

density between years 2014 and 2015 ($t=-5.375$, $p<0.0001$), and an insignificant increase between years 2015 and 2016 ($t=-0.543$, $p=0.8508$).

DISCUSSION

Alexandrium monilatum has established itself as a recurring HAB species in the York River region of the Chesapeake Bay. Cysts were present at all sampled sites in all years and were found in high densities across all three years of sampling (2014-2016; Fig. 1.3-1.6). Densities were high in the lower York River where blooms had been recorded in previous years (Marshall and Egerton 2009), especially at sites in the river channel. These findings suggest that there were ample cysts in the sediments of the York River region to support bloom-formation from year to year. These cysts may also help to expand the range of this species in the Bay as the cysts become resuspended or are moved via hydrodynamic processes.

Additionally, cyst density increased over the three years of the study. Much of the increase in cyst density occurred between years 2014 and 2015, even though no bloom occurred in 2014. Five water samples collected in August-September 2014 showed cell densities <1 cell/mL (K. Reece, VIMS, unpublished data), suggesting that little cyst excystment occurred in 2014. Even though no bloom was detected, it is possible that low levels of *A. monilatum* were able to reproduce in 2014, adding to the 2015 pre-bloom sediment cyst load. Alternatively, this increase in cyst density may be an artefact of which month the sediments were sampled. In 2014, sampling occurred primarily in July, while in 2015 and 2016, sampling occurred primarily in May. It is possible that in July of 2014 some of the cysts had already germinated, reducing the density of cysts in the sediments that could have been sampled. Although, if this were the case, we might have expected to have seen higher densities of vegetative cells in the water samples collected in August-September (see above).

If cyst density continues to increase, bloom severity might be expected to increase over time as well. The York River experiences deep physical mixing of the sediments (Dellapenna *et al*. 2003), which may mean that cysts are not easily buried to anoxic depths in this region. River dredging for navigational or fishing purposes, or other disturbances like storms, may also have an appreciable impact on the availability of viable cysts in the oxic sediment layer that can help to form blooms each year. Thus cysts produced over many years and remobilized from different depths may be readily available in any given year to form a bloom. This study quantified cysts in only the top centimeter of sediment, so underestimation of cysts available annually to produce blooms is a possibility.

Sediment samples were acquired using a grab, which could have led to the collection of disrupted sediments, where some of the surface floc and sediment was lost and replaced with older, deeper sediments. However, given the deep physical mixing of sediments in the York River, there is reason to believe that these deeper sediments could release viable cysts. A grab was sufficient for the purposes of this study, but future studies could apply the study design recommendations and findings of this study to obtain more accurate quantification of cysts. With special care not to disrupt the water-sediment interface when collecting samples, absolute cyst densities for a given sediment depth could be determined by using a coring device.

Overall cyst density was higher, and the cyst distribution larger, than anticipated. The original main study area was designed to encompass the full extent of previous years' *A. monilatum* blooms in the York River region, with the assumption that the cysts would be distributed within that range. However, cysts were widely distributed across the

study area, suggesting that expanding the sampling range would have led to the discovery of additional cysts. No sites in the study region were free of *A. monilatum* cysts. Future work to delineate the full extent of *A. monilatum* cyst distribution in the Chesapeake Bay would need to sample much more broadly, with sites further apart than those used in this study.

Blooms at the water's surface are heavily influenced by wind and currents (Shumway 1990), which lead to bloom patchiness and may spread vegetative cells long distances before they encyst and sink to the sediments. Bloom patchiness appears to translate to cyst distribution, making precise, small-scale cyst density prediction difficult, if not impossible. In order for sediment cyst mapping to work as a tool for understanding bloom dynamics, enough replicates are needed to account for this inherent bloom patchiness (Anderson *et al.* 1991). There was high variation in cyst densities between replicate grabs, leading to difficulties distinguishing differences between samples taken any closer together than 5 km. Additionally, when collecting triplicate grabs from a sampling site, the boat would drift away from the site. Efforts were made to keep all triplicate grabs within 100 m of the original grid site coordinates, although samples were recorded from as far off-site as 331 m (site Q in 2014). This implies that "replicate" grabs actually sample at a scale slightly smaller than the 500-m grid samples. With variance within site being so high, there is value in collecting triplicate grabs at each site. I would recommend that future studies continue to collect triplicate grabs. Differences between sites at the 5000-m scale could likely not have been detected without replicate grabs taken at each of these sites.

Sediment type is used in the Gulf of Maine to predict where dinoflagellate cysts will accumulate, with cysts generally associated with finer sediments like silts and clays (Anderson *et al.* 1991). An early study on *A. monilatum* cyst distribution in Florida found no correlation with sediment grain size (Owen and Norris 1982). It was not known whether *A. monilatum* cysts were more often found in silts and clays rather than sand in the Chesapeake Bay, so stratified random sampling by sediment type was not performed. Shallower sites in the study area tended to be sandier. The cut-off between silt and sand particles is 62.5 μm (Wentworth 1922), so it seems logical that *A. monilatum* cysts (30-60 μm) which are on the upper end of the silt scale would distribute in a manner more similar to fine sediments. Additionally, a cyst is lighter than a similarly-sized coarse sediment particle, so again the cyst is more likely to distribute with lighter fine sediments of a similar density. This study found a positive correlation between % fine sediments and cyst densities, even though there were still notable quantities of cysts at sites with more coarse sediments. Future sampling efforts might consider targeting sites with more fine grain sediments, or intentionally stratifying sampling sites to include a relatively equal number of both fine and coarse sediment sites.

Two sediment homogenization techniques were used and tested for DNA extraction. The "dry" method essentially follows the protocol of the PowerLyzer PowerSoil DNA Isolation kit (MO BIO, Carlsbad, CA); while the "wet" method was an attempt to provide more thorough homogenization of the sediments after initial results indicated high variance between replicate grab samples. Results from these two homogenization techniques were comparable, and showed no significant difference in samples processed in parallel for both techniques. The "wet" method may overestimate

the density of cysts from coarse sediments, as the cysts may preferentially be removed with the water fraction. The "dry" method is recommended for use in future sediment analysis because it is much easier to perform and has less room for error than the "wet" method.

DNA extracted from sediment samples was analyzed using qPCR to quantify the relative *A. monilatum* cyst densities using a species-specific set of primers. The forward primer Amon 174F has 100% species-specific binding for *A. monilatum,* according to an NCBI BLAST search on May 31, 2016, with a score of 46.1 bits (23), an E value of 0.005, 100% identity, and 0 gaps for the *A. monilatum* isolate JR07 18S ribosomal RNA gene, partial sequence (GenBank Accession # AY883005.1). There is potential for weak co-amplification of *A. hiranoi* and *pseudogoniaulax* (86% identity) as it matches from the 3' end with only a few nucleotides varying at the 5' end. However, these species are not known to be present in significant numbers in the Chesapeake Bay.

The number of gene copies in a cell varies throughout the cell's life stages; for example, *A. fundyense* cysts have 10X fewer gene copies than vegetative cells of the same species (Erdner *et al*. 2010). For this reason, qPCR standards ideally should be made from cells of the same life stage. Unfortunately, hypnozygotes are difficult to produce in a laboratory setting in the quality and quantity necessary for qPCR standards (Erdner *et al.* 2010). This study used qPCR standard material from cultured *A. monilatum* in log growth phase (the asexual, chain-forming stage) and so the qPCR output necessarily makes the assumption that gene copies in vegetative cells are similar to those in hypnozygotes. This may not be the case and could have resulted in significant over- or underestimation of the number of *A. monilatum* hypnozygotes present in sediment

samples collected in this study. Given these methodological caveats, this study determined presence and estimated magnitude of cyst densities in the bottom sediments in the southwestern portion of the Chesapeake Bay. Magnitude of *A. monilatum* cyst density still has immense value, highlighting cyst hot-spots and sites with 10 or 100X as many cysts as another site. There is still much to be learned about gene copy number in different life stages of *A. monilatum*, and future studies should determine the gene copy number of the target DNA sequence for the primary life stages being investigated using qPCR. Validating qPCR results through comparison with another method would provide confidence in the qPCR values, and provide information that could lead to a better understanding of DNA content within *A. monilatum* cysts.

An alternative method of cyst quantification is the primulin staining technique, a visual quantification method developed by Yamaguchi and others (1995), used in many field studies (Anderson *et al*. 2005; Erdner *et al*. 2010; Tobin and Horner 2011; McGillicuddy *et al*. 2014). This method was modified for use with *A. monilatum* as a way to perform visual cyst counts in an effort to validate qPCR results (see Appendix).

Erdner and others (2010), assessed whether qPCR was comparable to the primulin staining method. The qPCR method is faster and has higher throughput, but the reagents cost much more than those for the primulin method. However, the primulin method requires an in-depth knowledge of cyst morphology and taxonomy to identify cysts properly. The authors of the study performed a linear regression, and found that qPCR provided lower cyst counts than the visual primulin method, which they hypothesized could be due to the age or condition of the cysts. DNA breaks down fairly quickly after cell death, but the cyst wall does not, so a visual quantification method may count cysts

that qPCR would not; although neither method directly addresses the question of cyst viability, excystment studies (Anderson *et al.* 1991) would be needed to determine what proportion of cysts counted were capable of germination. The two quantification methods provided results that were within one order of magnitude of each other for 96.9% of their samples. They determined that qPCR could be used to accurately quantify cells, and emphasized that the choice between methods ultimately comes down to time and money.

Basic light microscopy was also tested as a visual quantification method to compare to qPCR. Using regular light microscopy, cysts could be distinguished from other cells and particles when there was minimal debris. However, distinguishing between different species that form cysts is challenging. Dinoflagellate cyst identification relies on characters such as shape, presence of ornaments, color, wall structure, and shape of the archeopyle--the hole through which the cell excysts (Anderson *et al.* 1991). The archeopyle is thought to be the best character for identifying cysts (Anderson *et al.* 1991). However, the archeopyle is only present once the dinoflagellate has left the cyst, and as such, it is not very useful for enumerating un-excysted, viable cysts. Morphological characteristics of *A. monilatum* resting cysts are generally not distinctive; the cysts are spherical (30-60 μm diameter) and have a prominent cyst wall without ornamentation.

In the Chesapeake Bay, there are a number of other bloom-forming species which produce resting cysts and may have significant cyst densities, these include: *Cochlodinium polykrikoides* (Marshall and Egerton 2013), *Levanderina fissa* (formerly known as *Gyrodinium uncatenum*; Tyler et al. 1982), *Gymnodinium,* and *Chattonella* spp. (Reece 2007-2014). There are also a number of species in the region that may produce cysts that are similar in appearance to *A. monilatum*, but which are not present in bloom

levels. Recent work using palynological methods to visually quantify *Alexandrium* spp. cysts in the Chesapeake Bay lumped together the co-occurring: *Alexandrium* spp., *Scrippsiella* spp., and *Prorocentrum minimum*, because they could not be clearly distinguished from one another (Van Hauwaert 2016). The results of this palynological survey however, were consistent with the qPCR results from this study, finding peak *Alexandrium* spp. cyst densities in the lower York River (Van Hauwaert 2016).

Given the uncertainties associated with qPCR and visual quantification methods available for *A. monilatum* cysts, an attractive alternative approach would be to use a fluorescence *in situ* hybridization (FISH) probe. Following methods from Hattenrath-Lehmann *et al.* (2016), our lab is currently developing a FISH assay for *A. monilatum* cysts that could be used to quantify cysts from environmental samples (see Appendix).

Environmental data were collected in an effort to identify factors that might help explain cyst distribution and density, or that could be used in a larger effort to model bloom dynamics of *A. monilatum* in the lower Chesapeake Bay. Previous studies have found that using cyst data to forecast blooms does not always work (McGillicuddy *et al.* 2011; Gracia *et al.* 2013), however, bloom distribution can be a good predictor of cyst distribution (Hattenrath-Lehmann *et al.* 2016). The model presented in this study described approximately 78% of the variation in cyst density based on sampling year, sediment type, and salinity. Sampling year likely represents unmeasured hydrodynamic processes that occurred during the previous year's bloom while *A. monilatum* was encysting and sinking to the sediments, among other things, this could include wind direction and speed or prevailing current patterns. Depth was not included in the model as it was confounded with sediment type, with fine sediments increasing with depth.

Shallower sites are more likely to have coarse sediments due to high energy wave action, tidal flow, and currents. Generally, as salinity increased, depth increased, as more saline waters were further out towards the mainstem of the Bay. In effect, salinity and sediment type revealed a lot about the site location where cyst density was measured. Again, salinity and sediment type may represent areas that experience certain hydrodynamic processes that were not directly measured, but that help to explain the way the particles (like cysts) moved and settled throughout the sampling region. Future cyst surveys should carefully consider how they stratify sampling across depth, sediment type, and salinity. Factors such as average surface water temperature in August (peak *A. monilatum* bloom season) in the previous year may help to predict cyst distribution. Having a better understanding of which environmental parameters seem to describe cyst distribution, we can make informed decisions on how to structure our sampling design to make it the most effective for our research question. Further determination of which environmental parameters should be recorded and included in the model could improve accuracy and help create a model that could be applied to other years or to nearby locations in the Chesapeake.

Alexandrium monilatum is not only established in the Chesapeake Bay as a recurring bloom-forming species (Marshall and Egerton 2009), but this study showed that it is also established in cyst-form in the bottom sediments of the York River region. High cyst densities were prevalent across the study area in the York River region over three consecutive years (2014-2016). This provides new perspective on the extent of this HAB species' distribution, potential impact, and range, and how cyst densities in the region may change from year to year. This was the first *A. monilatum*-specific study to use

qPCR to detect and quantify cysts in the Chesapeake, identifying areas with dense cyst concentrations that could help fuel future blooms. Future studies on *A. monilatum* cysts in the Chesapeake Bay should investigate seasonal timing and environmental cues for encystment and excystment, viability of cysts in the oxic sediment layers, hydrodynamic processes which influence bloom and cyst distribution, and should focus on expanding the range of sediment sampling to delineate the extent of the cyst distribution for this species in the Bay. With the range of HAB species increasing worldwide (as reviewed in: Landsberg 2002; Heisler *et al.* 2008), it is important that we continue to document the current and changing extent of our local HAB species, improving our understanding of HAB ecological dynamics so that we may manage for their current and future impacts.

LITERATURE CITED

Anderson DM, Fukuyo Y, Matsuoka K. 1991. Cyst methodologies. In: Manual on Harmful Marine Microalgae. p. 165–189.

Anderson DM, Keafer BA. 1985. Dinoflagellate cyst dynamics in coastal and estuarine waters. In: Proceedings of the Third International Conference on Toxic Dinoflagellates, St. Andrews, New Brunswick, Canada, June 8-12, 1985. p. 219–224.

Anderson DM, Stock CA, Keafer BA, Nelson AB, Thompson B, McGillicuddy, Jr. DJ, Keller M, Matrai PA, Martin JL. 2005. *Alexandrium fundyense* cyst dynamics in the Gulf of Maine. *Deep Sea Res Part II Top Stud Oceanogr,* 52:2522–2542.

Connell C, Cross J. 1950. Mass mortality of fish associated with the protozoan *Gonyaulax* in the Gulf of Mexico. *Science*, 112:359–363.

Dauer DM, Marshall HG, Donat JR, Lane MF, Doughten SC, Hoffman FA, Kurada R. 2010. Current status and long-term trends in water quality and living resources in the Virginia tributaries and Chesapeake Bay mainstem from 1985 through 2009. Final report submitted to Chesapeake Bay Program.

Dellapenna TM, Kuehl SA, Schaffner LC. 2003. Ephemeral deposition, seabed mixing and fine-scale strata formation in the York River estuary, Chesapeake Bay. *Estuar Coast Shelf Sci,* 58:621–643.

Erdner DL, Percy L, Keafer BA, Lewis J, Anderson DM. 2010. A quantitative real-time PCR assay for the identification and enumeration of *Alexandrium* cysts in marine sediments. *Deep Sea Res Part II Top Stud Oceanogr,* 57:279–287.

Gracia S, Roy S, Starr M. 2013. Spatial distribution and viability of *Alexandrium tamarense* resting cysts in surface sediments from the St. Lawrence Estuary, Eastern Canada. *Estuar Coast Shelf Sci,* 121-122:20–32.

Harding JM, Mann R, Moeller P, Hsia MS, Road FJ, Carolina S. 2009. Mortality of the veined rapa whelk, *Rapana venosa*, in relation to a bloom of *Alexandrium monilatum* in the York River, United States. *J Shellfish Res*, 28(2):363-367.

Hattenrath-Lehmann TK, Zhen Y, Wallace RB, Tang YZ, Gobler CJ. 2016. Mapping the distribution of cysts from the toxic dinoflagellate *Cochlodinium polykrikoides* in bloom-prone estuaries by a novel fluorescence *in situ* hybridization assay. *Appl Environ Microbiol,* 82:1114–1125.

Heisler J, Glibert PM, Burkholder JM, Anderson DM, Cochlan W, Dennison WC, Dortch Q, Gobler CJ, Heil CA, Humphries E, *et al*. 2008. Eutrophication and harmful algal blooms: A scientific consensus. *Harmful Algae,* 8:3–13.

Howell JF. 1953. *Gonyaulax monilata*, sp. nov., the causative dinoflagellate of a red tide on the East coast of Florida in August-September, 1951. *Trans Am Microsc Soc,* 72:153–156.

Hsia MH, Morton SL, Smith LL, Beauchesne KR, Huncik KM, Moeller PDR. 2006. Production of goniodomin A by the planktonic, chain-forming dinoflagellate *Alexandrium monilatum* (Howell) Balech isolated from the Gulf Coast of the United States. *Harmful Algae*, 5:290-299.

Lacasse O, Rochon A, Roy S. 2013. High cyst concentrations of the potentially toxic dinoflagellate *Alexandrium tamarense* species complex in Bedford Basin, Halifax, Nova Scotia, Canada. *Mar Pollut Bull,* 66:230–3.

Landsberg JH. 2002. The effects of harmful algal blooms on aquatic organisms. *Rev Fish Sci,* 10:113–390.

MacKiernan G. 1968. Seasonal distribution of dinoflagellates in the lower York River, Virginia [Thesis]. College of William & Mary. 104 p.

Marshall HG, Egerton TA. 2009. Phytoplankton blooms: their occurrence and composition within Virginia's tidal tributaries. *Va J Sci*, 60(3):149–164.

Marshall HG, Egerton TA. 2013. Assessing seasonal relationships between chlorophyll *a* concentrations to phytoplankton composition, biomass, and abundance, emphasizing the bloom producing algae (HAB and others) within the James, Elizabeth, and Lafayette rivers in Virginia. Final report submitted to Virginia Department of Environmental Quality.

McGillicuddy, Jr. DJ, Townsend DW, He R, Keafer BA, Kleindinst JL, Li Y, Manning JP, Mountain DG, Thomas MA, Anderson DM. 2011. Suppression of the 2010 *Alexandrium fundyense* bloom by changes in physical, biological, and chemical properties of the Gulf of Maine. *Limnol Oceanogr,* 56:2411–2426.

McGillicuddy, Jr. DJ, Brosnahan ML, Couture DA, He R, Keafer BA, Manning JP, Martin JL, Pilskaln CH, Townsend DW, Anderson DM. 2014. A red tide of *Alexandrium fundyense* in the Gulf of Maine. *Deep Sea Res Part II Top Stud Oceanogr,* 103:174–184.

Owen KC, Norris DR. 1982. Benthic resting cysts of *Gonyaulax monilata* Howell and their relationship to red tides in the Indian River, Florida. *Fla Sci,* 45:227–233.

Perry HM, Stuck KC, Howse HD. 1979. First record of a bloom of *Gonyaulax monilata* in coastal waters of Mississippi. *Gulf Res Rep,* 6:313–316.

Reece KS. 2007-2014. Enhanced surveillance of risk factors and health effects related to harmful algal blooms. Annual reports submitted to Virginia Department of Health.

Rogers JE, Leblond JD, Moncreiff CA. 2006. Phylogenetic relationship of *Alexandrium monilatum* (Dinophyceae) to other *Alexandrium* species based on 18S ribosomal RNA gene sequences. *Harmful Algae,* 5:275–280.

RStudio Team. 2015. RStudio: Integrated Development for R. RStudio, Inc., Boston, MA <http://www.rstudio.com/>.

Schlee J. 1973. Atlantic Continental Shelf and Slope of the United States sediment texture of the northeastern part: U.S. Geological Survey Professional Paper 529-L, 64 p.

Shepard FP. 1954. Nomenclature based on sand-silt-clay ratios. *J Sediment Petrol*, 24: 151-158.

Shumway SE. 1990. A review of the effects of algal blooms on shellfish and aquaculture. *J World Aquac Soc*, 21(2):65-104.

Tobin ED, Horner RA. 2011. Germination characteristics of *Alexandrium catenella* cysts from surface sediments in Quartermaster Harbor, Puget Sound, Washington, USA. *Harmful Algae,* 10:216–223.

Triki HZ, Daly-Yahia OK, Malouche D, Komiha Y, Deidun A, Brahim M, Laabir M. 2014. Distribution of resting cysts of the potentially toxic dinoflagellate *Alexandrium pseudogonyaulax* in recently-deposited sediment within Bizerte Lagoon (Mediterranean coast, Tunisia). *Mar Pollut Bull,* 84:172–81.

Tyler MA, Coats DW, Anderson DM. 1982. Encystment in a dynamic environment: deposition of dinoflagellate cysts by a frontal convergence. *Mar Ecol Prog Ser,* 7:163–178.

Van Hauwaert T. 2016. Recent dinoflagellate cysts from the Chesapeake estuary (Maryland and Virginia, U.S.A.): taxonomy and ecological preferences [Thesis]. Ghent University. 97 p.

[VA DEQ] Virginia Department of Environmental Quality. 2014. Quality assurance project plan (QAPP) for James River chlorophyll-*a* study. Special Study #14098.

Walker LM, Steidinger KA. 1979. Sexual reproduction in the toxic dinoflagellate *Gonyaulax monilata. J Phycol,* 15:312–315.

Wardle WJ, Ray SM, Aldrich AS. 1975. Mortality of marine organisms associated with offshore summer blooms of the toxic dinoflagellate *Gonyaulax monilata* Howell at Galveston, Texas. In: LoCicero VR, editor. Proceedings of the First International Conference on Toxic Dinoflagellate Blooms. Wakefield (MA): Science and Technology Foundation. p. 257-263.

Wentworth CK. 1922. A scale of grade and class terms for clastic sediments. *J Geol,* 30(5):377-392.

White AW, Lewis CM. 1982. Resting cysts of the toxic, red tide dinoflagellate *Gonyaulax excavata* in Bay of Fundy sediments. *Can J Fish Aquat Sci,* 39:1185–1194.

Yamaguchi M, Itakura S, Imai I, Ishida Y. 1995. A rapid and precise technique for enumeration of resting cysts of *Alexandrium* spp. (Dinophyceae) in natural sediments. *Phycologia,* 34:207–214.

TABLE 1.1.

2014 pre-bloom sediment cyst sampling of the 5000-m grid in the York River region. Values in bold italics are below the detection limit but have been left in to facilitate calculating summary statistics. Water quality parameters were measured at the surface.

Site	Sample Date	Time	Latitude N	Longitude W	Depth (m)	Temperature (°C)	Dissolved Oxygen (mg/L)	Salinity	*A. monilatum* Cyst Density (cysts/cc)	Mean (cysts/cc)
A-1	7/17/2014	10:08	37.37176	76.44955	4.88	27.30	3.47	17.63	***402***	
A-2	7/17/2014	10:10	37.37156	76.44962	4.88	27.32	3.18	17.64	***126***	1416
A-3	7/17/2014	10:12	37.37129	76.44968	5.21	27.32	3.14	17.66	3720	
B-1	7/17/2014	9:48	37.37243	76.39303	7.50	27.40	3.28	18.00	2760	
B-2	7/17/2014	9:51	37.37231	76.39331	7.62	27.40	3.14	18.00	***45***	2833
B-3	7/17/2014	9:55	37.37201	76.39366	6.10	27.40	3.11	17.97	5694	
C-1	7/17/2014	9:27	37.37254	76.33671	0.61	26.36	3.35	17.97	5024	
C-2	7/17/2014	9:30	37.37239	76.33666	0.61	26.36	3.06	17.98	***383***	2119
C-3	7/17/2014	9:32	37.37229	76.33675	0.61	26.49	2.94	18.14	951	
D-1	7/17/2014	10:57	37.32659	76.44857	2.99	27.66	3.50	18.16	***331***	
D-2	7/17/2014	10:59	37.32649	76.44860	3.17	27.67	3.55	18.16	363	2778
D-3	7/17/2014	11:02	37.32626	76.44859	3.26	27.65	3.52	18.17	7641	
E-1	7/17/2014	10:28	37.32720	76.39226	5.82	26.97	3.78	18.31	900	
E-2	7/17/2014	10:31	37.32695	76.39253	5.73	26.93	3.81	18.30	6520	5092
E-3	7/17/2014	10:32	37.32679	76.39266	5.82	26.95	3.79	18.30	7858	
F-1	7/17/2014	9:05	37.32830	76.33626	4.63	26.53	3.29	19.18	1043	
F-2	7/17/2014	9:07	37.32808	76.33630	5.24	26.54	3.31	19.25	8329	3207
F-3	7/17/2014	9:09	37.32792	76.33630	5.49	26.55	3.33	19.28	***249***	
G-1	6/30/2014	10:22	37.28030	76.56038	12.80	27.47	3.91	14.41	***233***	
G-2	6/30/2014	10:25	37.28049	76.56058	12.92	27.36	3.87	14.59	409	415
G-3	6/30/2014	10:32	37.28086	76.56109	12.89	27.63	3.93	14.31	602	
H-1	7/17/2014	11:25	37.28284	76.33481	2.65	26.74	7.77	19.24	***425***	
H-2	7/17/2014	11:28	37.28288	76.33495	2.74	26.74	7.24	19.24	***18***	***148***
H-3	7/17/2014	11:30	37.28285	76.33523	2.77	26.72	3.96	19.27	***0***	

Site	Sample Date	Time	Latitude N	Longitude W	Depth (m)	Temperature (°C)	Dissolved Oxygen (mg/L)	Salinity	*A. monilatum* Cyst Density (cysts/cc)	Mean (cysts/cc)
I-1	7/17/2014	8:31	37.28346	76.27891	5.21	25.70	3.44	20.39	***199***	
I-2	7/17/2014	8:41	37.28272	76.27998	6.55	25.71	3.40	20.35	4735	2883
I-3	7/17/2014	8:45	37.28244	76.28040	6.83	25.70	3.43	20.35	3714	
J-1	6/30/2014	9:59	37.23581	76.50324	7.68	26.67	3.86	16.18	645	
J-2	6/30/2014	10:00	37.23589	76.50327	7.77	26.78	3.82	16.13	1862	1402
J-3	6/30/2014	10:02	37.23587	76.50287	9.51	26.73	3.82	16.15	1700	
K-1	6/27/2014	12:26	37.23650	76.44705	11.86	28.00	4.83	16.40	1871	
K-2	6/27/2014	12:31	37.23640	76.44758	12.04	27.62	4.69	16.41	1288	1432
K-3	6/27/2014	12:35	37.23626	76.44784	11.64	27.65	4.53	16.40	1138	
L-1	6/27/2014	9:45	37.23714	76.39047	11.43	27.28	4.63	16.87	4176	
L-2	6/27/2014	9:55	37.23719	76.39056	11.49	27.36	4.23	16.89	2099	2836
L-3	6/27/2014	10:00	37.23690	76.39114	11.64	27.57	4.17	16.89	2233	
M-1	7/17/2014	12:06	37.23782	76.33445	11.70	26.60	3.87	19.95	***352***	
M-2	7/17/2014	12:12	37.23800	76.33593	12.04	26.60	3.92	19.94	12717	6229
M-3	7/17/2014	12:16	37.23818	76.33688	12.16	26.63	3.91	19.94	5617	
N-1	7/17/2014	11:47	37.23828	76.27778	6.16	26.28	3.85	19.78	1234	
N-2	7/17/2014	11:52	37.23753	76.27909	6.10	26.28	3.81	19.84	***381***	788
N-3	7/17/2014	11:57	37.23697	76.28004	6.28	26.24	3.75	20.02	747	
O-1	7/22/2014	10:22	37.19162	76.38827	0.61	25.99	3.69	20.50	***353***	
O-2	7/22/2014	10:27	37.19141	76.38899	1.01	26.04	3.72	20.53	***272***	***314***
O-3	7/22/2014	10:30	37.19130	76.38924	0.70	26.09	3.68	20.52	***317***	
P-1	7/22/2014	10:50	37.19260	76.33330	1.92	26.04	3.60	20.52	***14***	
P-2	7/22/2014	10:55	37.19230	76.33337	1.65	26.04	3.68	20.54	***12***	***40***
P-3	7/22/2014	10:57	37.19219	76.33339	1.83	26.11	3.71	20.50	***93***	
Q-1	7/22/2014	11:21	37.19125	76.27608	9.20	26.05	4.01	19.69	733	
Q-2	7/22/2014	11:23	37.19081	76.27612	9.91	26.08	4.02	19.68	1672	1516
Q-3	7/22/2014	11:28	37.19043	76.27616	9.97	26.06	4.05	19.69	2142	

Site	Sample Date	Time	Latitude N	Longitude W	Depth (m)	Temperature (°C)	Dissolved Oxygen (mg/L)	Salinity	*A. monilatum* Cyst Density (cysts/cc)	Mean (cysts/cc)
R-1	7/22/2014	11:43	37.14797	76.27660	4.36	26.23	4.21	20.27	***201***	
R-2	7/22/2014	11:56	37.14828	76.27616	4.63	26.31	4.11	20.22	1177	463
R-3	7/22/2014	11:58	37.14796	76.27641	4.51	26.31	4.11	20.23	***12***	
S-1	7/22/2014	12:41	37.10253	76.33219	2.87	26.45	3.59	20.34	1755	
S-2	7/22/2014	12:44	37.10262	76.33261	2.29	26.48	3.52	20.35	6080	3491
S-3	7/22/2014	12:45	37.10274	76.33305	2.59	26.50	3.54	20.37	2637	
T-1	7/22/2014	12:23	37.10305	76.27559	2.53	25.92	3.49	20.74	***141***	
T-2	7/22/2014	12:24	37.10295	76.27577	2.44	25.94	3.48	20.74	663	***311***
T-3	7/22/2014	12:26	37.10290	76.27586	2.32	25.94	3.49	20.74	***130***	

	Depth (m)	Temperature (°C)	Dissolved Oxygen (mg/L)	Salinity	*A. monilatum* Cyst Density (cysts/cc)
Minimum	0.61	25.70	2.94	14.31	0
Maximum	12.92	28.00	7.77	20.74	12717
Mean	6.01	26.69	3.85	18.74	1986
Standard Deviation	3.85	0.62	0.79	1.73	2629

TABLE 1.2.

2014 pre-bloom sediment sampling from the 500-m grid in the lower York River. Values in bold italics are below the detection limit but have been left in to facilitate calculating summary statistics. Water quality parameters were measured at the surface.

Site	Sample Date	Time	Latitude N	Longitude W	Depth (m)	Temperature (°C)	Dissolved Oxygen (mg/L)	Salinity	*A. monilatum* Density (cysts/cc)	Mean (cysts/cc)
12A	6/27/2014	12:57	37.25023	76.44716	2.90	28.12	4.55	16.85	2905	3156
12B	6/27/2014	13:04	37.25016	76.44140	2.80	28.23	4.40	16.99	2686	
12C	6/27/2014	12:38	37.24556	76.44688	4.33	27.80	4.70	16.68	3192	
12D	6/27/2014	13:13	37.24532	76.44144	3.14	27.98	4.65	16.72	3841	
16A	6/27/2014	10:37	37.25039	76.42469	1.68	27.50	5.11	16.85	2964	3062
16B	6/27/2014	10:44	37.25019	76.41871	5.97	27.28	5.09	16.69	3878	
16C	6/27/2014	10:29	37.24571	76.42466	4.08	27.50	5.74	16.56	1352	
16D	6/27/2014	10:19	37.24586	76.41893	5.85	27.59	4.52	16.83	4057	
22A	6/30/2014	9:36	37.24517	76.47550	2.59	26.72	3.75	17.24	1898	1871
22B	6/30/2014	9:30	37.24538	76.46961	2.80	26.58	3.79	17.28	1708	
22C	6/30/2014	9:44	37.24047	76.47529	7.71	26.79	3.79	17.18	865	
22D	6/30/2014	9:51	37.24084	76.46950	8.14	26.90	3.69	17.13	3013	
25A	6/30/2014	9:17	37.24544	76.45847	2.07	26.81	3.64	17.33	***339***	1381
25B	6/30/2014	9:25	37.24548	76.45261	3.51	26.94	3.90	17.22	1850	
25C	6/30/2014	9:02	37.24072	76.45872	8.53	26.76	3.08	17.19	1909	
25D	6/30/2014	8:52	37.24078	76.45271	8.47	26.56	3.60	17.14	1425	
41A	6/27/2014	11:24	37.23226	76.42995	12.89	28.20	4.74	16.38	1910	2982
41B	6/27/2014	10:55	37.23215	76.42406	12.34	26.76	5.15	16.32	2957	
41C	6/27/2014	11:11	37.22732	76.42982	7.77	28.32	4.64	16.34	2423	
41D	6/27/2014	11:03	37.22767	76.42426	4.72	27.54	4.57	16.64	4640	

Site	Sample Date	Time	Latitude N	Longitude W	Depth (m)	Temperature (°C)	Dissolved Oxygen (mg/L)	Salinity	*A. monilatum* Density (cysts/cc)	Mean (cysts/cc)
47A	6/27/2014	8:35	37.23248	76.39627	6.10	27.16	3.66	16.59	1972	2073
47B	6/27/2014	9:27	37.23270	76.39058	2.77	27.39	3.86	16.80	***263***	
47C	6/27/2014	9:05	37.22821	76.39590	2.50	27.20	3.71	16.65	5371	
47D	6/27/2014	9:18	37.22811	76.39037	1.62	27.68	3.95	17.50	687	
48A	6/27/2014	11:58	37.22731	76.46922	11.70	28.17	4.87	16.22	2072	2330
48B	6/27/2014	11:46	37.22723	76.46359	11.31	28.03	4.89	16.12	1789	
48C	6/27/2014	12:08	37.22253	76.46916	4.42	28.11	4.98	16.18	2946	
48D	6/27/2014	12:16	37.22252	76.46332	3.78	27.93	4.81	16.35	2514	

	Depth (m)	Temperature (°C)	Dissolved Oxygen (mg/L)	Salinity	*A. monilatum* Density (cysts/cc)
Minimum	1.62	26.56	3.08	16.12	263
Maximum	12.89	28.32	5.74	17.50	5371
Mean	5.59	27.45	4.35	16.78	2408
Standard Deviation	3.41	0.58	0.64	0.39	1239

TABLE 1.3.

2015 pre-bloom sediment cyst sampling of the 5000-m grid in the York River region. Values in bold italics are below the detection limit but have been left in to facilitate calculating summary statistics. Sample YR1-1 (May 19, 2015) was omitted from the dataset because the winch for the Ponar® broke after retrieving this sample, and the set of three replicate grabs could not be completed in one day. * indicate dissolved oxygen values that were converted from %DO to mg/L. ND=no data. Water quality parameters were measured at the surface.

Site	Sample Date	Time	Latitude N	Longitude W	Depth (m)	Temperature (°C)	Dissolved Oxygen (mg/L)	Salinity	*A. monilatum* Cyst Density (cysts/cc)	Mean (cysts/ cc)
A-1	5/25/2015	10:57	37.37183	76.44952	4.63	22.66	4.54	18.57	11778	
A-2	5/25/2015	11:00	37.37189	76.44936	4.63	22.68	4.66	18.57	8909	9135
A-3	5/25/2015	11:02	37.37198	76.449	4.66	22.70	4.52	18.57	6717	
B-1	5/25/2015	11:16	37.37252	76.39294	7.13	22.25	5.62	18.94	4309	
B-2	5/25/2015	11:19	37.3732	76.39256	6.80	22.21	5.02	18.94	7776	6662
B-3	5/25/2015	11:23	37.37336	76.39244	6.61	22.20	4.97	18.94	7901	
C-1	5/25/2015	11:58	37.37275	76.33701	<0.80	23.24	5.10	19.35	5348	
C-2	5/25/2015	12:00	37.37276	76.33701	<0.80	23.27	5.07	19.35	3114	3565
C-3	5/25/2015	12:02	37.37277	76.337	<0.80	23.28	5.09	19.36	2232	
D-1	5/25/2015	10:21	37.32679	76.44862	2.35	22.84	4.80	19.00	6633	
D-2	5/25/2015	10:24	37.32704	76.44801	1.89	22.86	4.64	18.99	1693	3493
D-3	5/25/2015	10:28	37.32644	76.44853	2.62	22.83	4.47	18.98	2154	
E-1	5/25/2015	9:57	37.327271	76.39204	5.33	21.84	4.98	19.15	25808	
E-2	5/25/2015	9:58	37.32781	76.39116	5.24	21.81	4.96	19.16	14092	24098
E-3	5/25/2015	10:01	37.32801	76.39079	5.24	21.80	5.12	19.10	32394	
F-1	5/25/2015	12:23	37.32826	76.33543	5.64	22.04	5.06	19.45	3792	
F-2	5/25/2015	12:25	37.32854	76.33534	5.55	22.04	5.04	19.45	7219	12972
F-3	5/25/2015	12:30	37.32777	76.33554	5.67	22.13	5.12	19.44	27904	
G-1	5/26/2015	9:51	37.27967	76.55953	12.22	22.06	*4.66	16.93	5254	
G-2	5/26/2015	9:57	37.28015	76.56053	12.89	22.10	*4.68	16.91	4846	4548
G-3	5/26/2015	10:02	37.28006	76.56051	12.16	22.02	5.69	16.97	3545	

Site	Sample Date	Time	Latitude N	Longitude W	Depth (m)	Temperature (°C)	Dissolved Oxygen (mg/L)	Salinity	*A. monilatum* Cyst Density (cysts/cc)	Mean (cysts/cc)
H-1	5/25/2015	9:25	37.28328	76.33443	1.89	21.00	5.10	19.55	***420***	***140***
H-2	5/25/2015	9:28	37.28348	76.33427	1.89	21.11	5.29	19.57	***0***	
H-3	5/25/2015	9:35	37.28302	76.33456	1.95	21.06	5.26	19.52	***0***	
I-1	5/25/2015	12:46	37.28323	76.27826	7.07	21.21	5.24	19.20	31392	17171
I-2	5/25/2015	12:50	37.28329	76.27827	7.07	21.16	5.28	19.25	13592	
I-3	5/25/2015	12:53	37.28341	76.2784	7.01	21.46	5.21	19.19	6529	
J-1	5/19/2015	12:35	37.23533	76.503	6.13	22.54	4.86	18.27	11325	8463
J-2	5/19/2015	ND	37.23541	76.50291	5.79	22.29	4.73	18.32	5109	
J-3	5/19/2015	ND	37.23501	76.50256	3.72	22.48	4.74	18.29	8955	
K-1	5/19/2015	12:04	37.23649	76.44759	12.22	22.69	5.90	18.41	9925	15264
K-2	5/19/2015	ND	37.23623	76.4466	12.62	22.76	5.74	18.62	8888	
K-3	5/19/2015	ND	37.2358	76.44556	13.26	22.70	5.45	18.43	26978	
L-1	5/19/2015	11:37	37.23713	76.39054	11.37	22.32	5.07	18.72	30283	25519
L-2	5/19/2015	ND	37.23658	76.39072	11.40	22.40	5.06	18.74	32572	
L-3	5/19/2015	ND	37.23627	76.39064	11.16	22.31	5.09	18.75	13701	
M-1	5/19/2015	10:50	37.23784	76.33398	11.95	20.93	4.68	20.05	71053	39244
M-2	5/19/2015	ND	37.2384	76.33431	11.98	20.96	4.99	20.06	9719	
M-3	5/19/2015	ND	37.23763	76.33411	12.01	20.55	4.63	20.09	36960	
N-1	5/25/2015	13:50	37.23872	76.27827	5.91	21.22	6.58	19.36	1412	892
N-2	5/25/2015	13:52	37.23881	76.27858	5.85	21.26	6.18	19.36	487	
N-3	5/25/2015	13:54	37.2389	76.27883	5.88	21.25	6.14	19.36	777	
O-1	5/26/2015	10:57	37.19264	76.38738	1.58	22.21	4.82	19.25	***0***	731
O-2	5/26/2015	11:01	37.19292	76.38729	1.71	22.18	4.88	19.29	1586	
O-3	5/26/2015	11:04	37.19313	76.38724	1.74	22.11	4.87	19.27	606	
P-1	5/26/2015	11:09	37.19286	76.33352	1.49	21.89	4.89	19.63	1400	573
P-2	5/26/2015	11:11	37.19295	76.33338	1.52	21.88	4.92	19.64	***320***	
P-3	5/26/2015	11:13	37.19302	76.33327	1.62	21.83	4.93	19.65	***0***	

Site	Sample Date	Time	Latitude N	Longitude W	Depth (m)	Temperature (°C)	Dissolved Oxygen (mg/L)	Salinity	*A. monilatum* Cyst Density (cysts/cc)	Mean (cysts/cc)
Q-1	5/26/2015	11:33	37.19328	76.27729	10.09	21.46	5.52	19.73	45583	
Q-2	5/26/2015	11:35	37.19324	76.27709	10.24	21.50	5.34	19.73	40658	59120
Q-3	5/26/2015	11:41	37.19316	76.27642	10.21	21.56	5.32	19.73	91118	
R-1	5/28/2015	9:07	37.14897	76.27594	4.57	21.85	4.48	21.15	472	
R-2	5/28/2015	9:10	37.14828	76.2762	4.39	21.78	4.46	21.20	***339***	689
R-3	5/28/2015	9:12	37.14846	76.27591	4.45	21.82	4.45	21.17	1255	
S-1	5/28/2015	10:25	37.10297	76.33184	2.47	24.37	3.77	19.18	35816	
S-2	5/28/2015	10:28	37.10317	76.33166	2.41	24.37	4.02	19.19	17479	35233
S-3	5/28/2015	10:33	37.10255	76.33147	2.56	24.38	4.05	19.23	52405	
T-1	5/28/2015	9:27	37.10316	76.27563	2.29	22.60	4.27	21.56	539	
T-2	5/28/2015	9:30	37.10321	76.27552	2.26	22.60	4.29	21.57	***110***	***216***
T-3	5/28/2015	9:33	37.10329	76.27523	2.47	22.60	4.30	21.57	***0***	
U-1	5/28/2015	9:50	37.05854	76.27437	3.29	21.76	4.57	21.93	***0***	
U-2	5/28/2015	9:54	37.05872	76.27422	3.08	21.77	4.54	21.93	***446***	***289***
U-3	5/28/2015	9:57	37.0589	76.27411	3.38	21.77	4.54	21.94	***421***	
PC1-1	5/25/2015	13:10	37.32952	76.22328	11.34	21.47	5.21	19.33	2185	
PC1-2	5/25/2015	13:13	37.32976	76.2235	11.52	21.52	5.17	19.33	936	2736
PC1-3	5/25/2015	13:17	37.32907	76.22314	11.31	21.28	5.09	19.33	5088	
YR1-2	5/26/2015	9:17	37.3242	76.6176	2.29	22.27	*4.44	15.94	2021	
YR1-3	5/26/2015	9:27	37.32468	76.61835	1.92	22.36	*4.58	15.71	812	1066
YR1-4	5/26/2015	9:30	37.32459	76.61762	1.89	22.36	*4.59	15.71	***365***	

	Depth (m)	Temperature (°C)	Dissolved Oxygen (mg/L)	Salinity	*A. monilatum* Cyst Density (cysts/cc)
Minimum	1.49	20.55	3.77	15.71	0
Maximum	13.26	24.38	6.58	21.94	91118
Mean	6.02	22.12	4.95	19.25	11818
Standard Deviation	3.87	0.78	0.50	1.28	17627

TABLE 1.4.

2016 pre-bloom sediment cyst sampling of select 5000-m grid sites in the York River region. Values in bold italics are below the detection limit but have been left in to facilitate calculating summary statistics. * indicate dissolved oxygen values that were converted from %DO to mg/L. ND=no data. Water quality parameters were measured at the surface.

Site	Sample Date	Time	Latitude N	Longitude W	Depth (m)	Temperature (˚C)	Dissolved Oxygen (mg/L)	Salinity	Dry *A. monilatum* Cyst Density (cysts/cc)	Wet *A. monilatum* Cyst Density (cysts/cc)	Dry Mean (cysts/ cc)	Wet Mean (cysts/cc)
C-1	5/25/2016	10:23	37.37302	76.33624	0.52	21.43	7.35	16.96	11794	5075		
C-2	5/25/2016	10:26	37.37306	76.33632	0.52	21.44	7.28	16.98	14556	4825	10086	3737
C-3	5/25/2016	10:29	37.37318	76.33629	0.52	21.51	7.29	16.96	3910	1310		
E-1	5/25/2016	9:59	37.32718	76.39330	5.79	20.33	5.87	17.27	12803	15567		
E-2	5/25/2016	10:02	37.32708	76.39333	5.79	20.37	5.87	17.26	18580	13448	16016	15909
E-3	5/25/2016	10:06	37.32707	76.39329	5.79	20.49	5.80	17.25	16665	18714		
G-1	5/19/2016	11:46	37.27979	76.56131	11.58	18.44	7.43	14.94	26544	26504		
G-2	5/19/2016	11:59	37.28019	76.56040	12.19	18.52	7.19	14.60	25024	29508	25750	29906
G-3	5/19/2016	12:02	37.27908	76.56012	10.67	18.59	7.29	14.59	25682	33706		
H-1	5/25/2016	9:38	37.28261	76.33531	2.50	20.60	6.23	18.35	***0***	***0***		
H-2	5/25/2016	9:40	37.28268	76.33546	2.47	20.51	6.16	18.35	1636	1220	545	1515
H-3	5/25/2016	9:42	37.28281	76.33552	2.50	20.56	6.11	18.35	***0***	3325		
L-1	5/19/2016	10:53	37.23741	76.39137	10.97	17.92	3.91	16.82	62673	63417		
L-2	5/19/2016	11:00	37.23705	76.39211	10.67	17.93	4.94	16.80	55279	39208	55881	43073
L-3	5/19/2016	11:05	37.23687	76.39268	10.67	17.97	5.27	16.79	49691	26593		
M-1	5/25/2016	9:12	37.23775	76.33429	11.28	18.92	6.09	16.43	23006	24791		
M-2	5/25/2016	9:18	37.23740	76.33352	11.28	18.94	5.77	16.44	52855	48063	37003	37228
M-3	5/25/2016	9:25	37.23773	76.33422	11.28	18.95	5.60	16.46	35148	38832		
P-1	5/19/2016	10:02	37.19238	76.33263	1.86	17.97	*0.97	17.35	6707	2774		
P-2	5/19/2016	10:19	37.19183	76.33467	ND	18.04	1.02	17.35	3691	1394	3466	2204
P-3	5/19/2016	10:25	37.19157	76.33494	1.98	18.04	0.99	17.35	***0***	2443		

Site	Sample Date	Time	Latitude N	Longitude W	Depth (m)	Temperature (˚C)	Dissolved Oxygen (mg/L)	Salinity	Dry *A. monilatum* Cyst Density (cysts/cc)	Wet *A. monilatum* Cyst Density (cysts/cc)	Dry Mean (cysts/ cc)	Wet Mean (cysts/cc)
Q-1	6/1/2016	8:47	37.19292	76.27684	10.58	21.88	0.34	19.21	43634	35931		
Q-2	6/1/2016	8:54	37.19324	76.27721	10.64	21.83	0.83	19.10	45808	30739	43236	38172
Q-3	6/1/2016	9:02	37.19316	76.27735	10.61	21.92	2.48	18.83	40266	47846		
S-1	6/1/2016	9:28	37.10276	76.27557	2.59	23.22	1.65	18.01	46335	50615		
S-2	6/1/2016	9:34	37.10338	76.27549	1.98	23.32	1.84	17.99	48805	37703	47653	44507
S-3	6/1/2016	9:37	37.10266	76.27528	1.65	23.29	2.10	18.01	47820	45204		
T-1	6/1/2016	9:53	37.10241	76.33218	2.90	24.78	2.42	16.20	6748	1399		
T-2	6/1/2016	9:58	37.10239	76.33223	2.90	24.82	2.52	16.12	2110	3649	4891	1934
T-3	6/1/2016	10:02	37.10239	76.33229	2.90	26.24	2.57	16.03	5814	754		

	Depth (m)	Temperature (˚C)	Dissolved Oxygen (mg/L)	Salinity	Dry *A. monilatum* Cyst Density (cysts/cc)	Wet *A. monilatum* Cyst Density (cysts/cc)
Minimum	0.52	17.92	3.77	14.59	0	0
Maximum	12.19	26.24	6.58	19.21	62673	63417
Mean	6.12	20.63	4.95	17.11	24453	21818
Standard Deviation	4.40	2.34	0.50	1.18	20172	19070

TABLE 1.5.

2014 sediment cyst density variance within each 500-m square (n=4), and between the 500-m squares (n=7) using the average cyst density per square. The variance within a square is greater than between squares in all but two cases, obscuring potential differences between squares.

Within Square	Variance
12	251474
16	1529861
22	781166
25	528815
41	1403751
47	5361367
48	257519
Between Squares	**463328**

TABLE 1.6.

2014 sediment cyst density variance within each 5000-m site (n=3), and between 5000-m sites (n=20) using the average log cyst density per site. The variance within site was greater than between sites in 8 of 20 cases.

Site	Variance
A	0.558174
B	1.285673
C	0.321357
D	0.601871
E	0.271965
F	0.587488
G	0.042973
H	0.767044
I	0.586867
J	0.065116
K	0.012636
L	0.027314
M	0.666655
N	0.065586
O	0.003236
P	0.245268
Q	0.059454
R	1.008974
S	0.075681
T	0.15898
Between Sites	**0.349830**

TABLE 1.7.

Sediment grain size analysis for 2016 sediment sampling sites. % coarse= gravel+sand, % fine=silt+clay. Basic sediment type was assigned by the particle size majority. *Sediment classification from Shepard (1954) as modified by Schlee (1973).

Site	Coarse Sediments		Fine Sediments		% Coarse	% Fine	Basic Sediment Type	Sediment Classification*
	% Gravel	% Sand	% Silt	% Clay				
C	0.00	91.26	4.37	4.37	91.26	8.74	Coarse	Sand
E	0.00	1.67	56.98	41.35	1.67	98.33	Fine	Clayey silt
G	0.00	4.97	42.93	52.10	4.97	95.03	Fine	Silty clay
H	0.00	98.02	0.29	1.69	98.02	1.98	Coarse	Sand
L	0.00	9.93	49.56	40.52	9.93	90.08	Fine	Clayey silt
M	0.00	24.08	47.11	28.80	24.08	75.91	Fine	Sand silt clay
P	0.00	98.34	0.00	1.66	98.34	1.66	Coarse	Sand
Q	0.00	6.91	53.20	39.90	6.91	93.10	Fine	Clayey silt
S	0.00	11.25	53.61	35.14	11.25	88.75	Fine	Clayey silt
T	47.27	46.33	2.66	3.73	93.60	6.39	Coarse	Gravelly sediment

TABLE 1.8.

ANOVA table from multiple linear regression to predict maximum log cyst densities in the York River region of the Chesapeake Bay based on year, sediment type, and salinity (N=30). ** p<0.01, *** p<0.001. $F_{(5,24)}$=21.07, p=4.563e^{-8}, R^2=0.7758.

Variable	Degrees of Freedom	Sums of Squares	Mean Squares	F value	Pr(>F)
Year	2	5.9940	2.9970	24.2234	1.747e-6 ***
Sediment Type	1	5.6975	5.6975	46.0507	5.101e-7 ***
Salinity	1	0.1869	0.1869	1.5109	0.230913
Sediment Type : Salinity	1	1.1532	1.1532	9.3210	0.005469 **
Residuals	24	2.9693	0.1237		

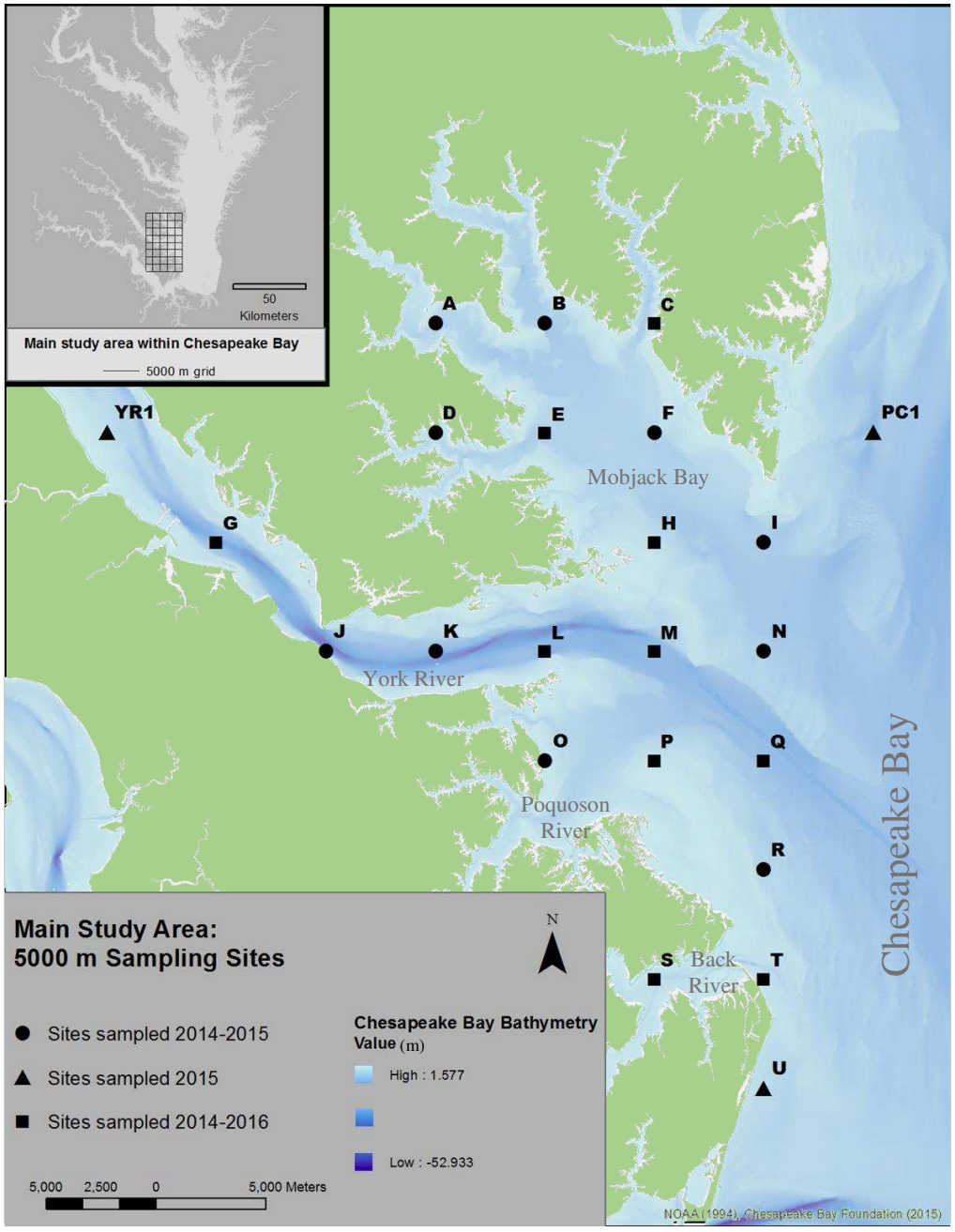

FIGURE 1.1.

Main study area with 5000-m grid sites denoted by letters. Sites that were sampled every year (2014-2016) are shown as squares, additional sites that were sampled in 2014-2015 are shown as circles, and sites that were sampled only in 2015 are shown as triangles.

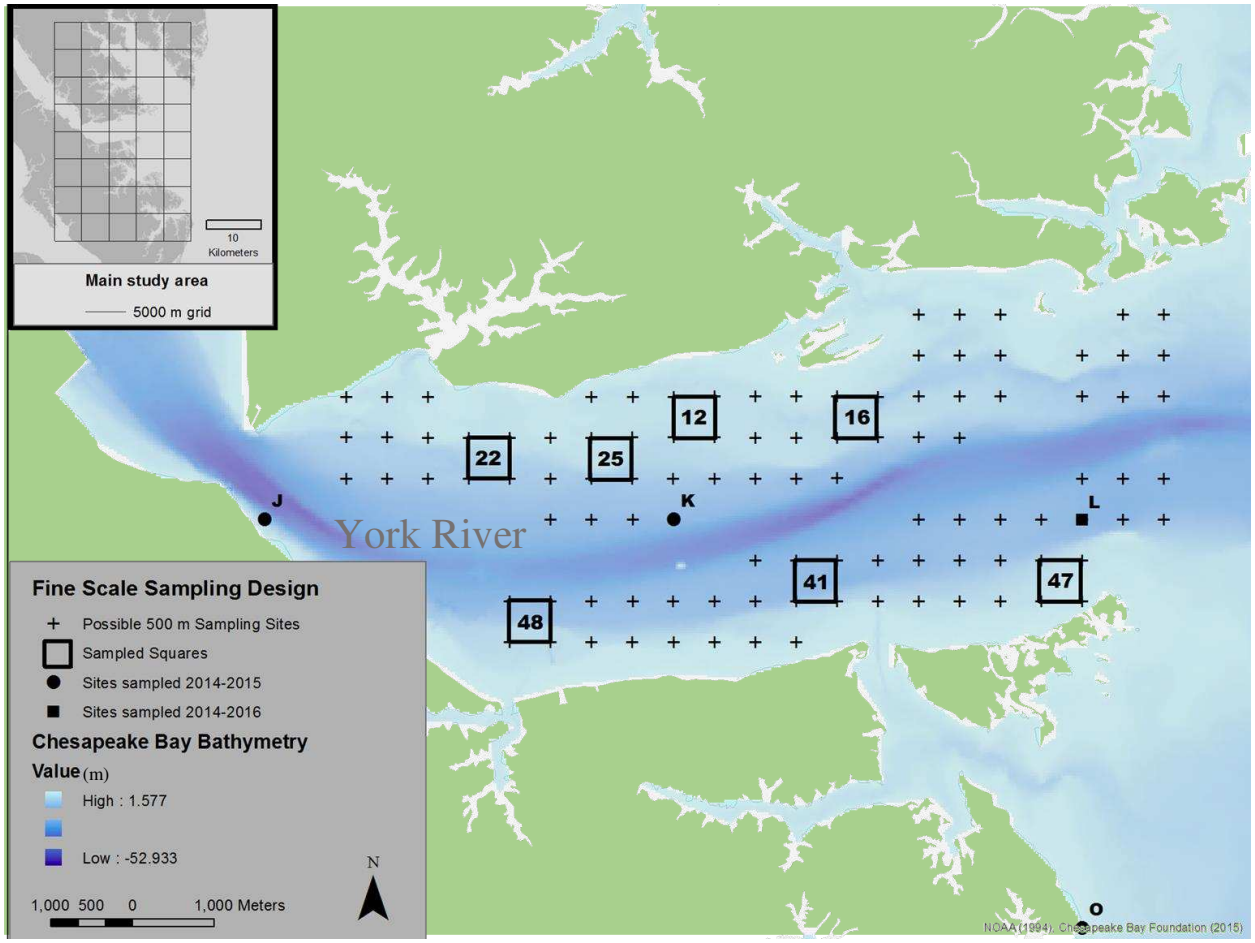

FIGURE 1.2.

Fine scale sampling of the lower York River with a 500-m grid of sites with depths between 1.2-12.2 m. Squares created by this grid were assigned numbers and seven non-overlapping squares were randomly selected for sampling in 2014. Sampled squares are outlined in bold and labeled with the number of the square.

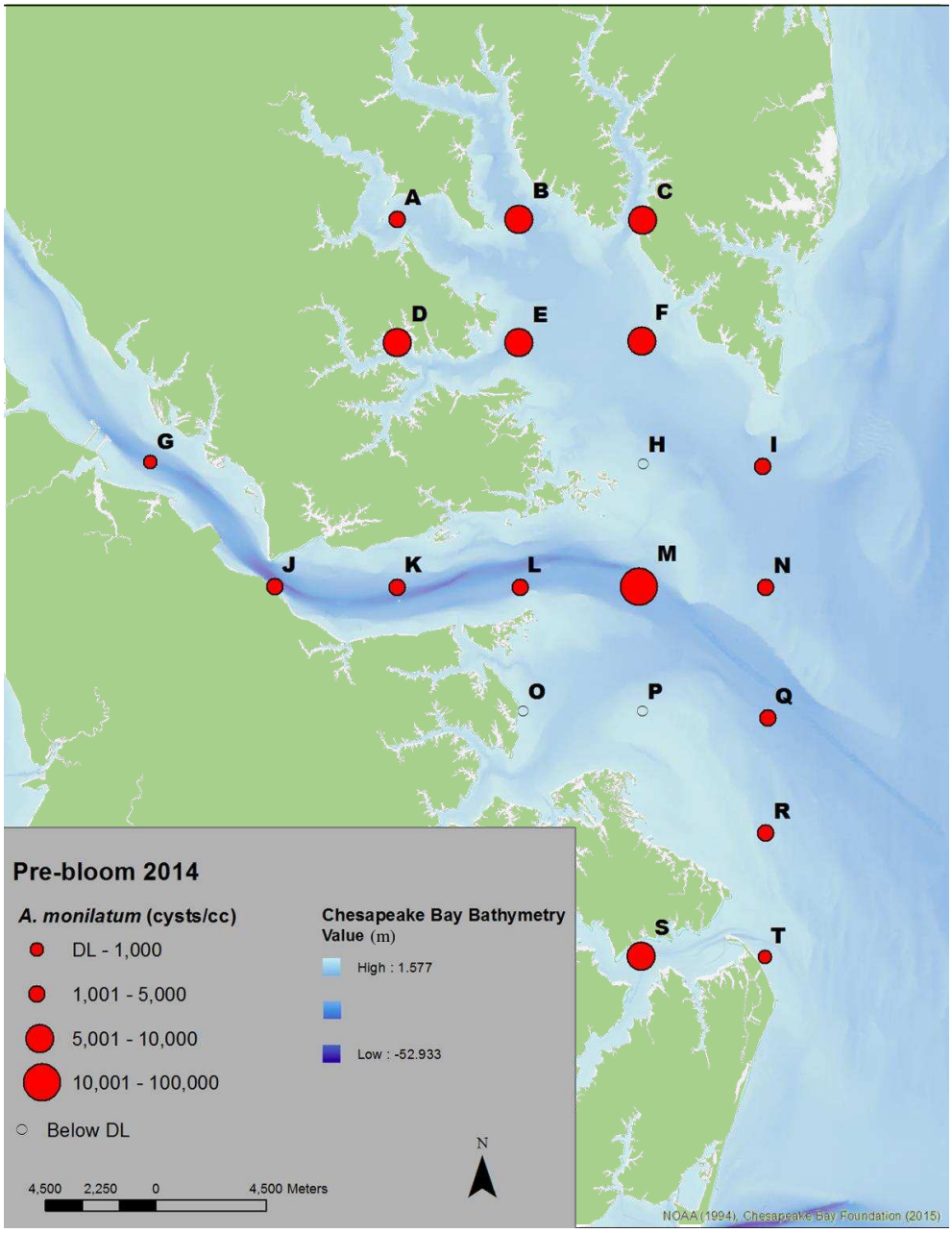

FIGURE 1.3.

Main study area with 5000-m grid sites denoted by letters. Results from the summer 2014 pre-bloom sampling season sediment grabs are shown, displaying the maximum *A. monilatum* cyst density sampled at each site. Open circles represent samples that were below the method detection limit.

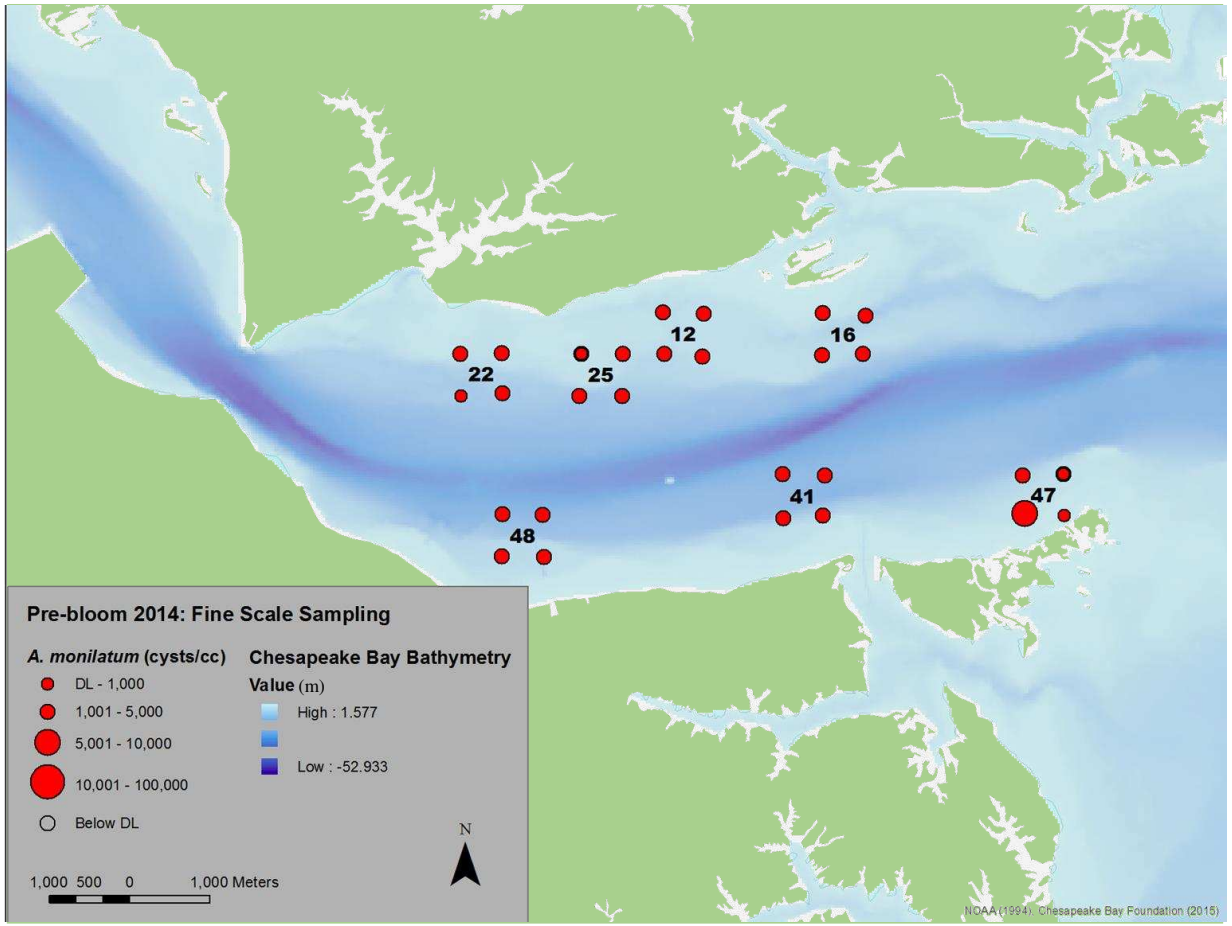

FIGURE 1.4.

Fine scale study in the lower York River with a 500-m grid of sites, results from the summer 2014 pre-bloom sampling season sediment grabs are shown. Open circles represent samples that were below the method detection limit.

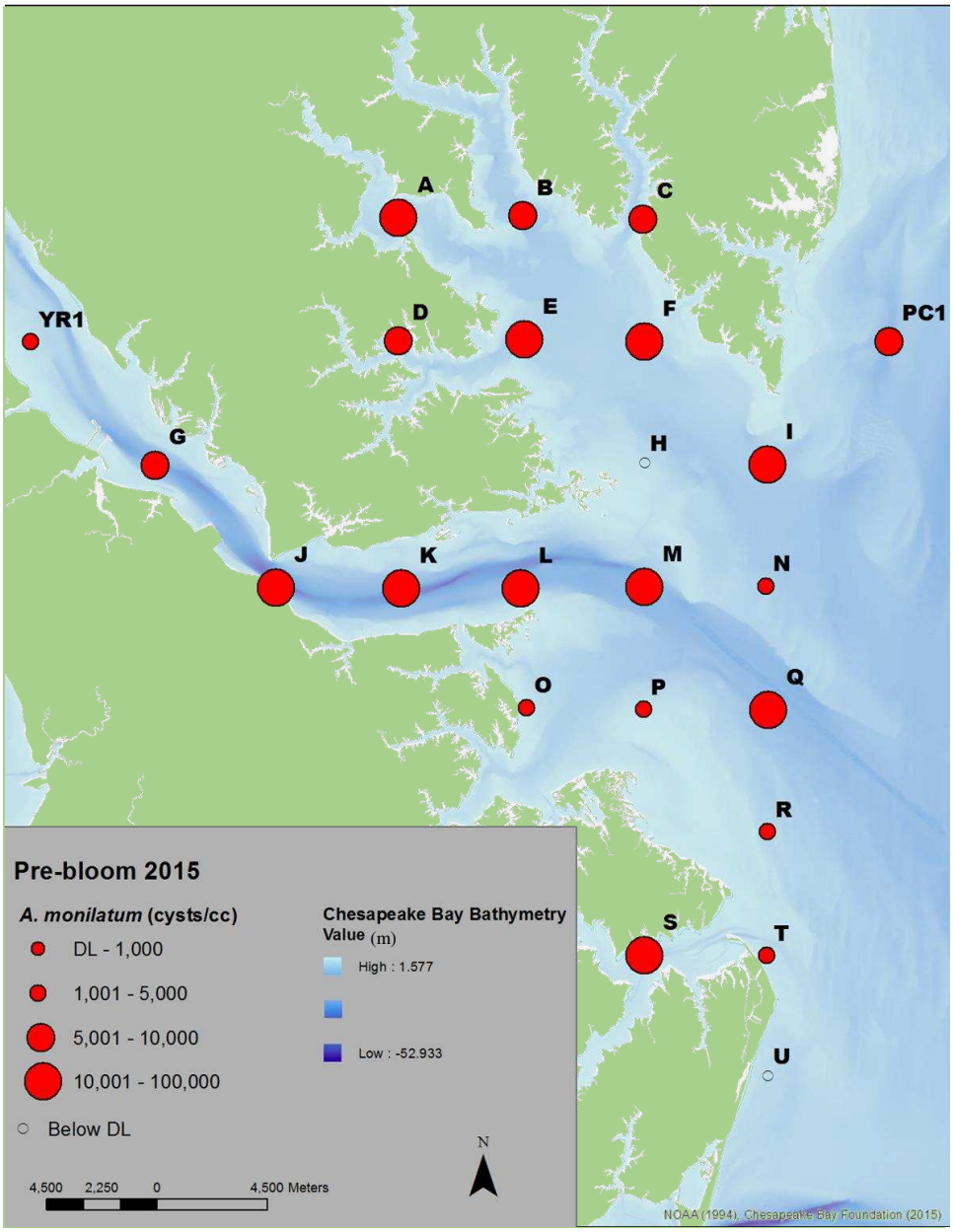

FIGURE 1.5.

Main study area with 5000-m grid sites denoted by letters. Results from the summer 2015 pre-bloom sampling season sediment grabs are shown, displaying the maximum *A. monilatum* cyst density sampled at each site. Density results transformed to "dry" method equivalent. Open circles represent samples that were below the method detection limit.

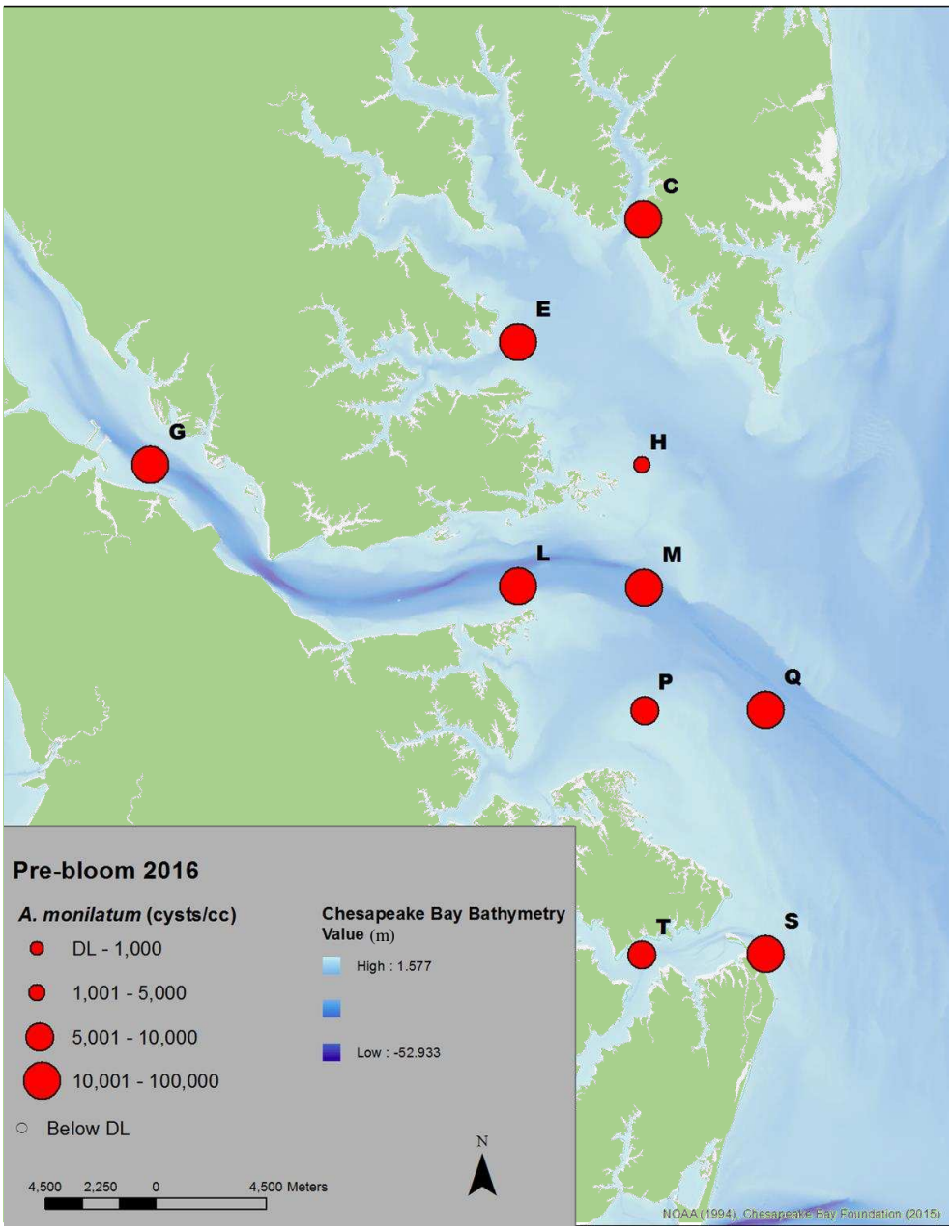

FIGURE 1.6.

Main study area with 5000-m grid sites denoted by letters. Results from the summer 2016 pre-bloom sampling season sediment grabs are shown, displaying the maximum *A. monilatum* cyst density sampled at each site. Open circles represent samples that were below the method detection limit.

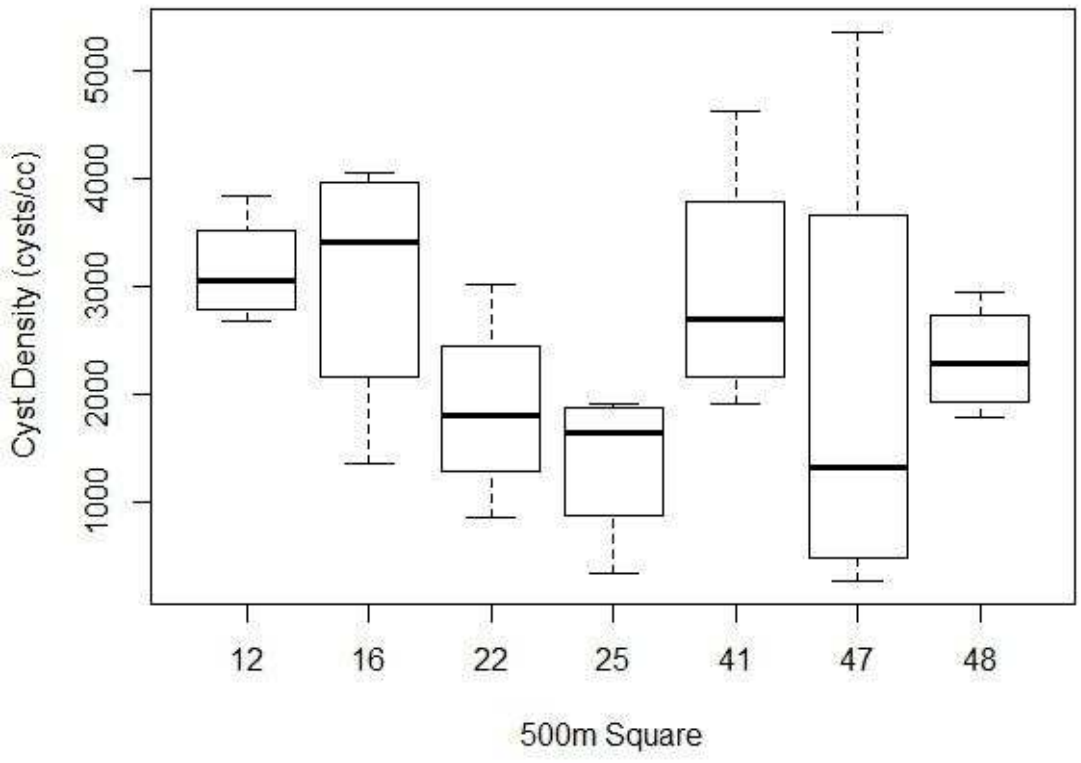

FIGURE 1.7.

Cyst density at each of the seven 500-m squares randomly selected for sampling in 2014 (see Fig. 1.2). There was no difference in cyst density between these squares (ANOVA; F=1.283, p=0.307).

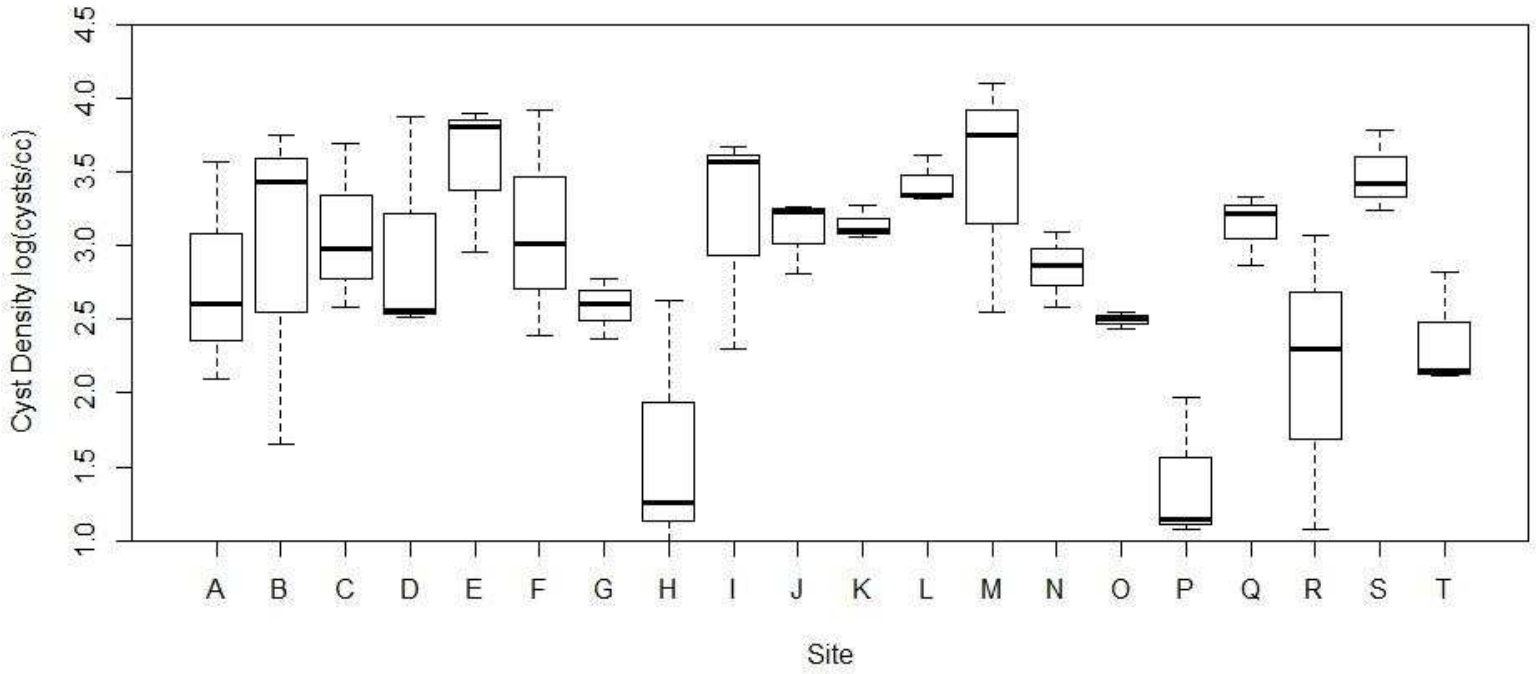

FIGURE 1.8.

2014 cyst density [$\log_{10}$ (cysts/cc)] by 5000-m site (see Fig. 1.1). There was a difference in cyst density between these sites (ANOVA; F=2.832, p=0.00276).

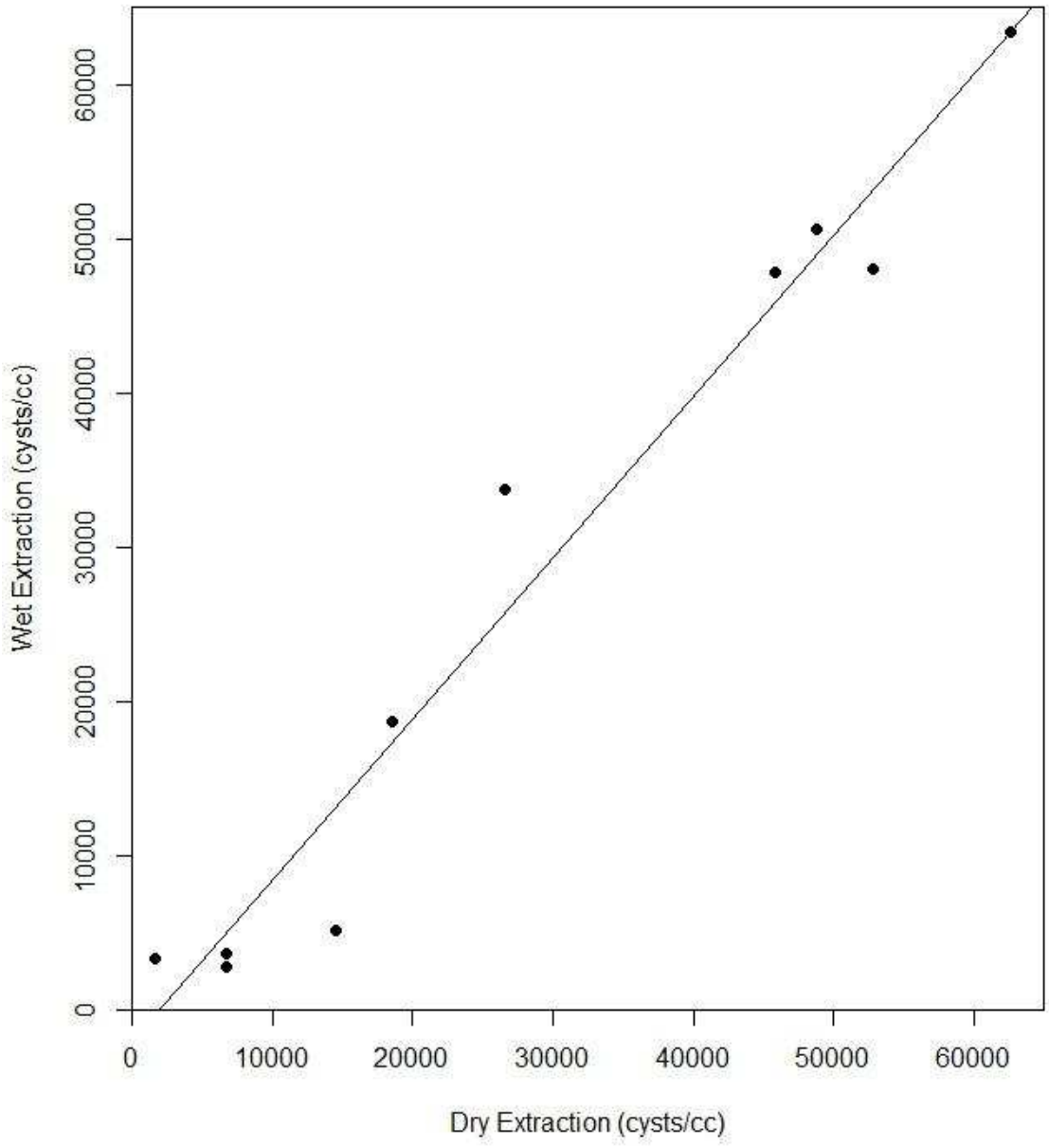

FIGURE 1.9.

Comparison of "wet" and "dry" DNA extraction methods applied in 2016 using simple linear regression, and the maximum cyst density of the three grabs at each site. $y=1.0462x-2090$, $R^2=0.9588$, $F=210.6$, $p=4.98x10^{-7}$. 95% CI of slope 0.880-1.213.

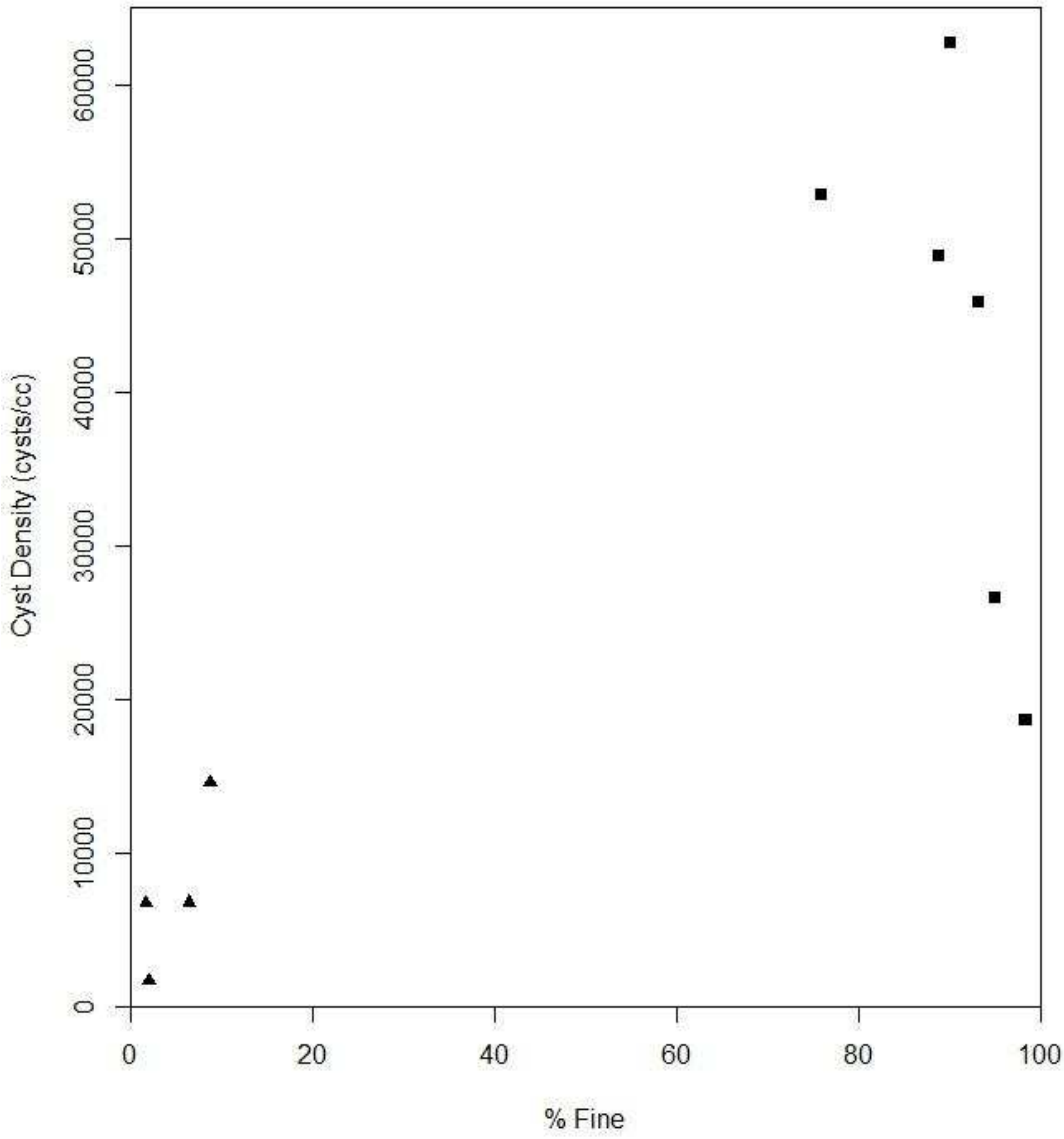

FIGURE 1.10.

Maximum cyst densities (from the “dry” extraction method) for the 2016 sites with % fine sediments. Triangles represent samples which were grouped into the “coarse” group; squares represent samples grouped into the “fine” group.

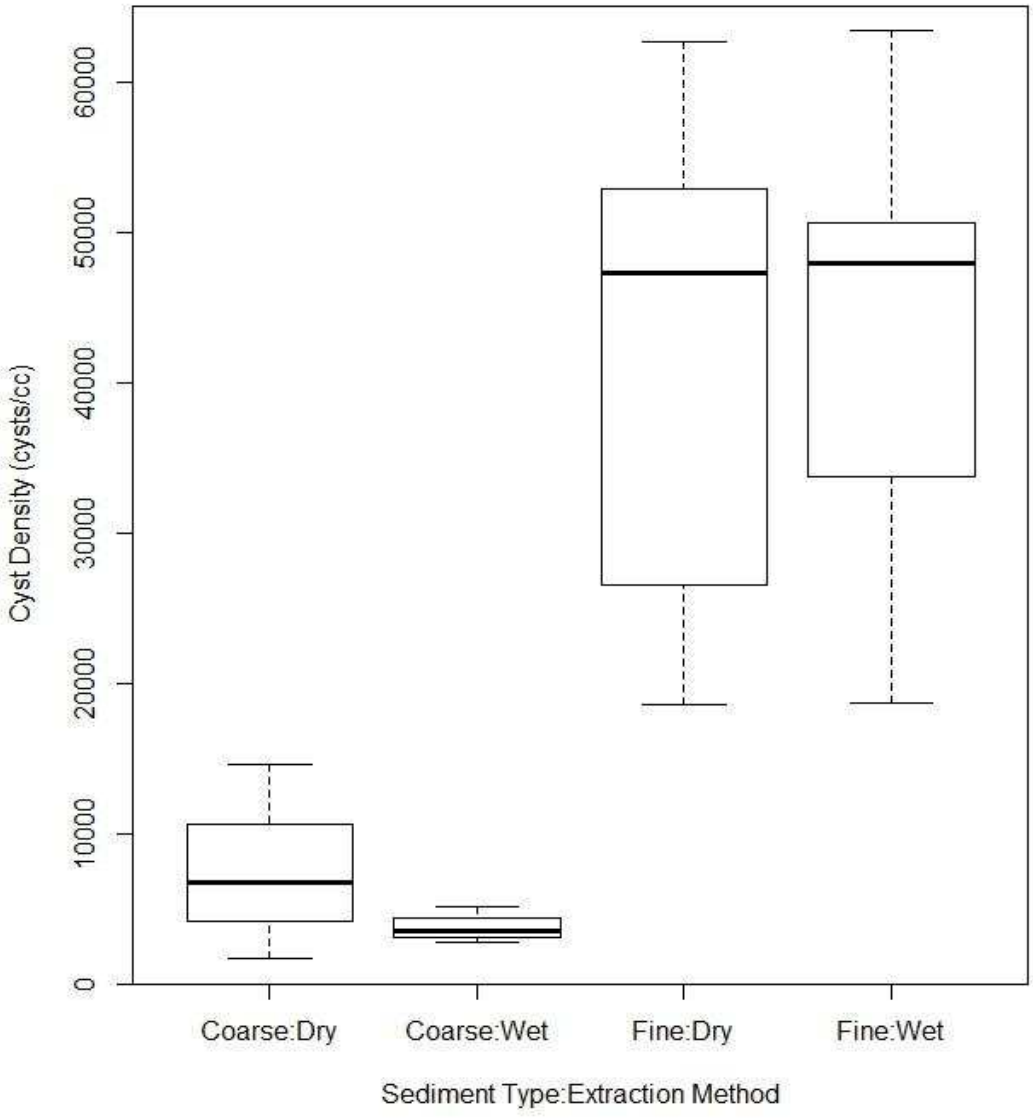

FIGURE 1.11.

Maximum cyst densities extracted by the “dry” and “wet” methods for both coarse and fine samples collected in 2016.

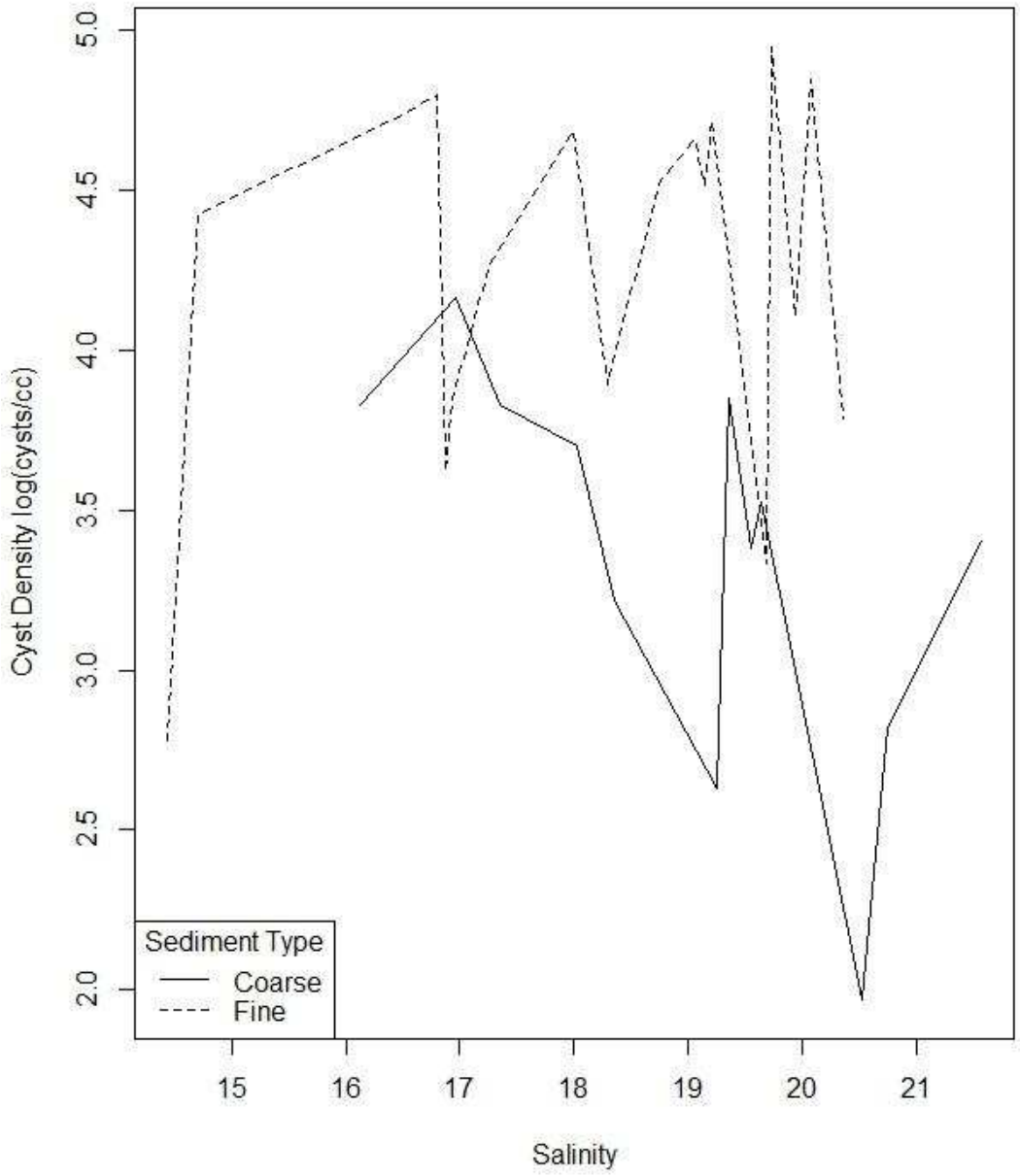

FIGURE 1.12.

Cyst density interaction plot for sediment type and salinity.

CHAPTER 2:

EXPOSURE OF *CRASSOSTREA VIRGINICA* TO *ALEXANDRIUM MONILATUM*

ABTRACT

The harmful algal bloom (HAB) species *Alexandrium monilatum* produces the lipophilic toxin "goniodomin A", and has long been associated with finfish and shellfish mortalities in the Gulf of Mexico. Recent blooms of this species in the southern Chesapeake Bay have reached record-high densities, particularly in the lower York River, raising concerns about potential impacts on fishery and aquaculture resources in the region. Laboratory HAB toxicity bioassay methods developed at the Virginia Institute of Marine Science were modified to investigate potential adverse health impacts of *A. monilatum* on adult triploid eastern oysters, *Crassostrea virginica*. Oyster behavior and mortality were monitored and routine paraffin histology was performed to analyze tissue damage. A 48-hour fed toxicity bioassay led to no mortality or tissue damage. However, histopathological analyses and cell counts suggested that *A. monilatum* cells may have been consumed by some oysters. A 96-hour unfed toxicity bioassay led to high mortality (67%) and erosion of the gill and mantle epithelial tissues in 94% of oysters exposed to live *A. monilatum* or *A. monilatum* lysate (n=33). Oysters exhibited avoidance behavior by not feeding in the presence of *A. monilatum.*

In the summer of 2015, oysters were deployed in the lower York River near Goodwin Island to assess effects of exposure to natural *A. monilatum* blooms in comparison to laboratory bioassay results. A subsample of six oysters was collected weekly before, during, and after the 2015 *A. monilatum* bloom. Oysters were processed using routine paraffin histology. There was no mortality, but minor epithelial erosion of the mantle was seen in half of the oysters collected during the *A. monilatum* bloom (n=12). Cells resembling *A. monilatum* were observed in external (gill and mantle) and internal (stomach and intestine) oyster tissues during the bloom. Results from field and laboratory studies suggest that adult *C. virginica* consume *A. monilatum* cells and that oysters can exhibit at least modest health impacts following exposure to *A. monilatum*.

INTRODUCTION

The harmful algal bloom (HAB) species *Alexandrium monilatum* has long been associated with finfish and invertebrate kills in the Gulf of Mexico (Connell and Cross 1950; Wardle *et al*. 1975). Laboratory studies using live, cultured cells suggest that *A. monilatum* produces one or more toxins that have negative impacts on shellfish (May *et al*. 2010) and finfish (Gates and Wilson 1960; Aldrich *et al*. 1967; Sievers 1969; Wilson *et al*. 1975). Early research on the toxicity of cultured *A. monilatum* suggested toxic substances were released upon cell lysis (Gates and Wilson 1960; Aldrich *et al*. 1967), with toxicity peaking a month into population decline (Aldrich *et al*. 1967). Crude cell extracts exhibited hemolytic (Bass *et al*. 1983), and purportedly neurotoxic properties in laboratory bioassays (Bass and Kuvshinoff 1983). Laboratory exposures using crude cell extracts showed toxicity to crickets, cockroaches, crayfish, frogs, and mice (Bass 1986; Bass and Kuvshinoff 1983; Clemons *et al*. 1980). More recent work found that the primary toxin produced by *A. monilatum* is the polyether macrolide "goniodomin A" (Hsia *et al*. 2006). Studies have suggested that this lipophilic toxin interferes with the structure and function of actin, disrupting the actin-myosin complex (Furukawa *et al*. 1993; Yasuda *et al*. 1998; Matsunaga *et al*. 1999), cytoskeleton (Mizuno *et al*. 1998), and other actin-mediated processes like angiogenesis–the formation of new blood vessels (Abe *et al*. 2002).

Several emerging toxin-producing HAB species, including *A. monilatum*, have been identified recently in Virginia waters (Marshall *et al*. 2008). In 2007, Chesapeake

Bay witnessed its first bloom of *A. monilatum* since the mid-1960s (MacKiernan 1968; Marshall *et al.* 2008). Following this recent re-emergence, this HAB species has bloomed in the southern Chesapeake Bay almost annually, peaking in density around late August or early September (Marshall and Egerton 2009, 2013). Both historically, and in the last few years, these blooms have appeared to originate near the mouth of the York River in Virginia, but the spatial distribution of *A. monilatum* in the region seems to be increasing (Dauer *et al.* 2010). Additionally, bloom concentrations recorded in the York River in the last few years have reached densities a full order of magnitude (>5X) higher than any *A. monilatum* blooms reported in the Gulf of Mexico (Perry *et al.* 1979). Bloom patches in the Bay quantified using quantitative real-time polymerase chain reaction (qPCR) assays have indicated densities >200,000 cells/mL (K. Reece, VIMS, unpublished data).

Research animals held in flow-through systems receiving York River water at the Virginia Institute of Marine Science (VIMS) during the 2007 *A. monilatum* bloom were inadvertently exposed to high cell densities of this toxin-producing species. This led to the mortality of an entire rapa whelk colony (n>200; *Rapana venosa;* Harding *et al.* 2009), and cownose rays (n=4; *Rhinoptera bonasus*) which were being fed oysters grown in the York River near VIMS (R. Fisher, VIMS, pers. comm.). In recent years there have been anecdotal reports of blue crab and larval and adult oyster mortalities during local *A. monilatum* blooms.

Crassostrea virginica is an iconic, ecologically and economically important molluscan species in the Chesapeake Bay. However, natural oyster populations in the Bay have been diminished by a long history of overfishing and the devastating impacts of habitat degradation and infectious disease (Newell 1988). Progress in selective breeding

for disease resistance has in recent years led to development of a lucrative oyster aquaculture industry in Virginia (valued at $16.0 million for 2015) that is currently leading East Coast oyster production (Hudson and Murray 2016).

Preliminary laboratory exposures of larval and adult *C. virginica* to live, whole cells of *A. monilatum* and lysate have resulted in significant morbidity and mortality (Reece *et al*. 2012). The ability of oysters to maintain their health during and after a HAB event has important implications for the industry as well as for Chesapeake Bay restoration efforts. Oysters of approximately market size were the focus of this study because this size class is consumed as seafood, and oyster mortalities in this size class would represent a large financial loss to the industry. With the high densities of *A. monilatum* blooms seen in the Chesapeake, and the apparent expansion of bloom range from year to year, there is a critical need to understand the impact of these blooms and their toxins.

The primary objective of this study was to determine the impact of *A. monilatum* on the health of adult *C. virginica*. This was accomplished by developing and conducting toxicity bioassays with adult oysters and laboratory-cultured *A. monilatum*, and through the completion of a field sentinel study with oysters deployed in natural *A. monilatum* bloom waters.

METHODS

HAB toxicity bioassay methods developed at VIMS (Lovko *et al*. 2003; Reece *et al*. 2012) were modified to investigate adverse health impacts of different *A. monilatum* cell density treatments on triploid *C. virginica* oysters that were near market size (market size: shell height ≥ 76 mm). Laboratory challenges of oysters were conducted using a range of different *A. monilatum* cell densities in an effort to characterize dose-responses for *A. monilatum* densities seen in the field during natural bloom events. Replicate glass vessels each containing one test oyster were assigned to a treatment to look at toxic effects based on exposure over a given time period. A number of parameters were recorded during the bioassays, including cell removal and oyster health indicators such as, feeding behavior (valves open/closed), mortality, and sub-lethal health effects identified by histopathology.

Alexandrium monilatum Culture

A single-cell clonal culture of *A. monilatum* isolated from a 2007 York River bloom was maintained in log growth phase at ~23° C with approximately 110 µmol photons m^{-2} sec^{-1} of light on a 14:10-h light:dark cycle. The growth medium used was L1.5, a derivative of L1 medium (Guillard and Morton 2003) with 1.5X $NaNO_3$, made-up in autoclaved, 0.22-µm filtered, York River water adjusted to a salinity of 20. Nutrient analyses (NH_3, NO_x, NO_2, O-PO_4) of the L1.5 medium were performed by the VIMS Analytical Services Laboratory (see below).

	NH_3	**NO_x**	**NO_2**	**O-PO_4**
L1.5 Nov15	0.0343	25.7800	0.0410	1.2000
L1.5 Jan16	0.0349	22.5300	0.0406	1.0800

48-hour Fed Toxicity Bioassay

Triploid *C. virginica* (shell height 41.5-72.1 mm, average 55.9±7.6 s.d. mm) that were grown-out in the York River (Lease 13471) were harvested and purchased from Chessie Seafood (Wicomoco, VA) on October 30, 2014. Before the experiment, oysters were kept in the York River on subtidal racks at VIMS for one week. Four days prior to start of the experiment, oysters were moved into the laboratory into tanks with artificial seawater (salinity ~22) to acclimate and were not fed prior to the experiment. Six oysters were processed just before the experiment to provide baseline oyster health data. Thirty oysters (6 per treatment) were used in the toxicity bioassay and were exposed to one of five different treatments (approximately 0-, 250-, 500-, 2500-, 5000-cells/mL) of live, cultured *A. monilatum* for 48 hours. Live *A. monilatum* from the culture described above was used at full strength for the highest density treatment and then diluted with fresh growth medium to obtain the lower treatment densities. During the trial, oysters were placed individually into replicate glass containers holding 300 mL of the assigned treatment; these containers were constantly aerated to keep cells in suspension.

Oysters were fed 64 µL of Shellfish Diet 1800® (Reed Mariculture, Campbell, CA) at 0 and 24 hours to induce filtering; this amount was determined using Reed Mariculture feeding guidelines for broodstock using "dry meat weight" estimates. "Dry meat weight" estimates were calculated using the average "total wet weight" (includes shell weight) for an oyster used in this experiment, and a "total wet weight" to "dry meat weight" ratio calculated from Table 1 in Mercado-Silva (2005).

Throughout the bioassay (at 0, 2, 6, 17.25, 25, 29.75, 41.25, 44.5, and 48.25 hours) 1-mL water samples were collected from each container for cell counts.

Alexandrium monilatum cell counts were performed by counting all of the cells in 3 10-µL subsamples, taking the average of these three counts and multiplying by 100. The change in cell density (Δ cell density=final cell density-initial cell density) for each replicate container was calculated and recorded. Oysters were checked for mortality, which was defined as a lack of response to physical stimulus (prodding with a glass Pasteur pipette), at 2.5, 4, 6.25, 7.75, 17, 19, 21, 23, 25.25, 29.5, 41, 44.5, and 47.75 hours. Qualitative observations of oyster feeding behavior (valves open/closed) and production of pseudofeces were made at these times. After the bioassay, oyster shell height (umbo to furthest point on shell) and width (widest point) were recorded, the oysters were shucked, meat wet weight was recorded, and a standard transverse section including digestive tract, digestive glands, gills, mantle, and gonad was removed for histopathological processing (see **Histopathology**).

96-hour Unfed Toxicity Bioassay

Triploid *C. virginica* (shell height 61.5-107.7 mm, average 88.6±9.8 s.d. mm) that were grown-out on the York River (Leases 17225 and 20133) were harvested and purchased from Chessie Seafood (Wicomoco, VA) on October 29, 2015 and January 11, 2016, respectively. Oysters were scrubbed to remove biofouling organisms and rinsed with deionized water prior to being moved into tanks in the laboratory with artificial seawater (salinity ~22). Oysters harvested October 29, 2015 were not fed for four days preceding the experimental trial, which began November 2, 2015. Oysters harvested January 11, 2016 were kept in the laboratory and fed Shellfish Diet 1800® (Reed Mariculture, Campbell, CA) until two days prior to the experimental trial, which began January 28, 2016. During these periods before the experimental trials, oysters were

acclimated to laboratory conditions and temperatures (23-24° C). Study size and effort involved with this 96-hour bioassay necessitated splitting the experiment into two separate trials, each lasting 96 hours. Live *A. monilatum* treatment replicates were randomized between the November 2015 and January 2016 trials; however, all lysate and live, non-toxic dinoflagellate control treatment replicates were run in the January 2016 trial.

Forty-six oysters (4-6 per treatment) were used in the toxicity bioassay and each individual oyster was assigned to one of eight different treatments: live *A. monilatum* (in approximately 0-, 1000-, 2000-, 4000-, 6300-, or 7600-cells/mL), *A. monilatum* lysate (made from culture to approximate 5000 cells/mL–see below), and a live, non-toxic dinoflagellate control. Live *A. monilatum* treatments were prepared as described above (see **48-hour Fed Toxicity Bioassay**). Lysate of *A. monilatum* was prepared through freeze-thaw (-80° C), followed by probe sonication of *A. monilatum* culture material on ice at full power (100 W) using a Misonix XL2000 Microson Ultrasonic Cell Disruptor (Misonix, Farmingdale, NY). Live, non-toxin-producing dinoflagellate *Levanderina fissa* (formerly known as *Gyrodinium uncatenum)* was used as a fed control to observe feeding behavior of the oysters at high cell density (~6300-cells/mL) to account for density-dependent changes in filtering. *Levanderina fissa* was approximately the same size as *A. monilatum* (~30-50 μm) and was grown in culture in the laboratory under the same conditions as *A. monilatum.* An additional two treatments without oysters were used to account for density-dependent growth or mortality of *A. monilatum* in the absence of a grazer, and consisted of "low-" (~1000-cells/mL) and "high-" (~7600-cells/mL) density treatments. During the trial, oysters were placed individually into replicate glass

containers holding 600 mL of the assigned treatment (non-toxic dinoflagellate treatments only received 550 mL), these containers were constantly aerated to keep cells in suspension.

Six oysters were processed just before each trial to provide baseline oyster health data (n=12). Oysters were not provided with an additional food source during the trials. Every 12 hours throughout the bioassay, oyster feeding behavior (valves open/closed) and mortality were recorded. Oysters that were found to be dead were processed at the time of observation. At 96 hours all remaining oysters were processed. Oyster processing was performed as described above (see **48-hour Fed Toxicity Bioassay**). At 0 and 96 hours (or at the time death was observed), 1 mL of water was collected from each container for a cell count using a Sedgewick-Rafter slide. The change in cell density (Δ cell density) was calculated and recorded for each replicate container.

Histopathology

Oyster tissues were fixed with Davidson's solution (Shaw and Battle 1957). Sections were cut at 6 μm and stained with hematoxylin and eosin (H&E) stain. Sections were visually scanned under a microscope at 100-400X for general health, signs of tissue damage, presence of *A. monilatum*-like cell bodies, and notable infections from common oyster parasites (e.g. *Perkinsus marinus, Haplosporidium nelsoni*). Tissue damage was generally limited to gill and mantle epithelial erosion. This type of damage was ranked using gill and mantle erosion severity estimations ranging from 0-3 depending on the severity of the erosion: 0=normal tissue, 1=disruption/erosion present focally (or just a few epithelial cells show pathology throughout section), 2=disruption/erosion present multi-focally but with normal structure still present in places, 3=disruption/erosion severe

and widespread. “Rank sum” represented the sum of the gill and mantle erosion ranks for an individual oyster.

Field Sentinel Study

Oysters were deployed in cages in the field during the 2015 HAB season to compare exposure to natural *A. monilatum* blooms, to exposure to laboratory-cultured *A. monilatum*. Triploid *C. virginica* that were grown-out on the York River (Lease 20133) were harvested and purchased from Chessie Seafood (Wicomoco, VA) on July 15, 2015. Oysters were stored at 10° C until July 17, 2015 when a cage holding 96 of these oysters was deployed just off of the bottom, adjacent to a protected oyster reef off the north side of Goodwin Island in the York River (37.22670°N 76.40939°W; Fig. 2.1). In the last few years, this area has experienced high density *A. monilatum* blooms on an almost annual basis (K. Reece, VIMS, unpublished data).

The site was sampled weekly from the last week of July through the first week of September, and then biweekly for the rest of September. During each sampling, the cage was checked for oyster mortalities, and a sub-sample of six oysters was collected for processing identical to that described in the previous sections. Concurrent 100-mL surface water grab samples were collected to determine *A. monilatum* cell densities above the cage using quantitative real-time PCR (qPCR) assays. Water samples were kept cool and in the dark until they could be filtered through 3-µm Nitex filters which were stored frozen at -20° C until DNA extraction (see below). Depth from the vessel’s depth gauge, and general surface water quality data (temperature, dissolved oxygen, salinity) using a YSI 650 MDS (YSI Inc., Yellow Springs, OH) were collected most weeks. Water depth at this site was approximately 2.4 m, and mean salinity was approximately 21.3.

On August 14, 2015 a brief study of *A. monilatum* cell density difference with depth was conducted at the field site, with sampling at 09:30, 13:30, 17:30, and 21:30. Using the YSI, measurements of temperature, pH, dissolved oxygen, and salinity were taken at the water's surface (0 m) and near the bottom (2 m). Additionally, a 100-mL water sample was collected at each time point from each depth using a Niskin bottle. The water samples were filtered and stored as described above.

DNA Extraction

Cultured *A. monilatum* (see ***Alexandrium monilatum* Culture**) were used as standard material for qPCR. Cell counts of the culture, performed using light microscopy, were used to determine a volume of culture to be filtered onto a 3-µm Nitex filter to represent a 100-mL sample with 5000 cells/mL (500,000 cells). These filters were stored at -20° C until ready for DNA extraction. DNA was extracted from frozen filters from all standards and samples according to the manufacturer's instructions for the QIAamp Fast DNA Stool Mini kit (Qiagen, Germantown, MD) with the following modifications. The frozen filters were transferred to 5-mL microcentrifuge tubes for extraction. Five times the volume of Buffer AL, proteinase K, and ethanol were used in each extraction reaction. The optional, higher heat, 95° C water bath was used to lyse cells after adding InhibitEX. After the 95° C bath and 15 s of vortexing, Buffer AL and then proteinase K were added directly into the microcentrifuge tube with the filter. The first centrifugation step was omitted. Extracted DNA was eluted twice with 100 µL of the kit's elution reagent, and eluted DNA was stored at -20° C until qPCR analysis could be performed.

An alternative "non-bloom" extraction protocol was created for samples that were expected to have low *A. monilatum* densities by using 5X the volume of sample for

extraction in the QIAamp Fast DNA Stool Mini kit protocol (Qiagen, Germantown, MD). These samples were run with standards extracted using the same "non-bloom" protocol.

Quantitative Real-time PCR

A pair of primers targeting the 18S ribosomal RNA gene were used for qPCR (Eurofins MWG Operon, Louisville, KY): a species-specific forward primer (VA DEQ 2014) was designed based on an *A. monilatum* sequence deposited in NCBI's GenBank by Rogers *et al*. in 2006 (Accession# AY883005.1), and a reverse primer designed to target Alveolates (K. Reece, VIMS, unpublished data).

Primer set used (5'-3'):	
	Am-SSU-174F CAATCAAACCTGACTCTTGTGGG
	Am-SSU-409R GCCTGCTGCCTTCCTTAGATGTGGT

Reaction volumes of 10 µL included 5.00 µL of 1.00 µM Fast SYBR® Green Master Mix (ThermoFisher Scientific, Waltham, MA), 0.90 µL at 0.90 µM of forward primer Am-SSU-174F and reverse primer Am-SSU-409R, 2.20 µL of dH_2O, and 1.00 µL of DNA template. Cycling conditions consisted of 1 cycle at 95° C for 20 s, followed by 40 cycles of 95° C for 3 s, 60° C for 30s, 75.5° C for 30 s, followed by 1 cycle of 95° C for 15 s, 60° C for 1 min, 95° C for 15 s, and 60° C for 15 s, followed by melt curve analysis. Six standards were included on each plate, made up of a 10-fold serial dilution of an extracted standard ranging from 5×10^{-3} to 5×10^{3} cells/mL. The range of detection based on the standard curve was 5-5000 cells/mL. Samples that were expected to be over 5000 cells/mL were run with 10-fold serial dilutions to ensure that at least one sample came up within the range of detection. Each reaction was run in triplicate using the 7500 Fast Real-Time PCR System (Applied Biosystems®, Foster City, CA), with the software

determining the threshold cycle values (C_t) and providing interpolated values for cells/mL for each reaction based on the standard curve. The average of the interpolated cells/mL values from the triplicate reactions were used for reporting purposes. Negative qPCR results (i.e. when no fluorescence was detected and the system recorded the sample quantity as “undetermined”) were recorded as “0 cells/mL”.

RESULTS

48-hour Fed Toxicity Bioassay

No mortality or tissue damage was seen in any of the oysters in the 48-hour fed toxicity bioassay (Table 2.1). Histological analysis of one oyster (E6) from the highest density treatment (5000-cells/mL) showed cell bodies which resembled *A. monilatum* in the stomach, intestines, and gills (Fig. 2.2).

Periodic cell counts revealed that the majority of *A. monilatum* was removed from the water column in all of the treatments within 48 hours (Fig. 2.3). The lowest cell density treatment (250-cells/mL) was depleted in 2-17.25 hours, the 500-cells/mL treatment was depleted by 5 of the 6 oysters in 2-29.75 hours, and the 2500-cells/mL treatment was depleted in 25-29.75 hours. In one of the highest density replicates, the cell density was reduced by approximately 6200 cells/mL in 48 hours; this oyster (E4) was the first oyster to deplete the *A. monilatum* in this treatment (by 29.75 hours), but cell counts then increased back up to about 250 cells/mL by the end of the 48-hour experiment. Five of the six oysters in the highest cell density treatment showed an increase in cell density in the last four hours of the experiment. The sixth oyster (E6) never fully depleted the *A. monilatum.* Feces and pseudofeces were observed in all of the oyster containers in the highest *A. monilatum* treatment (5000-cells/mL). Three of the oysters were never observed with their valves open during the experiment (A2, B5, and C4), however, all of these oysters produced feces by 48 hours.

96-hour Unfed Toxicity Bioassay

Mortality and tissue damage were seen in oysters in the 96-hour unfed toxicity bioassay. Oyster mortality and behavior data involving valve opening and response to

tactile stimulation during the 96 hours are presented in Table 2.2. Overall, 22 of the 45 oysters in the experiment were dead by 96 hours. All 22 of these oysters were exposed to some form of *A. monilatum* (live cell or lysate). There was no mortality observed in either the fed or unfed control oysters (NT-6300 or AMON-0 respectively; n=12), while 67% of oysters exposed to some form of *A. monilatum* were dead by 96 hours (22 of 33). There was no obvious dose-response over regular time intervals, and over 96 hours different *A. monilatum* treatments produced 50-80% mortality (Fig. 2.4). The highest mortality (80%, n=5) was observed in the 2000-cells/mL live cell treatment, and lowest mortality (50%, n=4) in the most dense live *A. monilatum* cell treatment (7600-cells/mL); all other *A. monilatum* treatments (including the lysate) showed 67% mortality (n=6 in each treatment). *Alexandrium monilatum* lysate produced mortality at 24 hours, before any of the live *A. monilatum* treatments (Fig. 2.4). None of the oysters in the highest density live *A. monilatum* treatment (7600-cells/mL) were observed filtering before 72 hours and this was the last treatment to show mortality.

Sixteen of the oysters were never observed with their valves open during the experiment (Table 2.2). Fourteen of these oysters were exposed to algal material: two oysters received the non-toxic dinoflagellate *L. fissa,* and 12 oysters were exposed to some density of *A. monilatum* material. Eight of those 12 oysters exposed to *A. monilatum* had a decrease in cell density over the course of the experiment (i.e. negative Δ cell densities, Table 2.3). All 8 of those oysters with negative Δ cell densities showed histological signs of erosion, and 5 of the 8 were dead by 96 hours (Table 2.3). Four oysters exposed to some density of *A. monilatum* had positive Δ cell densities. Three of these showed histological signs of erosion but none of these oysters were dead by 96

hours (Table 2.3). The one oyster which was never observed with its valves open had a positive Δ cell density, showed no signs of erosion, was not dead by 96 hours, and was the heaviest oyster in the experiment, with a wet meat weight of 11.124 g (AMON-7600 OYR3).

Thirty-eight percent (17 of 45) of oysters exhibited a slowed response, or were unresponsive, to tactile stimulation at least once during the 96 hours (Table 2.2). Eleven oysters (including one unfed control) were observed at least once during the 96 hours with valves slightly open and unresponsive to prodding, these oysters were not gaping yet 73% (n=8) were dead by 96 hours. This behavior (slightly open and unresponsive) was seen in all treatments except for the non-toxic dinoflagellate and highest live *A. monilatum* density (7600-cells/mL) treatments. Eight oysters at least once during the 96 hours exhibited a slowed response when prodded, 88% of these oysters (n=7) were dead by 96 hours. This behavior (slowed response) was seen in only the *A. monilatum* lysate, and live *A. monilatum* density treatments of 4000- and 6300-cells/mL.

A few whole *A. monilatum* cells were discovered in cell counts of lysate material (22-44 cells/mL). These cells had a "fuzzy" appearance in all 6 replicates and indicated that not all cells were fully lysed during the freeze-thaw and sonication process. Cell counts from the final time point exhibited *A. monilatum* cells which appeared partly digested in four of the vessels containing oysters, all of these oysters produced excess mucus and *A. monilatum* were observed in their gills when shucked for histopathological analysis. The "low" (1000-cells/mL) density *A. monilatum* treatment without oysters had a Δ cell density of 1433±646 s.d. cells/mL (n=3). The "high" (7600-cells/mL) density *A. monilatum* treatment without oysters had a Δ cell density of 391±941 s.d. cells/mL (n=2).

Ninety-four percent (31 of 33) of oysters exposed to some form of *A. monilatum* (live cell or lysate) exhibited histopathological signs of epithelial necrosis and erosion in the gill (Fig. 2.5), mantle (Fig. 2.6), or both. However, no damage was seen in any internal tissues. The oysters which did not exhibit erosion were AMON-7600 OYR3, which was described above, and AMON-1000 OYR1. Two control oysters that were not exposed to *A. monilatum* also exhibited erosion (BLBL2 OYR4 and NT-6300 OYR4). For oysters exposed to *A. monilatum* (live cell or lysate; n=33), 79% exhibited severe gill erosion and 63% exhibited moderate mantle erosion (Fig. 2.7). Erosion rank sum is the rank of gill and mantle erosion combined, and was calculated to give a sense of total erosion damage to an oyster. Fifty-six percent of the oysters exposed to *A. monilatum* (live cell or lysate) were ranked as "5" on a 0-6 scale, indicating severe gill erosion and moderate mantle erosion (Fig. 2.7). Oysters exposed to *A. monilatum* lysate all exhibited an erosion rank of 4 or 5, and all of those oysters exhibited severe gill erosion. Oysters exposed to live *A. monilatum* at 2000-cells/mL also all exhibited an erosion rank of 4 or 5, but one of the oysters exhibited only moderate gill erosion (Fig. 2.7).

Other histopathological observations included the presence of parasitic cells and possible *A. monilatum* cells. Six oysters exhibited either *P. marinus* (dermo) or *H. nelsoni* (MSX) cells, with no obvious relation to erosion or mortality (Table 2.3). Seventy-eight percent (21 of 27) of oysters exposed to live *A. monilatum* cells exhibited cells that resembled the HAB dinoflagellate. These cells were located between the gills (20 oysters) and adjacent to the mantle external to the oyster (3 oysters; Table 2.3). All of the oysters with cells resembling *A. monilatum* in their tissues exhibited moderate to severe erosion of at least one tissue type (gill or mantle; Fig. 2.8).

Field Sentinel Study

No oyster mortality was seen in the field sentinel study. Field sentinel study site water quality data, including *A. monilatum* cell densities for each sampling event, are presented in Table 2.4. There was no *A. monilatum* in the water sample taken when the oyster cage was deployed on July 17, 2015. Over the course of the bloom season, *A. monilatum* cell densities reached up to 3374 cells/mL at this site (August 6, 2015) and were below the detection limit by August 27, 2015 (Fig. 2.9). Histopathological data showed that cases of epithelial erosion (measured on the same scale as the laboratory experiments) occurred near the peak of the bloom, and again about a month and a half later (Fig. 2.9). The presence of cells that resembled *A. monilatum* in the histopathological sections was highest during the bloom and immediately following the bloom (Fig. 2.9).

Overall, 25% of the oysters in this study exhibited histopathological signs of epithelial erosion (12 of 48). Seventy-five percent of these cases were minor focal erosion of the external epithelium of the mantle, often between the lobes of the mantle in the periostracal groove (Table 2.5). There was one case of focal erosion in the stomach epithelium in an oyster that was sampled on July 28, 2015 when the *A. monilatum* density was 25 cells/mL. There were two cases of overall moderate epithelial erosion that both occurred when the highest *A. monilatum* cell density sample was collected (August 6, 2015); one of these oysters exhibited focal erosion in both the gills and mantle, the other exhibited moderate mantle erosion.

Cells that resembled the HAB dinoflagellate *A. monilatum* in histopathological sections were found in 23 of 48 oysters (48%) either between the gills, inside the stomach

lumen, inside the intestinal lumen, and/or adjacent to the mantle external to the oyster (Table 2.5; Fig. 2.10). These cells were found in more than one location in many of the oysters. For oysters with these cells, 40% of the observations were in the stomach, 40% in the intestine, 12.5% in the gill, and 7.5% adjacent to the mantle. Fifty-seven percent of the oysters with cells resembling *A. monilatum* in their tissues exhibited no signs of epithelial erosion, however, in the oysters sampled on August 6 and 13, 2015 during the peak of the *A. monilatum* bloom, all of the oysters that exhibited epithelial erosion (n=6) also contained cells resembling *A. monilatum.*

Other histopathological observations included the presence of parasitic cells; twelve oysters exhibited either *P. marinus* (dermo) or *H. nelsoni* (MSX) cells (Table 2.5). Half of the oysters processed on August 19 and 27, 2015 exhibited *H. nelsoni* cells in the gills, and at least one oyster in each sample after those dates exhibited these cells. One oyster with *H. nelsoni* cells in the gills (out of 11) exhibited minor focal gill erosion (2W02). One oyster (8W03) collected on September 28, 2015, exhibited *P. marinus* cells in the intestinal epithelium. Overall, there was no pattern between parasite presence and erosion or mortality.

The results from the August 14, 2015 study of cell density difference with depth at the field sentinel study site are presented in Table 2.6 (Fig. 2.11). *Alexandrium monilatum* cell densities were always higher at the surface, with the highest cell density at both depths collected at 17:30 (0 m: 9126 cells/mL; 2 m: 2678 cells/mL). At 13:30, the cell densities differed by more than an order of magnitude (0 m: 3236 cells/mL; 2 m: 273 cells/mL), but the absolute difference in cell density was largest at 17:30 (6448 cells/mL difference). By 21:30, the cell density range between depths was 595-925 cells/mL.

DISCUSSION

Exposure to live cells and lysates of *A. monilatum* caused adverse behavioral and health impacts in the adult eastern oyster, *C. virginica*, ranging from delayed feeding to mortality. Laboratory and natural bloom exposures (field sentinel study) both caused negative health effects in oysters, however, severity of these impacts varied considerably between these studies.

The 48-hour toxicity bioassay did not result in mortality or tissue damage, however, concentrations of *A. monilatum* cells declined significantly over the assay period. One oyster contained cells resembling *A. monilatum* in its digestive tissues. These cells exhibited hyper-basophilic, "U"-shaped, nuclei with condensed chromosomes matching earlier descriptions of *A. monilatum* (Connell and Cross 1950). This suggests that at least some oysters were filtering and ingesting *A. monilatum*. In contrast, control treatments without oysters showed that *A. monilatum* cell densities increased over 96 hours at both low (1000-cells/mL increased to 2433±646 s.d. cells/mL) and high (7600-cells/mL increased to 7991±941 s.d. cells/mL) densities. This supports the hypothesis that the oysters were interacting with the dinoflagellates, presumably by ingesting them or incorporating them into pseudofeces. Pseudofeces are comprised of mucus and rejected food particles that are sorted by the labial palps as the oyster filters. Oysters in higher density *A. monilatum* treatments appeared to produce more pseudofeces than those in the control or lower density treatments, suggesting that some of the *A. monilatum* cells removed from the water column were rejected and incorporated into pseudofeces. The toxin-producing HAB species *Heterocapsa circularisquama* has been found to induce pseudofeces production in the short-neck clam, *Ruditapes philippinarum,* with cells of *H.*

circularisquama identified in the pseudofeces (Basti *et al.* 2011). Interestingly, there is evidence that *A. monilatum* may pass through the digestive tract of the oyster and remain viable (May *et al.* 2010), which could partly explain why cell concentrations in the highest density treatment increased towards the end of the 48 hours.

The absence of pathology and mortality in the 48-hour toxicity bioassay corroborated similar findings from studies of short-term exposure of adult *C. virginica* to *A. monilatum.* In one study, adult oysters exposed to live, laboratory-cultured *A. monilatum* (550 cells/mL) for 24 hours, suffered no mortality (May *et al.* 2010). Ray and Aldrich (1966) also performed 24-hour exposures of *C. virginica* to live, laboratory-cultured *A. monilatum* (~950 cells/mL). They found no significant decline in *A. monilatum* cell density over the 24 hours and no oyster mortality, with the majority of oysters never observed open during the duration of the exposure. Although not quantified, observations in this study indicated that many of the oysters in this bioassay exhibited avoidance by remaining closed and not feeding for the first 24 hours. Thus, my 48-hour assay and the two earlier studies suggest that exposure duration may need to be longer to ensure that oysters receive sufficient exposure to elicit quantifiable health impacts. Therefore, a longer bioassay was conducted to circumvent temporary avoidance behavior by the oysters, and to allow a long enough exposure time for any pathology or mortality due to *A. monilatum* exposure to develop.

High mortality (67%) occurred in oysters exposed to *A. monilatum* (live cell or lysate) during a subsequent 96-hour toxicity bioassay. Similar numbers of oysters across the concentration range of *A. monilatum* treatments exhibited mortality, however, the lysate treatment caused mortality more rapidly than any of the live *A. monilatum*

treatments. This could suggest that the toxin is endogenous and that cell lysis liberates toxins, making them more bioavailable to the oysters. This would corroborate early findings of Gates and Wilson (1960), who found heat- or freeze-treated *A. monilatum* cells to be more toxic to finfishes. As blooms undergo senescence, cells lyse and release endogenous toxins, in some cases causing massive fish kill events (Landsberg 2002).

It is not unusual for the first sign of pathology to be seen in the gills when bivalves are exposed to toxic dinoflagellate cultures in the laboratory (Basti *et al*. 2011, 2015b). In this study, 94% of oysters exposed to *A. monilatum* (live cell or lysate) exhibited epithelial erosion and necrosis in the gill or mantle, many showing severe gill erosion and moderate mantle erosion, especially in the lysate treatment. Gill and mantle are both tissues that are in contact with the environment, and the damage done to these tissues during these bioassays was enough to fatally compromise the overall health of these oysters. Generally, damage could only be seen under a microscope after histopathological processing. In contrast to "gill disease", a bivalve disease of unknown etiology characterized by macroscopic white and yellow "spots", perforations and indentations along the edge of the gills (Smolarz *et al*. 2006), gross gill pathology was only rarely observed in this study. However, elevated mucus production was observed in many of the oysters exposed to *A. monilatum* in the 96-hour study. Basti and colleagues (2011) hypothesized that mucus production in the gill may reduce contact between toxic algae and gill tissues. Other HAB species have also been shown to damage the gill tissues of bivalves in similar exposure experiments. Basti and colleagues (2011) showed gill pathology due to *H. circularisquama* in the short-neck clam, with major damage and mortality (>90%) within 96 hours. Reduced clearance and respiration rates preceded gill

damage that included: hypertrophy, hyperplasia, necrosis, and denuding of cilia. Additionally, damage was greater in the gill than in any of the other 8 organs evaluated in exposures of *Mytilus galloprovincialis* to *H. circularisquama* (Basti *et al.* 2015).

Extensive gill hemorrhage could lead to bivalve death (Basti *et al.* 2015). Gill tissue necrosis can interfere with food intake and respiration, leading to emaciation and weakness (Smolarz *et al.* 2006). Oyster responses to, or lack of responses to, tactile stimuli in this study may have been signs of the severe gill damage that many oysters exhibited. Notably, some oysters were slightly open and unresponsive to a tactile stimulus, as if they were incapable of full valve closure. Other oysters had their valves open, some almost gaping, but when prodded, very slowly closed their valves. Ray and Aldrich (1966) limited oyster exposures with *A. monilatum* to 24 hours because longer assays led to oysters losing the ability to close, which frequently led to death. These signs are also similar to those seen in *A. monilatum* toxin extract injection studies done with mice (Erker *et al.* 1985), cockroaches (Clemons *et al.* 1980), frogs, and crayfish (Bass and Kuvshinoff 1983). Mice exhibited sedation, ataxia, dyspnea, convulsions, and loss of reflexes prior to death (Erker *et al.* 1985). Cockroaches exhibited weakness, loss of righting ability, and paralytic extension of legs (Clemons *et al.* 1980), while frogs and crayfish exhibited a loss of coordination and reflexes (Bass and Kuvshinoff 1983). Many of the clinical signs in these studies imply paralysis or a loss of reflexes, actions that involve muscle control. These clinical signs would seem to match well with a toxin like goniodomin A, produced by *A. monilatum*, which has been shown to interfere with actin function (Furukawa *et al.* 1993; Yasuda *et al.* 1998; Matsunaga *et al.* 1999). Actin is

involved in both muscular contraction and basic cellular structure, so *A. monilatum* toxin exposure could directly and/or indirectly interfere with valve closure.

Valve state (open/closed) observations were recorded in both bioassays in the hopes that the data would reveal information about oyster feeding or avoidance behavior. Unfortunately, these data did not correlate well with cell removal data, observations of fecal production, or with the evidence of toxic effects from exposure to *A. monilatum*. This suggests that infrequent observation of valve state is not a strong predictor of oyster feeding behavior; the chances of missing when the oyster is open or feeding are very high. An alternative method that has been used to measure valve gape as a proxy for *A. monilatum* clearance rate is through the use of optical fibers (May *et al.* 2010). This method involves measuring the axial displacement of two optical fibers–a stationary emitting fiber, and a receiving fiber that is attached via a PVC arm to the top valve of the oyster–as the oyster opens and closes its valves (Frank *et al*. 2007). The downsides to this method are that the optical fibers require specialized equipment, fine calibration, and limit the number of oysters that can be assessed for valve gape at one time.

Even with valve state not being a great predictor of when an oyster was feeding, none of the oysters in the highest *A. monilatum* density treatment were observed filtering before 72 hours. None of the other treatments showed a similar, consistent response. This delay could perhaps indicate active avoidance of exposure to *A. monilatum* by the oysters. One of these oysters in particular was never observed feeding. This oyster had the highest wet meat weight of all oysters from both bioassays (>11 g) and survived the 96-hour exposure without any ill effects. This may indicate that larger oysters have enough reserves to avoid feeding for longer periods of time. If this is the case, larger (wet

meat weight) oysters may have an advantage during prolonged blooms. This result suggests that oysters may be able to exhibit avoidance behavior, staying closed or delaying feeding when *A. monilatum* is present, which corroborates findings from previous laboratory studies (Ray and Aldrich 1966; Sievers 1969; May *et al.* 2010). Other avoidance behaviors that have been reported when adult oysters were exposed to *A. monilatum* in the laboratory have included significantly reduced valve gape and clearance rate (2-hour exposures with initial *A. monilatum* densities of 550 cells/mL; May *et al.* 2010), and opening less frequently than control oysters (1.3% v. 55.2% of observations, respectively, over 24 hours; Ray and Aldrich 1966). Avoidance behavior has been recorded in other bivalve species exposed to toxin-producing HAB dinoflagellates; short-neck clams make a brief attempt at valve closure when exposed to *H. circularisquama* (Basti *et al.* 2011).

One of the goals of the toxicity bioassays was to develop a dose-response curve to identify a 48- or 96-hour median lethal dose (LD_{50}) or median effect dose (ED_{50}). Some experiments have been able to produce dose-response curves for HAB exposure to bivalves, with pathology or mortality increasing with HAB cell density and with duration of exposure (Basti *et al.* 2015). However, oyster avoidance behavior and inconsistent feeding behavior in this study prevented determination of dose-response curves. Overall, within the range of *A. monilatum* densities tested in this study, toxicity did not increase with cell density.

Results of the field sentinel study differed from those of either toxicity bioassay, revealing no mortality, with only minor tissue erosion coinciding with the peak of the early-August *A. monilatum* bloom. Epithelial erosion in field oysters occurred primarily

on the external edges of the mantle where it covers the gills, an organ that is exposed to the ambient environment while the oyster is filtering. Most of this tissue damage occurred during the peak of the bloom, suggesting that there may be a causal relationship between exposure to *A. monilatum* and tissue damage. There were however, in both the field sentinel study and the 96-hour toxicity bioassay, a few cases of epithelial erosion that may not be related to *A. monilatum* exposure.

A few field sentinel study oysters exhibited tissue erosion about 1.5 months after termination of the *A. monilatum* bloom. While it is possible that these are residual effects from the bloom, or delayed erosion due to *A. monilatum* toxin remaining in the water column (Aldrich *et al.* 1967 found toxicity peaked 6-7 weeks after the population reached its maximum density in the laboratory), it is equally likely that there is another cause for this tissue damage. Epithelial erosion is a common non-specific observation in oysters. Similarly, stomach epithelium erosion seen in one field oyster before *A. monilatum* reached bloom densities (July 28, 2015: 25 cells/mL) could have been caused by some other irritant, as no other oysters exposed in the laboratory or field showed signs of internal tissue damage. A baseline oyster from the 96-hour bioassay harvested from the York River in January, a time of year when *A. monilatum* is inactive and overwintering in the sediments, also exhibited minor signs of gill erosion. A control oyster exposed to non-toxic dinoflagellate *L. fissa* at 6300 cells/mL exhibited moderate gill and mantle epithelial erosion. It is possible that some other irritant led to this erosion, or that there was accidental cross-contamination between this treatment and an *A. monilatum* treatment. Despite these few exceptions, there does seem to be some relationship between *A. monilatum* exposure and epithelial erosion.

In the 96-hour toxicity bioassay, 78% of oysters exposed to live *A. monilatum* contained cells resembling *A. monilatum* in the gills or adjacent to the mantle, and all of these oysters exhibited moderate to severe erosion in at least one of these tissues. During the *A. monilatum* bloom in the field sentinel study (August 6 and 13, 2015), all oysters that exhibited tissue erosion had cells resembling *A. monilatum* in their tissues, but not vice versa. In contrast to the 96-hour unfed toxicity bioassay, overall, most of the field study sentinel oysters with these cells did not exhibit epithelial erosion.

Cells resembling *A. monilatum* were found in both external (gill and mantle) and internal (stomach and intestine) tissues during and after the *A. monilatum* bloom in field sentinel study oysters. This provides support to the 48-hour toxicity bioassay which suggested that oysters might consume *A. monilatum*. The brief study of *A. monilatum* cell density difference with depth at the field sentinel study site showed that *A. monilatum* cells were in fact found at the depth of the oyster cage, although in lower densities than those seen during the day at the water's surface. Absolute confirmation that the cells observed in these oyster tissues were *A. monilatum* will be tested by our laboratory using species-specific molecular tools. A fluorescent *A. monilatum*-specific DNA probe will allow testing of fluorescent *in situ* hybridization (FISH) methods in the histological sections. This will allow us to verify the presence/absence of *A. monilatum* inside of oyster tissues and to compare these observations to histopathological observations made in this study.

Other planned future work will help sort out the likely causes of tissue erosion by quantifying goniodomin A in all of the oysters from these three studies, relating toxin values back to severity of epithelial erosion, *A. monilatum* exposure density, and

mortality. Bass and Kuvshinoff (1983) stated that, "liberation of [*A. monilatum*] toxins upon [cell] death and cytolysis exposes aquatic organisms at buccal and/or respiratory surfaces where delicate and vital membrane processes could be affected and the toxin might enter the blood or body fluids". They hypothesized that these toxins could pose a risk to human and animal health through inhalation of aerosolized toxins or through ingestion of toxin-contaminated foods. *Alexandrium monilatum* toxins are harmful to mammals. Intraperitoneal (IP) injection and oral administration of goniodomin A in rats produced inflammation and necrosis in the liver and thymus (Terao *et al.* 1989), and IP injection in mice induced mortality within 24 hours (LD50 2.9 µg/g; Bass 1986). The potential for *A. monilatum* and its toxins to impact human health through natural exposure is currently unknown. Bioaccumulation of other HAB-produced toxins in shellfish during natural exposure to seasonal blooms can have serious human health impacts after consumption of HAB-toxin-contaminated seafood (Shumway 1990).While adult *C. virginica* health is negatively impacted by *A. monilatum*, it is not known whether *A. monilatum* toxin bioaccumulates in oyster tissues. If toxin quantification shows that oysters do bioaccumulate goniodomin A, studies should be performed to identify what quantities of toxin pose a risk to human health. Toxicity bioassays in which oysters that have been exposed to live *A. monilatum* are fed to higher trophic level organisms could show if toxin can be quantified, and toxic effects observed, at higher trophic levels. Alternatively, following quantification of goniodomin A in oyster tissues, bioassays using purified toxin can be performed as a proxy to test for exposure limits for human health and seafood safety.

Why did the field-deployed oysters display far fewer signs of potential health effects after exposure to *A. monilatum* than those from the 96-hr unfed toxicity bioassay? The field-deployed oysters in this study were placed in an area with fairly high tidal flushing near the mouth of the York River, so it is not entirely surprising that toxic effects were minimal at this location. A brief study at the field site performed on August 14, 2015 showed that *A. monilatum* cell density differed both over time and with depth. Surface *A. monilatum* densities were consistently higher than at 2 m, the approximate depth of the deployed oysters. Cell density differences were greatest during the daytime, but both densities peaked at 17:30, with densities at 2 m as high as 2678 cells/mL. In the laboratory studies, densities as low as 1000 cells/mL had health impacts on adult oysters. This brief study also showed that the *A. monilatum* cell density changed considerably within hours, and that at 2 m the high cell density did not persist for more than 8 hours. Observed variations in cell densities at this site could be explained by diel vertical migration of *A. monilatum,* as well as by tides, winds, and currents that could have moved the bloom throughout the day. It is likely that some combination of these effects was responsible for the variation seen in this study. This high variation in *A. monilatum* cell density over time may be beneficial to the oyster, providing opportunities to filter-feed when HAB densities are low and to use avoidance behaviors for short periods when the surrounding waters are dense with *A. monilatum.*

Generally, *A. monilatum* cell densities recorded during the field sentinel study were on the lower end of the densities tested in the laboratory bioassays. The difference in effect on oysters between the field and the 96-hour unfed toxicity bioassay may indicate inherent differences in toxicity of *A. monilatum* in the field versus in the

laboratory, or could be due to toxin accumulation in laboratory-cultured material. Toxin can accumulate over time in culture material as the population undergoes phased log growth and senescence. In the natural environment in high-energy areas with lots of flushing, toxins are likely diluted. Future field studies should select multiple *A. monilatum* bloom sites which experience different amounts of flushing, to test for differences in toxicity to adult *C. virginica*.

Variation in toxicity has been seen in other marine HAB species, such as *Prorocentrum minimum* (as reviewed in Wikfors 2005) and *Alexandrium fundyense* (Anderson *et al.* 2014). Toxicity varies throughout the population growth phase, and time of peak toxicity varies between HAB species (Aldrich *et al.* 1967; Anderson *et al.* 1990; Dyble *et al.* 2006). For *A. tamarense*, toxin content was found to be affected by temperature and N- and P- supply (Anderson *et al.* 1990), and varied with nutrient source (Leong *et al.* 2004); this information was originally published in reference to *A. tamarense*, but was most likely *A. fundyense* based on recent phylogenetic analyses and reassignment of geographic ranges (John *et al.* 2014). Nitrogen limitation appears to increase toxin content in the marine HAB species *Karenia brevis* (Hardison *et al.* 2012). In freshwater HAB-forming cyanobacteria, toxin production can depend on light intensity (Dyble *et al.* 2006), as well as the presence or absence of specific genes in different strains, and gene expression that may be mediated by environmental conditions such as total nitrogen (as reviewed in Camargo and Alonso 2006). In short, toxin-production and toxicity of HAB species is highly variable between and within species. More research is needed on toxicity and toxin production in *A. monilatum* in the Chesapeake Bay.

Further research is required to determine whether or not *A. monilatum* poses a significant seafood safety risk. Variation in toxin production by *A. monilatum* and the amount of flushing and dilution at a site may be important factors controlling the health impacts of *A. monilatum* on *C. virginica*. Healthy oysters may be able to avoid *A. monilatum* exposure and its effects. However, it is clear that adult oysters exposed to *A. monilatum* or its lysate can experience erosion in external tissues and, at least in the context of laboratory challenges, an appreciable degree of mortality. Severity of toxic effects to oysters in the field likely depends on the actual concentration of *A. monilatum* bloom toxins at the site, as well as the ability of the oyster to avoid filtering during times of high bloom density or high toxin content in the water column.

LITERATURE CITED

Abe M, Inoue D, Matsunaga K, Ohizumi Y, Ueda H, Asano T, Murakami M, Sato Y. 2002. Goniodomin A, an antifungal polyether macrolide, exhibits antiangiogenic activities via inhibition of actin reorganization in endothelial cells. *J Cell Physiol,* 190:109–116.

Aldrich DV, Ray SM, Wilson WB. 1967. *Gonyaulax monilata*: Population growth and development of toxicity in cultures. *J Protozool,* 14:639–649.

Anderson DM, Kulis DM, Sullivan JJ, Hall S, Lee C. 1990. Dynamics and physiology of saxitoxin production by the dinoflagellates *Alexandrium* spp. *Mar Biol,* 104:11–524.

Anderson DM, Couture DA, Kleindinst JL, Keafer BA, McGillicuddy, Jr. DJ, Martin JL, Richlen ML, Hickey JM, Solow AR. 2014. Understanding interannual, decadal level variability in paralytic shellfish poisoning toxicity in the Gulf of Maine: the HAB Index. *Deep Sea Res Part II Top Stud Oceanogr,* 103:264–276.

Bass EL. 1986. Use of the cricket *Acheta domestica* L. as a bioassay organism for the toxic extract from *Gonyaulax monilata* (Dinophyceae). *J Phycol,* 22:546–549.

Bass EL, Kuvshinoff BW. 1983. Evidence for a neuroactive component in the toxic extract from *Gonyaulax monilata*. *Comp Biochem Physiol,* 75C:131–134.

Bass EL, Pinion JP, Sharif ME. 1983. Characteristics of a hemolysin from *Gonyaulax monilata* Howell. *Aquat Toxicol,* 3:15–22.

Basti L, Endo M, Segawa S. 2011. Physiological, pathological, and defense alterations in manila clams (short-neck clams), *Ruditapes philippinarum*, induced by *Heterocapsa circularisquama*. *J Shellfish Res*, 30(3):829–844.

Basti L, Endo M, Segawa S, Shumway SE, Tanaka Y, Nagai S. 2015. Prevalence and intensity of pathologies induced by the toxic dinoflagellate, *Heterocapsa circularisquama*, in the Mediterranean mussel, *Mytilus galloprovincialis*. *Aquat Toxicol*, 163:37–50.

Camargo JA, Alonso Á. 2006. Ecological and toxicological effects of inorganic nitrogen pollution in aquatic ecosystems: a global assessment. *Environ Int*, 32:831 – 849.

Clemons GP, Pham DV, Pinion JP. 1980. Insecticidal activity of *Gonyaulax* (Dinophyceae) cell powders and saxitoxin to the German cockroach. *J Phycol,* 16:305–307.

Connell C, Cross J. 1950. Mass mortality of fish associated with the protozoan *Gonyaulax* in the Gulf of Mexico. *Science*, 112:359–363.

Dauer DM, Marshall HG, Donat JR, Lane MF, Doughten SC, Hoffman FA, Kurada R. 2010. Current status and long-term trends in water quality and living resources in the Virginia tributaries and Chesapeake Bay mainstem from 1985 through 2009. Final report submitted to Chesapeake Bay Program.

Dyble J, Tester PA, Litaker RW. 2006. Effects of light intensity on cylindrospermopsin production in the cyanobacterial HAB species *Cylindrospermopsis raciborskii*. *Afr J Mar Sci*, 28(2):309–312.

Erker EF, Slaughter LJ, Bass EL, Pinion JP, Wutoh J. 1985. Acute toxic effects in mice of an extract from the marine algae *Gonyaulax monilata*. *Toxicon*, 23(5):761–767.

Frank DM, Hamilton JF, Ward JE, Shumway SE. 2007. A fiber optic sensor for high resolution measurement and continuous monitoring of valve gape in bivalve molluscs. *J Shellfish Res*, 26(2):575–580.

Furukawa K, Sakai K, Watanabe S, Maruyama K, Murakami M, Yamaguchi K, Ohizumi Y. 1993. Goniodomin A induces modulation of actomyosin ATPase activity mediated through conformational change of actin. *J Biol Chem,* 268:26026–26031.

Gates JA, Wilson WB. 1960. The toxicity of *Gonyaulax monilata* Howell to *Mugil cephalus*. *Limnol Oceanogr*, 5(2):171–174.

Guillard RRL, Morton SL. 2003. Culture methods. In: Manual on Harmful Marine Microalgae. p. 77–97.

Harding JM, Mann R, Moeller P, Hsia MS, Road FJ, Carolina S. 2009. Mortality of the veined rapa whelk, *Rapana venosa*, in relation to a bloom of *Alexandrium monilatum* in the York River, United States. *J Shellfish Res*, 28(2):363-367.

Hardison DR, Sunda WG, Litaker RW, Shea D, Tester PA. 2012. Nitrogen limitation increases brevetoxins in *Karenia brevis* (Dinophyceae): implications for bloom toxicity. *J Phycol*, 48:844–858.

Hsia MH, Morton SL, Smith LL, Beauchesne KR, Huncik KM, Moeller PDR. 2006. Production of goniodomin A by the planktonic, chain-forming dinoflagellate *Alexandrium monilatum* (Howell) Balech isolated from the Gulf Coast of the United States. *Harmful Algae*, 5:290-299.

Hudson K, Murray TJ. 2016. Virginia shellfish aquaculture situation and outlook report. p.20.

John U, Litaker RW, Montressor M, Murray S, Brosnahan ML, Anderson DM. 2014. Formal revision of the *Alexandrium tamarense* species complex (Dinophyceae) taxonomy: the introduction of five species with emphasis on molecular-based (rDNA) classification. *Protist*, 165(6):779–804.

Landsberg JH. 2002. The effects of harmful algal blooms on aquatic organisms. *Rev Fish Sci*, 10(2):113–390.

Leong SCY, Nagashima Y, Taguchi S. 2004. Variability in toxicity of the dinoflagellate *Alexandrium tamarense* in response to different nitrogen sources and concentrations. *Toxicon*, 43:407–415.

Lovko VJ, Vogelbein WK, Shields JD, Haas LW, Reece KS. 2003. A new larval fish bioassay for testing the pathogenicity of *Pfiesteria* spp. (Dinophyceae). *J Phycol*, 39:600-609.

MacKiernan G. 1968. Seasonal distribution of dinoflagellates in the lower York River, Virginia [Thesis]. College of William & Mary. 104 p.

Marshall HG, Egerton TA, Johnson R, Semcheski M, Bowman N, Mansfield N. 2008. Re-occurring harmful algal blooms in the tidal waters of Virginia, USA. Ocean Sciences Meeting; March 2-7, 2008; Orlando, Florida.

Marshall HG, Egerton TA. 2009. Phytoplankton blooms: their occurrence and composition within Virginia's tidal tributaries. *Va J Sci*, 60(3):149–164.

Marshall HG, Egerton TA. 2013. Assessing seasonal relationships between chlorophyll *a* concentrations to phytoplankton composition, biomass, and abundance, emphasizing the bloom producing algae (HAB and others) within the James, Elizabeth, and Lafayette rivers in Virginia. Final report submitted to Virginia Department of Environmental Quality.

Matsunaga K, Nakatani K, Murakami M, Yamaguchi K, Ohizumi Y. 1999. Powerful activation of skeletal muscle actomyosin ATPase by goniodomin A is highly sensitive to troponin/tropomyosin complex. *J Pharm Exp Ther*, 291(3):1121–1126.

May SP, Burkholder JM, Shumway SE, Hegaret H, Wikfors GH, Frank D. 2010. Effects of the toxic dinoflagellate *Alexandrium monilatum* on survival, grazing and behavioral response of three ecologically important bivalve molluscs. *Harmful Algae*, 9:281-293.

Mercado-Silva N. 2005. Condition index of the eastern oyster, *Crassostrea virginica* (Gmelin, 1791) in Sapelo Island Georgia--effects of site, position on bed and pea crab parasitism. *J Shellfish Res,* 24:121–126.

Mizuno K, Nakahata N, Ito E, Murakami M, Yamaguchi K, Ohizumi Y. 1998. Goniodomin A, an antifungal polyether macrolide, increases the filamentous actin content of 1321N1 human astrocytoma cells. *J Pharm Pharmacol,* 50:645–648.

Newell R. 1988. Ecological changes in Chesapeake Bay: are they the result of overharvesting the American oyster, *Crassostrea virginica*? In: Understanding the Estuary: Advances in Chesapeake Bay Research; March 1988; Baltimore, MD. Chesapeake Research Consortium Publication 129. p.536-546.

Perry HM, Stuck KC, Howse HD. 1979. First record of a bloom of *Gonyaulax monilata* in coastal waters of Mississippi. *Gulf Res Rep,* 6:313–316.

Ray SM, Aldrich D V. 1966. Ecological interactions of toxic dinoflagellates and molluscs in the Gulf of Mexico. In: Animal Toxins. p. 75–83.

Reece KS, Vogelbein WK, Carnegie RB. 2012. Assessing the impacts of emerging harmful algal bloom species on shellfish restoration and aquaculture in Chesapeake Bay. Final report submitted to VA Sea Grant. Award #NA10OAR4170085.

Rogers JE, Leblond JD, Moncreiff CA. 2006. Phylogenetic relationship of *Alexandrium monilatum* (Dinophyceae) to other *Alexandrium* species based on 18S ribosomal RNA gene sequences. *Harmful Algae,* 5:275–280.

Shaw BL, Battle HI. 1957. The gross and microscopic anatomy of the digestive tract of the oyster *Crassostrea virginica* (Gmelin). *Can J Zool,* 35:325–347.

Shumway SE. 1990. A review of the effects of algal blooms on shellfish and aquaculture. *J World Aquac Soc*, 21(2):65-104.

Sievers AM. 1969. Comparative toxicity of *Gonyaulax monilata* and *Gymnodinium breve* to annelids, crustaceans, molluscs and a fish. *J Protozool,* 16:401–404.

Smolarz K, Wolowicz M, Stachnik M. 2006. First record of the occurrence of "gill disease" in *Mytilus edulis trossulus* from the Gulf of Gdansk (Baltic Sea, Poland). *J Invertebr Pathol,* 93:207–209.

Terao K, Ito E, Murakami M, Yamaguchi K. 1989. Histopathological studies on experimental marine toxin poisoning III. Morphological changes in the liver and thymus of male ICR mice induced by goniodomin A, isolated from the dinoflagellate *Goniodoma pseudogoniaulax*. *Toxicon,* 27(2):269-271.

[VA DEQ] Virginia Department of Environmental Quality. 2014. Quality assurance project plan (QAPP) for James River chlorophyll-*a* study. Special Study #14098.

Wardle WJ, Ray SM, Aldrich AS. 1975. Mortality of marine organisms associated with offshore summer blooms of the toxic dinoflagellate *Gonyaulax monilata* Howell at Galveston, Texas. In: LoCicero VR, editor. Proceedings of the First International Conference on Toxic Dinoflagellate Blooms. Wakefield (MA): Science and Technology Foundation. p. 257-263.

Wikfors GH. 2005. A review and new analysis of trophic interactions between *Prorocentrum minimum* and clams, scallops, and oysters. *Harmful Algae,* 4:585–592.

Wilson WB, Ray SM, Aldrich DV. 1975. *Gymnodinium breve*: population growth and development of toxicity in cultures. In: Proceedings of the First International Conference on toxic dinoflagellate blooms. p. 127–141.

Yasuda M, Nakatani K, Matsunaga K, Murakami M, Momose K, Ohizumi Y. 1998. Modulation of actomyosin ATPase by goniodomin A differs in types of cardiac myosin. *Eur J Pharmacol,* 346:119–123.

TABLE 2.1.

48-hour fed toxicity bioassay results by oyster. Oyster IDs include a replicate number and a prefix based on the treatment assigned: "BL"=baseline oysters, "A"-"E"=live *A. monilatum* treatments. "Amon Treatment" indicates the initial approximate *A. monilatum* cell density. Δ cell density=final cell density-initial cell density. "Amon Location" indicates tissues where cells resembling *A. monilatum* were found.

Oyster ID	Amon Treatment	Shell Height (mm)	Shell Width (mm)	Wet Meat Weight (g)	Δ Cell Density (cells/mL)	Mortality (Y=1, N=0)	Hour Processed	Amon Location
BL1		59.2	40.8	2.546		0	0	
BL2		60.7	46.4	4.061		0	0	
BL3		58.3	35.1	2.747		0	0	
BL4		48.1	31.9	1.434		0	0	
BL5		41.8	37.0	5.006		0	0	
BL6		63.6	39.7	9.610		0	0	
A1	0	44.0	38.0	1.473	-33	0	48	
A2	0	68.3	41.8	3.906	0	0	48	
A3	0	56.8	33.6	2.621	0	0	48	
A4	0	59.8	46.3	3.715	0	0	48	
A5	0	65.2	40.0	2.190	0	0	48	
A6	0	65.5	39.2	4.336	0	0	48	
B1	250	54.5	31.8	2.445	-100	0	48	
B2	250	58.9	39.7	4.046	-167	0	48	
B3	250	54.0	37.7	2.434	-233	0	48	
B4	250	57.8	29.4	2.156	-100	0	48	
B5	250	54.7	39.9	2.624	-267	0	48	
B6	250	41.5	36.5	2.719	-233	0	48	
C1	500	50.9	39.1	3.113	-567	0	48	
C2	500	56.4	38.0	2.480	-200	0	48	
C3	500	56.2	46.5	3.457	-333	0	48	
C4	500	48.2	34.2	2.232	-367	0	48	
C5	500	53.5	37.2	2.848	-700	0	48	
C6	500	49.7	26.5	1.361	-533	0	48	
D1	2500	47.4	29.3	1.707	-2400	0	48	
D2	2500	47.7	36.6	1.949	-1700	0	48	
D3	2500	67.3	34.6	3.802	-2833	0	48	
D4	2500	64.0	44.8	4.013	-2900	0	48	
D5	2500	72.1	40.7	4.218	-2933	0	48	
D6	2500	58.8	37.2	2.687	-2767	0	48	
E1	5000	51.3	39.6	2.773	-4533	0	48	
E2	5000	63.4	38.0	3.635	-3167	0	48	
E3	5000	57.9	42.7	3.354	-3500	0	48	
E4	5000	46.7	41.8	2.257	-6200	0	48	
E5	5000	49.2	33.9	1.815	-3133	0	48	
E6	5000	60.2	35.6	3.249	-3600	0	48	gills, stomach, intestine

TABLE 2.2.

Behavioral observations of oysters in the 96-hour unfed toxicity bioassay. Oyster IDs include a replicate number (OYR#) and a prefix based on the treatment assigned: "BLBL1"=baseline oysters from the November 2015 trial, "BLBL2"=baseline oysters from the January 2016 trial, "AMON"=live *A. monilatum* treatments and was followed by the approximate average cell density for that treatment group, "NT"=non-toxic dinoflagellate treatment (fed control) and was followed by the approximate average cell density, "AMLYS"=*A. monilatum* lysate and was followed by the approximate average cell density the treatment represented. Responses to tactile stimulation were recorded every 12 hours: 0=valves closed, 1=valves open and oyster responsive, 2=valves slightly open but oyster not responsive, 3=valves open but oyster response very slow and/or valves did not fully close, black=oyster gaping and unresponsive—dead.

Oyster ID	Wet Meat Weight (g)	Hour							
		12	24	36	48	60	72	84	96
AMON-0 OYR1	5.230	0	0	0	0	0	0	0	0
AMON-0 OYR2	8.386	0	1	1	1	0	0	0	2
AMON-0 OYR3	7.947	1	0	0	0	0	0	0	0
AMON-0 OYR4	8.786	0	0	0	0	0	0	0	0
AMON-0 OYR5	3.499	0	0	0	0	0	0	0	1
AMON-0 OYR6	3.586	0	0	0	1	0	0	0	0
NT-6300 OYR1	5.425	0	0	0	0	0	0	0	1
NT-6300 OYR2	6.641	0	0	0	1	0	0	0	0
NT-6300 OYR3	5.613	0	0	0	0	0	0	0	1
NT-6300 OYR4	2.851	0	0	0	0	0	0	0	0
NT-6300 OYR5	5.768	0	0	0	0	0	0	0	0
NT-6300 OYR6	3.103	0	1	1	0	0	0	0	0
AMON-1000 OYR1	5.432	0	0	1	1	2	1	1	2
AMON-1000 OYR2	6.170	0	0	0	1	0	0	2	
AMON-1000 OYR3	5.623	0	0	2	2	2	2		
AMON-1000 OYR4	4.570	0	0	0	1	0			
AMON-1000 OYR5	2.760	0	0	0	0	0	0	0	0
AMON-1000 OYR6	3.809	0	0	0	0				
AMON-2000 OYR1	7.460	0	0	0	0	2	2	2	
AMON-2000 OYR2	7.968	0	0	0	0	0	2		
AMON-2000 OYR3	8.733	0	0	0	0	0	0		
AMON-2000 OYR5	4.590	0	0	0	0	0	0	0	0
AMON-2000 OYR6	4.866	0	1	0	1	2			
AMON-4000 OYR2	10.491	0	0	0	2	0	0	0	0
AMON-4000 OYR3	7.690	0	0						
AMON-4000 OYR4	7.048	0	0	0					
AMON-4000 OYR5	5.549	0	0	0	0	0	0	0	0
AMON-4000 OYR6	5.472	0	0	1	1	3			

Oyster ID	Wet Meat Weight (g)	Hour							
		12	24	36	48	60	72	84	96
AMON-4000 OYR7	1.999	1	1	0	3	3			
AMON-6300 OYR5	1.930	1	1	1	3				
AMON-6300 OYR6	9.022	0	0	0	0	0	0	0	0
AMON-6300 OYR7	3.100	0	0	0	0	0	3		
AMON-6300 OYR8	3.635	0	0	0	0	3	1	1	1
AMON-6300 OYR9	4.801	0	0	3					
AMON-6300 OYR10	5.071	0	0	1	2				
AMON-7600 OYR1	7.769	0	0	0	0	0	0	0	
AMON-7600 OYR2	7.81	0	0	0	0	0	0	0	1
AMON-7600 OYR3	11.124	0	0	0	0	0	0	0	0
AMON-7600 OYR4	5.833	0	0	0	0	0	1		
AMLYS-5000 OYR1	5.146	0							
AMLYS-5000 OYR2	3.561	0	0	0	0	0	0	1	0
AMLYS-5000 OYR3	2.460	1	1						
AMLYS-5000 OYR4	1.692	0	2	1	1	2	3		
AMLYS-5000 OYR5	6.524	0	0	0	0	0	0	0	0
AMLYS-5000 OYR6	6.245	0	0	3	2				

TABLE 2.3.

96-hour unfed toxicity bioassay results by oyster. Oyster IDs include a replicate number (OYR#) and a prefix based on the treatment assigned: “BLBL1”=baseline oysters from the November 2015 trial, “BLBL2”=baseline oysters from the January 2016 trial, “AMON”=live *A. monilatum* treatments and was followed by the approximate average cell density for that treatment group, “NT”=non-toxic dinoflagellate treatment (fed control) and was followed by the approximate average cell density, “AMLYS”=*A. monilatum* lysate and was followed by the approximate average cell density the treatment represented. Δ cell density=final cell density-initial cell density. Erosion ranking for both gill and mantle: 0=normal, 1=disruption/erosion present focally (or just a few epithelial cells showed pathology throughout section), 2=disruption/erosion present multi-focally but with normal structure still present in places, 3=disruption/erosion severe and widespread. Rank sum=gill+mantle erosion ranking. ND=no data. “Amon Location” indicates tissues where cells resembling *A. monilatum* were found. Observations of *H. nelsoni* cells (in gill), and *P. marinus* cells (in intestinal epithelium) are noted.

Oyster ID	Shell Height (mm)	Shell Width (mm)	Wet Meat Weight (g)	Δ Cell Density (cells/mL)	Mortality (Y=1, N=0)	Hour Processed	Erosion Ranking			Amon Location	Comments
							Gill	Mantle	Rank Sum		
BLBL1 OYR1	87.9	44.8	6.255		0	0	0	0	0		
BLBL1 OYR2	99.6	45.0	6.592		0	0	0	0	0		
BLBL1 OYR3	87.4	47.7	6.643		0	0	0	0	0		
BLBL1 OYR4	105.1	52.7	9.305		0	0	0	0	0		
BLBL1 OYR5	87.4	40.7	6.135		0	0	0	0	0		
BLBL1 OYR6	86.5	51.0	6.769		0	0	0	0	0		

Oyster ID	Shell Height (mm)	Shell Width (mm)	Wet Meat Weight (g)	Δ Cell Density (cells/mL)	Mortality (Y=1, N=0)	Hour Processed	Erosion Ranking			Amon Location	Comments
							Gill	Mantle	Rank Sum		
BLBL2 OYR1	87.9	44.8	6.255		0	0	0	0	0		
BLBL2 OYR2	99.6	45.0	6.592		0	0	0	0	0		
BLBL2 OYR3	87.4	47.7	6.643		0	0	0	0	0		
BLBL2 OYR4	105.1	52.7	9.305		0	0	1	0	1		
BLBL2 OYR5	87.4	40.7	6.135		0	0	0	0	0		
BLBL2 OYR6	86.5	51.0	6.769		0	0	0	0	0		*H. nelsoni.*
AMON-0 OYR1	91.6	41.0	5.230	0	0	96	0	0	0		
AMON-0 OYR2	106.4	47.4	8.386	0	0	96	0	0	0		
AMON-0 OYR3	89.9	49.4	7.947	0	0	96	0	0	0		
AMON-0 OYR4	90.0	44.2	8.786	0	0	96	0	0	0		
AMON-0 OYR5	88.1	44.2	3.499	0	0	96	0	0	0		
AMON-0 OYR6	76.2	52.0	3.586	0	0	96	0	0	0		
NT-6300 OYR1	102.4	45.0	5.425	-5706	0	96	0	0	0		
NT-6300 OYR2	78.5	43.5	6.641	-6906	0	96	0	0	0		

Oyster ID	Shell Height (mm)	Shell Width (mm)	Wet Meat Weight (g)	Δ Cell Density (cells/mL)	Mortality (Y=1, N=0)	Hour Processed	Erosion Ranking			Amon Location	Comments
							Gill	Mantle	Rank Sum		
NT-6300 OYR3	82.0	42.9	5.613	-5438	0	96	0	0	0		
NT-6300 OYR4	82.3	41.2	2.851	-6806	0	96	2	2	4		Gross signs of erosion.
NT-6300 OYR5	61.5	54.0	5.768	-6341	0	96	0	0	0		
NT-6300 OYR6	73.0	49.6	3.103	-6413	0	96	0	0	0		
AMON-1000 OYR1	82.1	53.9	5.432	-800	0	96	0	0	0		
AMON-1000 OYR2	92.2	41.5	6.170	-768	1	96	3	0	3		
AMON-1000 OYR3	88.4	48.8	5.623	-947	1	84	3	2	5		Mucus. Dead oyster.
AMON-1000 OYR4	99.8	41.8	4.570	107	1	72	3	2	5	gills	
AMON-1000 OYR5	81.2	47.0	2.760	479	0	96	2	2	4	gills	Mucus.
AMON-1000 OYR6	83.1	50.3	3.809	-915	1	60	2	0	2	gills	
AMON-2000 OYR1	101.4	41.1	7.460	-1530	1	96	3	2	5	gills	Mucus. Dead oyster.
AMON-2000 OYR2	103.2	35.9	7.968	-1352	1	84	3	2	5	gills	Mucus. Dead oyster.
AMON-2000 OYR3	97.9	48.5	8.733	-1250	1	84	3	2	5	gills	
AMON-2000 OYR5	107.7	34.0	4.590	-2088	0	96	2	2	4	gills, mantle	Mucus.

Oyster ID	Shell Height (mm)	Shell Width (mm)	Wet Meat Weight (g)	Δ Cell Density (cells/mL)	Mortality (Y=1, N=0)	Hour Processed	Erosion Ranking			Amon Location	Comments
							Gill	Mantle	Rank Sum		
AMON-2000 OYR6	102.4	42.3	4.866	-2826	1	72	3	2	5	gills	Mucus.
AMON-4000 OYR2	102.4	42.1	10.491	-3792	0	96	3	1	4		
AMON-4000 OYR3	91.0	51.1	7.690	-2348	1	36	3	1	4	gills	Mucus.
AMON-4000 OYR4	101.4	46.3	7.048	-1834	1	48	3	2	5	gills, mantle	*P. marinus.*
AMON-4000 OYR5	88.5	44.3	5.549	7777	0	96	0	1	1		
AMON-4000 OYR6	78.0	53.3	5.472	-4149	1	72	3	2	5	gills	Mucus. Gross signs of erosion.
AMON-4000 OYR7	80.3	43.9	1.999	-1659	1	72	3	2	5	gills	Gross signs of erosion. Adductor muscle easily came free of shell.
AMON-6300 OYR5	77.8	38.6	1.930	-6200	1	60	3	ND	ND	gills	
AMON-6300 OYR6	82.7	50.5	9.022	-2195	0	96	3	2	5	gills	*H. nelsoni.*
AMON-6300 OYR7	78.2	38.4	3.100	-3511	1	84	3	0	3	gills	Mucus. Gross signs of erosion.
AMON-6300 OYR8	82.0	56.7	3.635	-5450	0	96	3	1	4	gills	Mucus. *P. marinus.*
AMON-6300 OYR9	86.4	42.7	4.801	-5969	1	48	3	2	5	gills	Mucus.
AMON-6300 OYR10	76.1	43.0	5.071	-3936	1	60	3	2	5	gills	Mucus.
AMON-7600 OYR1	90.7	43.2	7.769	1672	1	96	2	1	3	gills	Dead oyster.

Oyster ID	Shell Height (mm)	Shell Width (mm)	Wet Meat Weight (g)	Δ Cell Density (cells/mL)	Mortality (Y=1, N=0)	Hour Processed	Erosion Ranking			Amon Location	Comments
							Gill	Mantle	Rank Sum		
AMON-7600 OYR2	86.5	51.1	7.810	-6449	0	96	3	2	5	gills	Mucus.
AMON-7600 OYR3	89.6	47.4	11.124	2299	0	96	0	0	0		*P. marinus.*
AMON-7600 OYR4	88.6	40.1	5.833	-5080	1	84	3	2	5	mantle	Dead oyster. *H. nelsoni.*
AMLYS-5000 OYR1	91.6	40.9	5.146	-26	1	24	3	2	5		
AMLYS-5000 OYR2	72.8	47.3	3.561	-29	0	96	3	2	5		
AMLYS-5000 OYR3	75.9	46.5	2.460	-16	1	36	3	2	5		Adductor muscle easily came free of shell.
AMLYS-5000 OYR4	86.5	37.1	1.692	-28	1	84	3	1	4		Gross signs of erosion.
AMLYS-5000 OYR5	84.0	45.4	6.524	-22	0	96	3	2	5		Possible erosion/infection in stomach epithelium.
AMLYS-5000 OYR6	88.3	44.1	6.245	-25	1	60	3	1	4		Gross signs of erosion.

TABLE 2.4.

Field sentinel study sampling data. Values in bold italics are below the detection limit. ND=no data. Water quality parameters were measured at the surface.

Sample Date	**Time**	**Latitude N**	**Longitude W**	**Depth (m)**	**Temperature (°C)**	**Dissolved Oxygen (mg/L)**	**Salinity**	***A. monilatum* Cell Density (cells/mL)**	**Comments**
7/17/2015	10:40	37.2267	76.40939	ND	ND	ND	ND	***0***	Oysters deployed
7/28/2015	ND	ND	ND	ND	ND	ND	ND	25	Week 1 sampling
8/6/2015	12:17	37.22667	76.40942	2.5	28.98	8.76	20.84	3374	Week 2 sampling
8/13/2015	15:26	37.22667	76.40942	2.2	28.55	13.44	20.64	1341	Week 3 sampling
8/15/2015	13:15	37.22667	76.40942	ND	ND	ND	ND	174	
8/19/2015	11:31	37.22677	76.40983	2.5	27.64	12.50	21.11	465	Week 4 sampling
8/27/2015	10:40	37.22658	76.40919	ND	26.69	4.61	21.56	***1***	Week 5 sampling
9/4/2015	11:21	37.22660	76.40929	2.5	27.66	3.63	21.49	***0***	Week 6 sampling
9/17/2015	8:38	37.22671	76.40932	2.5	25.19	3.87	22.33	***0***	Week 7 sampling

TABLE 2.5.

Field sentinel study results by oyster. The first number of the Oyster ID represents the week sampled, "W" represents the location of the oyster cage, and the last two numbers identify the individual oyster with a replicate number. Erosion rank sum for all tissue types: 0=normal, 1=disruption/erosion present focally (or just a few epithelial cells show pathology throughout section), 2=disruption/erosion present multi-focally but with normal structure still present in places, 3=disruption/erosion severe and widespread. "Amon Location" indicates tissues where cells resembling *A. monilatum* were found. Observations of *H. nelsoni* cells (in gill), and *P. marinus* cells (in intestinal epithelium) are noted.

Oyster ID	Date Processed	Shell Height (mm)	Shell Width (mm)	Wet Meat Weight (g)	Erosion Rank Sum	Amon Location	Comments
1W01	7/28/2015	73.1	50.5	6.136	0	intestine	
1W03	7/28/2015	77.6	72.1	8.66	0	stomach	
1W04	7/28/2015	75.3	50.1	5.78	0		
1W07	7/28/2015	72.9	49.9	8.77	1		Focal erosion in stomach epithelium.
1W08	7/28/2015	80.6	59.3	8.82	0	intestine, stomach	
1W09	7/28/2015	71.8	59.4	9.20	0		
2W01	8/6/2015	69.6	45.3	7.474	2	intestine, stomach, gills, mantle	Focal erosion in gills and mantle.
2W02	8/6/2015	72.4	58.9	5.77	2	intestine, stomach, gills	*H. nelsoni.* Moderate mantle erosion.
2W03	8/6/2015	63.6	46.9	4.49	0	intestine, stomach	
2W04	8/6/2015	93.9	53.4	6.04	0	stomach	

Oyster ID	Date Processed	Shell Height (mm)	Shell Width (mm)	Wet Meat Weight (g)	Erosion Rank Sum	Amon Location	Comments
2W05	8/6/2015	81.9	50.9	8.47	0	intestine, stomach, gills, mantle	
2W06	8/6/2015	87.6	54.8	7.83	0		
3W01	8/13/2015	71.7	52.7	9.299	1	intestine, stomach	Focal mantle erosion.
3W02	8/13/2015	74.8	56.6	7.26	1	intestine, gills	Focal mantle erosion.
3W03	8/13/2015	77.0	50.3	10.39	1	intestine, stomach	Focal mantle erosion.
3W04	8/13/2015	77.2	50.0	4.79	0		
3W05	8/13/2015	73.7	66.3	10.13	1	intestine, stomach	Focal mantle erosion.
3W06	8/13/2015	87.7	41.1	5.11	0	stomach	
4W01	8/19/2015	81.8	44.2	5.952	0	stomach	*H. nelsoni.*
4W02	8/19/2015	76.1	54.5	7.962	0	intestine	*H. nelsoni.*
4W03	8/19/2015	74.8	48.1	8.02	0	stomach	*H. nelsoni.*
4W04	8/19/2015	83.7	53.3	9.173	0	intestine	
4W05	8/19/2015	71.2	52.8	8.17	0		
4W06	8/19/2015	69.9	54.2	6.09	0	stomach, gills	
5W01	8/27/2015	81.3	53.5	6.732	0	intestine, stomach	

Oyster ID	Date Processed	Shell Height (mm)	Shell Width (mm)	Wet Meat Weight (g)	Erosion Rank Sum	Amon Location	Comments
5W02	8/27/2015	78.5	50.0	7.933	0	intestine, stomach	
5W03	8/27/2015	100.6	61.2	15.315	0	mantle	*H. nelsoni.*
5W04	8/27/2015	81.0	50.3	10.32	0		*H. nelsoni.*
5W05	8/27/2015	73.8	56.4	5.283	0		*H. nelsoni.*
5W06	8/27/2015	83.9	48.0	6.33	0	intestine	
6W01	9/4/2015	79.6	48.1	12.538	0		
6W02	9/4/2015	82.5	51.6	10.079	0		
6W03	9/4/2015	79.8	60.0	9.917	0		*H. nelsoni.*
6W04	9/4/2015	85.1	55.2	9.341	0		*H. nelsoni.*
6W05	9/4/2015	88.1	53.2	7.806	0		
6W06	9/4/2015	84.0	54.9	10.287	0		
7W01	9/17/2015	99.8	63.1	13.949	0		
7W02	9/17/2015	69.2	48.8	9.965	0		
7W03	9/17/2015	78.5	59.1	9.494	0		
7W04	9/17/2015	76.5	56.0	7.489	0		

Oyster ID	Date Processed	Shell Height (mm)	Shell Width (mm)	Wet Meat Weight (g)	Erosion Rank Sum	Amon Location	Comments
7W05	9/17/2015	83.7	54.5	8.201	0	intestine	*H. nelsoni.*
7W06	9/17/2015	87.9	50.4	7.898	1		Focal mantle erosion.
8W01	9/28/2015	84.6	59.8	9.448	1		Focal mantle erosion.
8W02	9/28/2015	72.1	62.2	7.013	1		*H. nelsoni.* Focal mantle erosion.
8W03	9/28/2015	84.4	55.9	7.960	0		*P. marinus.*
8W04	9/28/2015	83.4	48.7	8.764	1		Focal mantle erosion.
8W05	9/28/2015	81.0	51.9	7.972	1		Focal mantle erosion.
8W06	9/28/2015	79.7	50.0	6.512	0		

TABLE 2.6.

Study of *A. monilatum* cell density difference with depth on August 14, 2015 at the field sentinel study site. Samples were taken at the surface (0 m) and at 2 m every 4 hours from 9:30 to 21:30. ND=no data.

Sample Depth (m)	**Time**	**Latitude N**	**Longitude W**	**Depth (m)**	**Temperature (°C)**	**Dissolved Oxygen (mg/L)**	**Salinity**	***A. monilatum* Cell Density (cells/mL)**
0	9:24	37.22654	76.40928	2.3	27.02	10.03	20.94	1209
2	9:29	37.22645	76.40914	2.3	26.93	8.95	20.96	282
0	13:30	37.22661	76.40932	ND	27.91	13.99	21.03	3236
2	13:32	37.22653	76.40924	ND	27.63	12.6	21.03	273
0	17:23	37.22661	76.40932	2.2	28.67	17.43	20.82	9126
2	17:26	37.22666	76.40926	2.3	28.22	16.03	20.95	2678
0	21:47	37.22657	76.40937	ND	27.23	10.67	20.98	925
2	21:48	37.22664	76.40944	ND	27.24	10.64	20.99	595

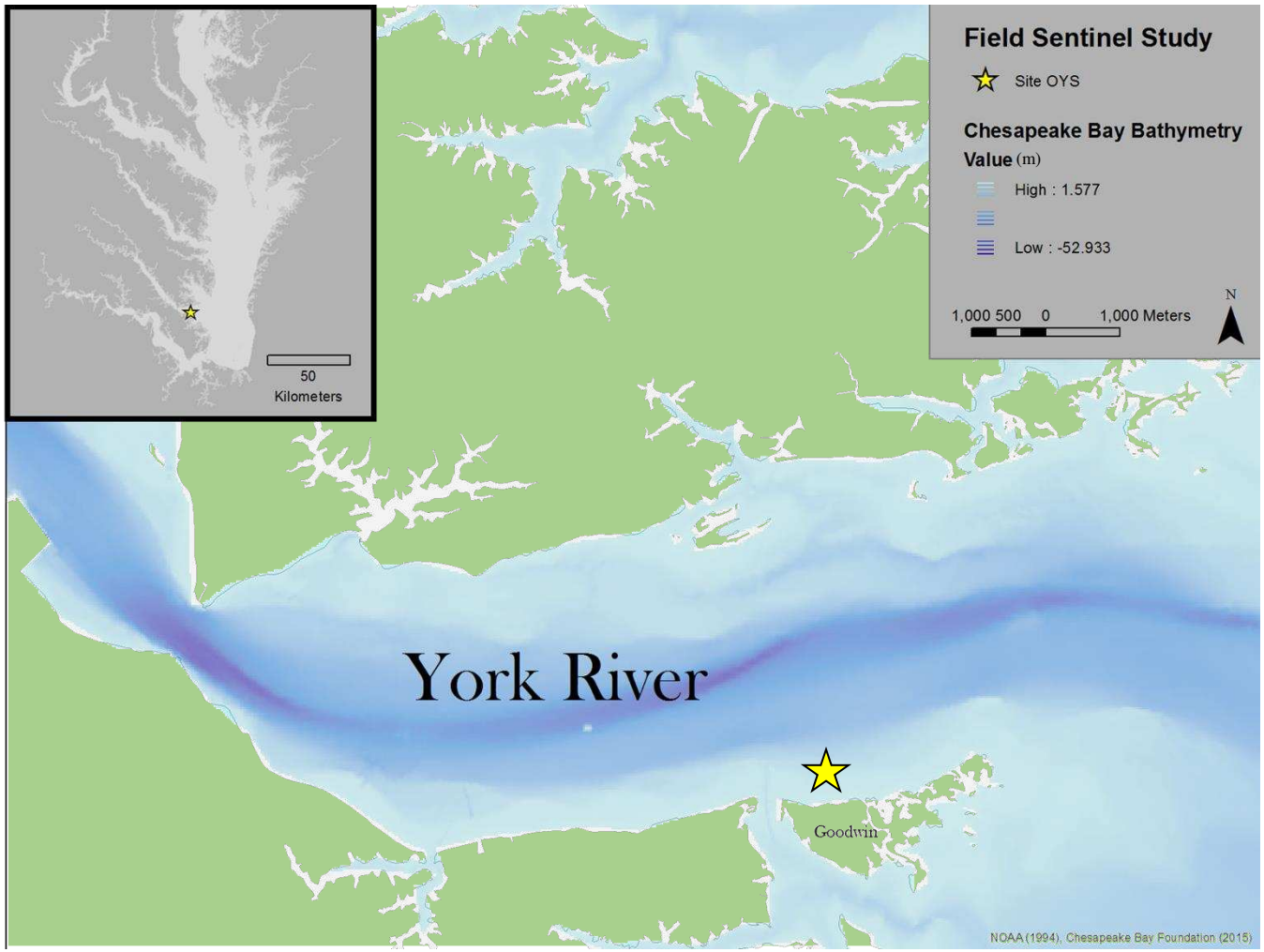

FIGURE 2.1.

Location of *C. virginica* field sentinel study site (star) off of Goodwin Island in the lower York River.

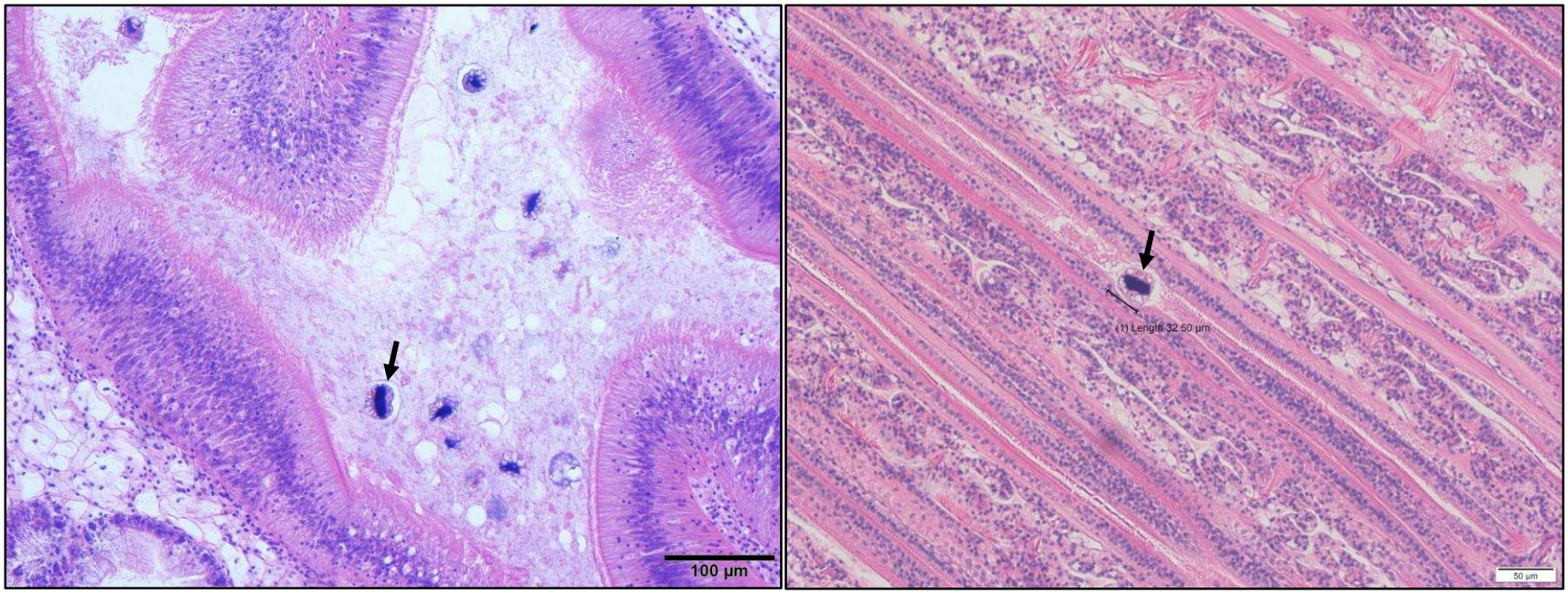

FIGURE 2.2.

Histological sections (H&E stain) of an oyster (*C. virginica*) that was exposed to 5000 cells/mL of *A. monilatum* for 48 hours in the 48-hour fed toxicity bioassay. Cell bodies (examples indicated by arrows) that resembled dinoflagellates of the same size and description as *A. monilatum* were seen in the stomach (left), and gills (right).

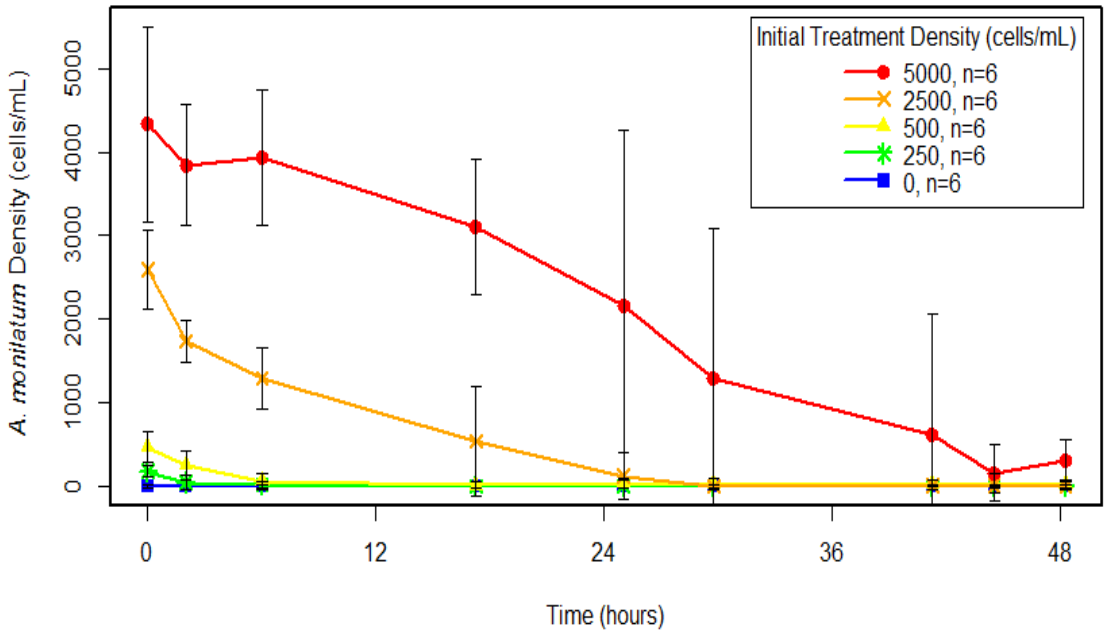

FIGURE 2.3.

Removal of *A. monilatum* cells during the 48-hour fed toxicity bioassay. Cell density is reported with standard error.

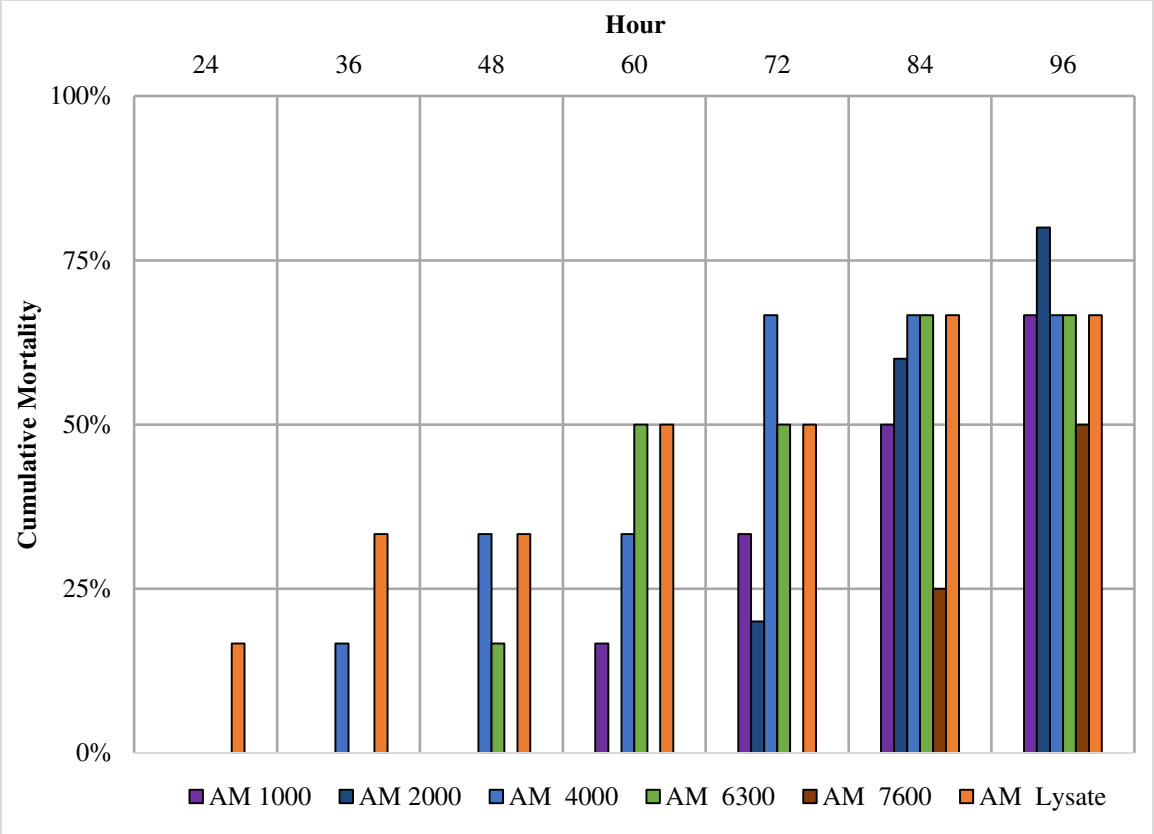

FIGURE 2.4.

Cumulative mortality during the 96-hour unfed toxicity bioassay in all treatments exposed to *A. monilatum* (live cell or lysate). There was no mortality by 12 hours, so only data from 24-96 hours is displayed. Treatment names have been abbreviated and include the cell density. n=6 for all treatments, except AM 2000 (n=5) and AM 7600 (n=4).

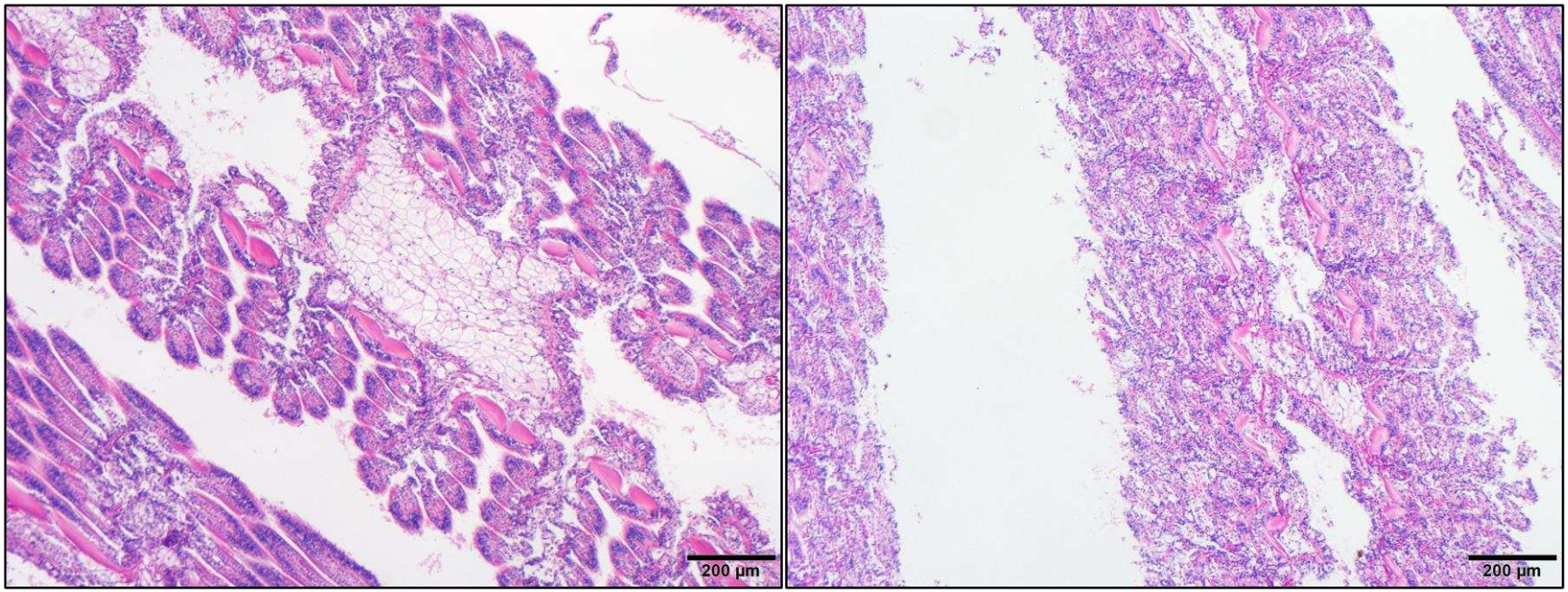

FIGURE 2.5.

Histological sections (H&E stain) of oyster (*C. virginica*) gills from the 96-hour unfed toxicity bioassay: healthy gill from control oyster AMON-0 OYR2 (left) and severely eroded gill from oyster AMON-1000 OYR4 (right) that was exposed to 1000 cells/mL of *A. monilatum* and was dead by 72 hours. The eroded gill exhibits a general loss of structure.

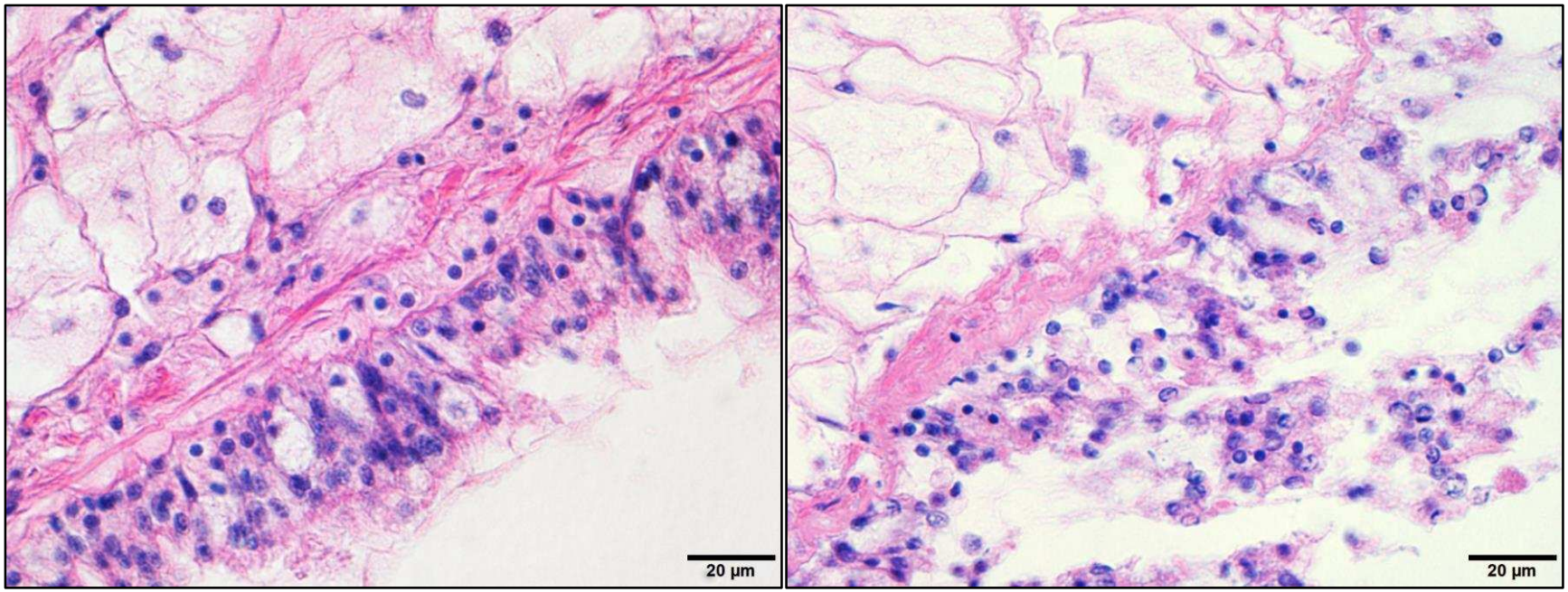

FIGURE 2.6.

Histological sections (H&E stain) of oyster (*C. virginica*) mantle epithelia from the 96-hour unfed toxicity bioassay: healthy mantle epithelium from control oyster AMON-0 OYR2 (left) and moderate erosion of the mantle epithelium of oyster AMON-1000 OYR3 (right) that was exposed to 1000 cells/mL of *A. monilatum* and was dead by 84 hours. The crescent-shaped nuclear morphology of the necrotic, eroded cells (right) was seen in all observations of erosion in both mantle and gill.

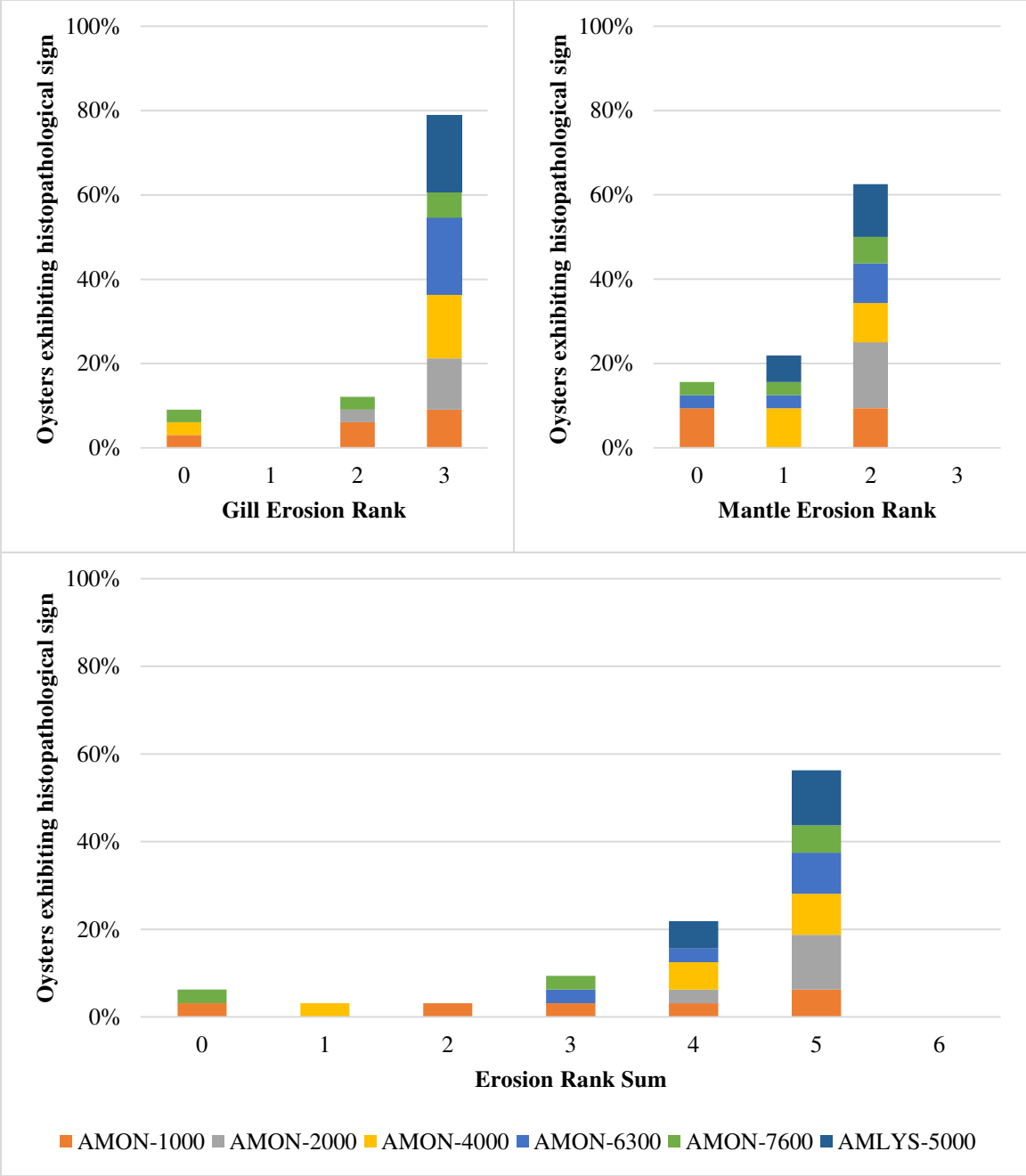

FIGURE 2.7.

Epithelial erosion rankings by treatment for oysters from the 96-hour unfed toxicity bioassay that were exposed to *A. monilatum* (live cell or lysate): gill (upper left), mantle (upper right), and rank sum (bottom). Treatment names have been abbreviated and include the cell density. N=33 for gill erosion rank, with n=6 for all treatments, except AM 2000 (n=5) and AM 7600 (n=4). N=32 for mantle erosion rank and erosion rank sum, with n=6 for all treatments, except AM 2000 and AM 6300 (n=5), and AM 7600 (n=4).

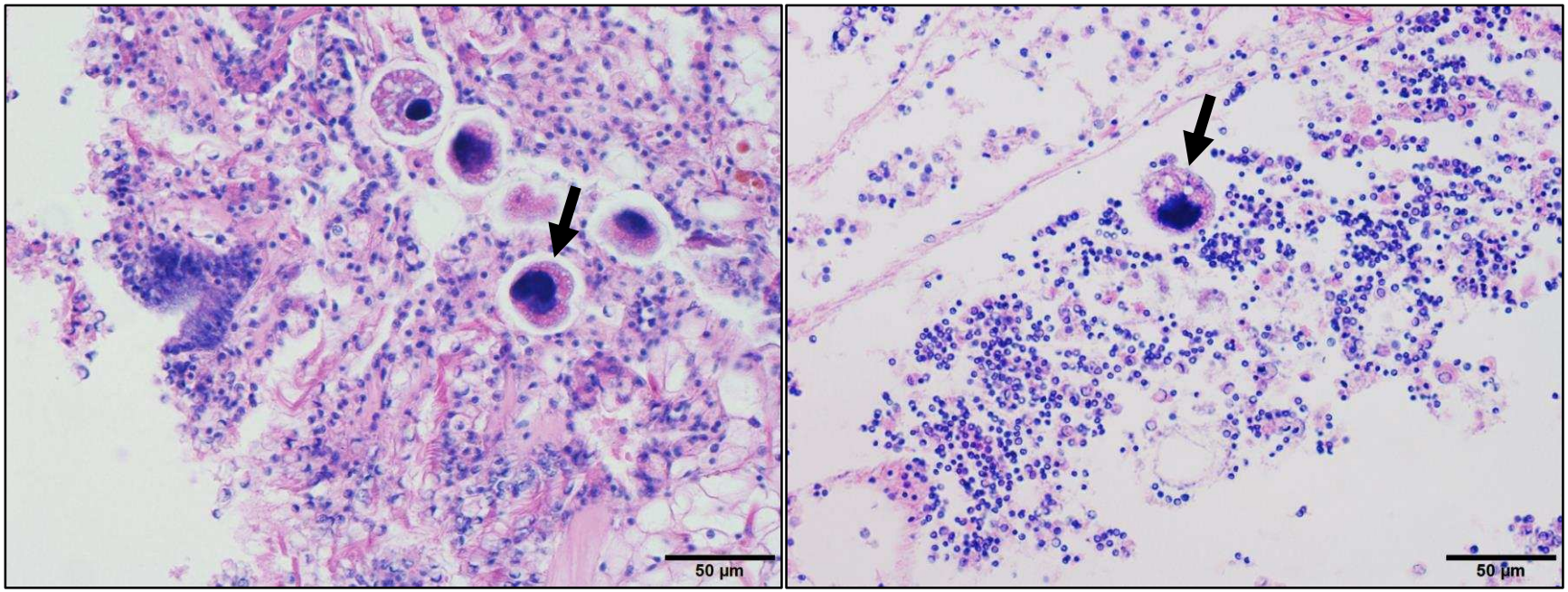

FIGURE 2.8.

Histological sections (H&E stain) of severely eroded oyster gills with cell bodies (examples indicated by arrows) resembling *A. monilatum* from the 96-hour unfed toxicity bioassay: oyster AMON-4000 OYR3 (left) that was exposed to 4000 cells/mL of *A. monilatum* and was dead by 36 hours, and oyster AMON-6300 OYR8 (right) that was exposed to 6300 cells/mL of *A. monilatum* for 96 hours.

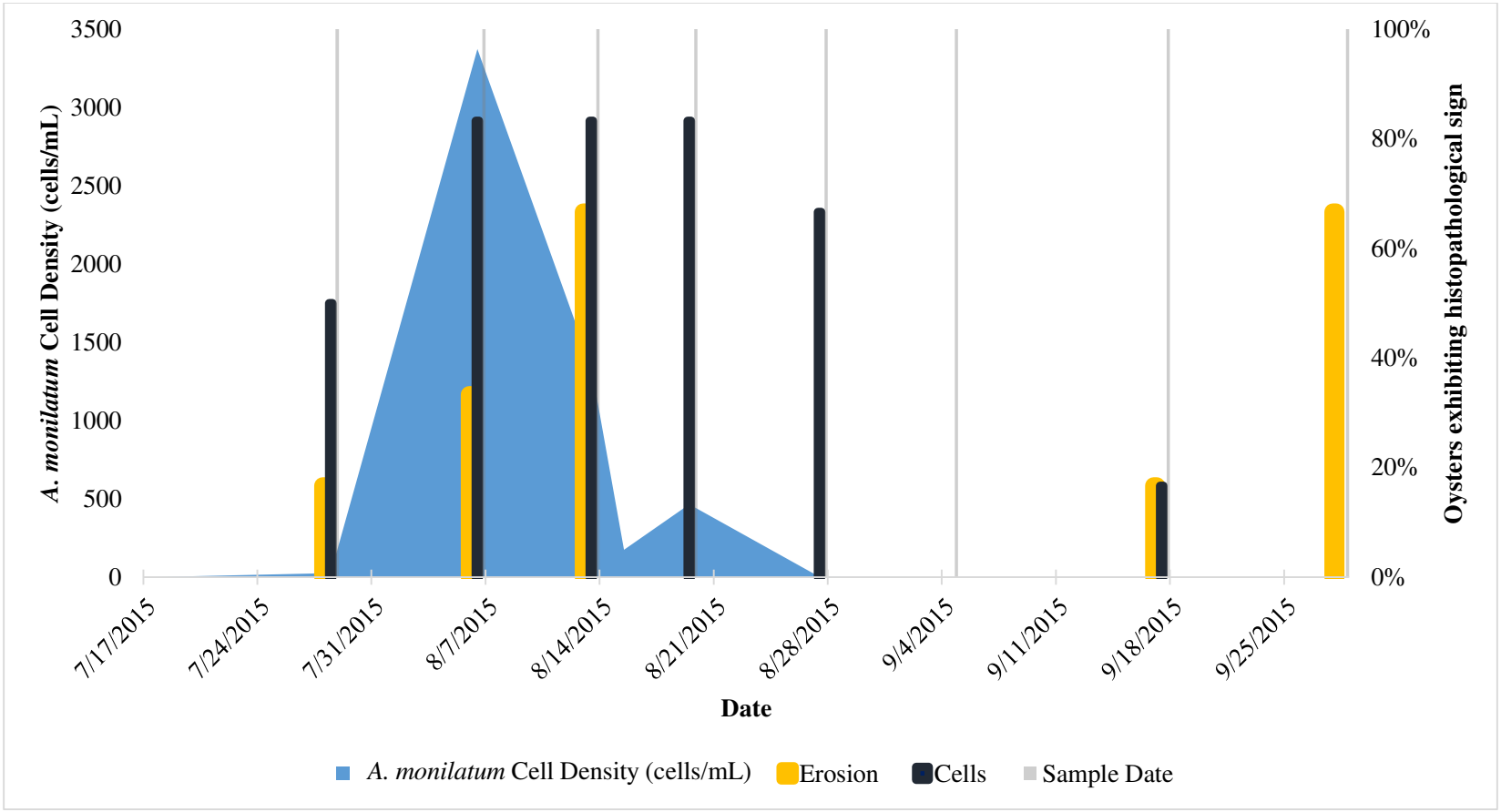

FIGURE 2.9.

Alexandrium monilatum cell density at the field sentinel study site from July 17, 2015 to September 17, 2015 with oyster histopathological results through September 28, 2015. Grey vertical bars indicate oyster sampling events for the field sentinel study, six oysters were sampled during each event. “Erosion” represents the percentage of oysters in a sample exhibiting epithelial erosion, and “Amon” represents the percentage of oysters exhibiting cells resembling *A. monilatum* in the histological sample section.

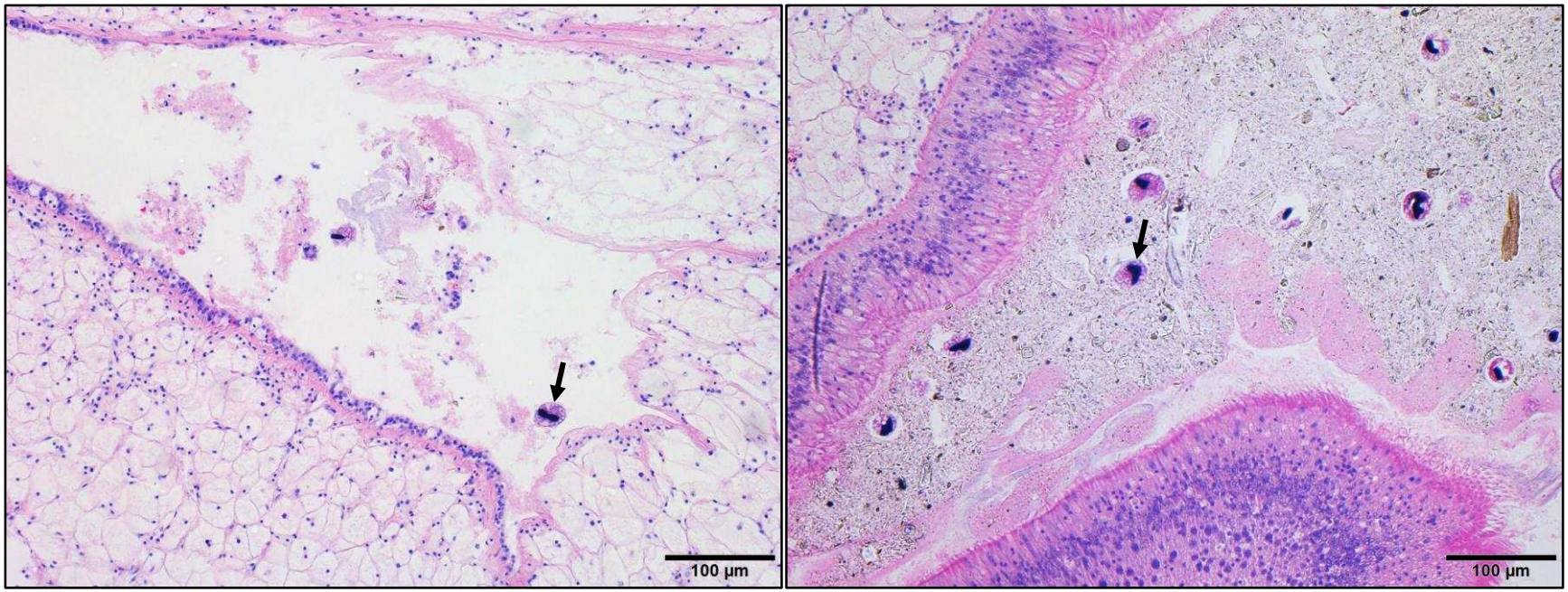

FIGURE 2.10.

Histological sections (H&E stain) of oysters (*C. virginica*) with cell bodies (examples indicated by arrows) resembling *A. monilatum* from the field sentinel study: cells adjacent to the mantle epithelium of oyster 2W01 (left) collected on August 6, 2015 at the peak of the *A. monilatum* bloom (3374 cells/mL), and cells in the intestinal lumen of oyster 4W04 (right) collected on August 19, 2015 when the *A. monilatum* cell density was 465 cells/mL.

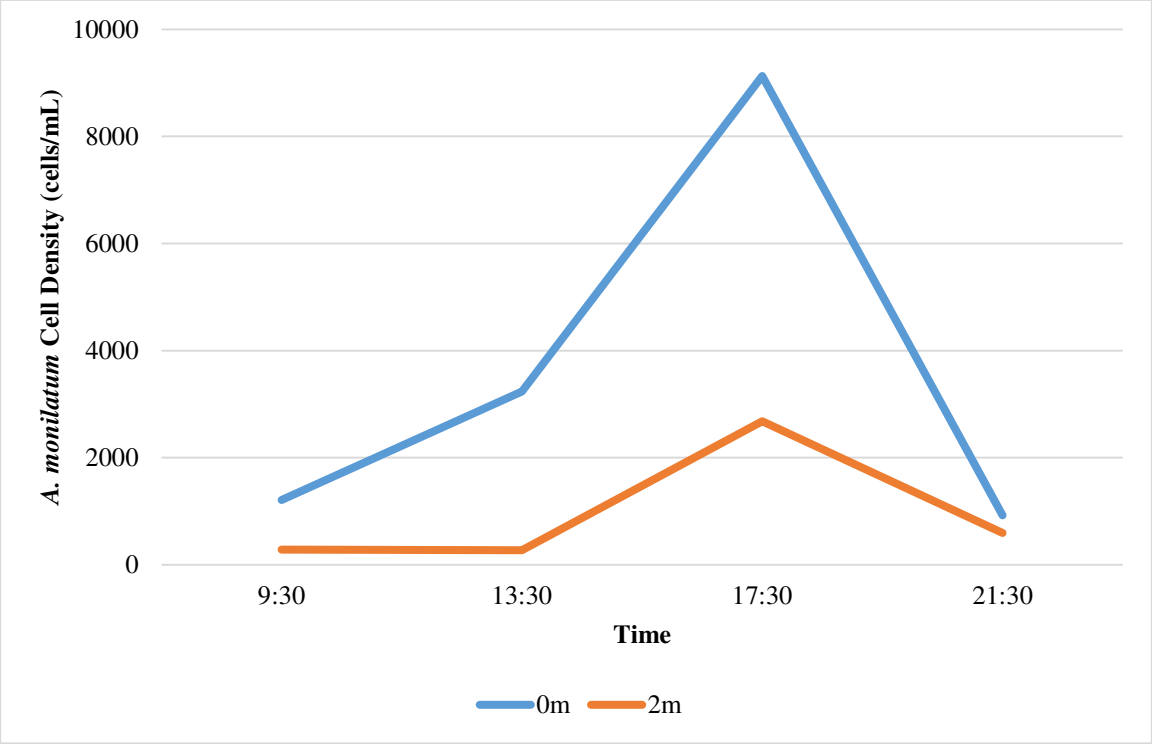

FIGURE 2.11.

Study of *A. monilatum* cell density difference with depth on August 14, 2015 at the field sentinel study site (sunset was at 20:00).

GENERAL CONCLUSION

In addition to improving the overall scientific understanding of this little-studied, locally re-emerging harmful algal bloom (HAB) species, this research examined the validity of current scientific and oyster aquaculture industry concerns regarding *Alexandrium monilatum* impacts on oyster health. In the first *A. monilatum*-specific cyst quantification and mapping study in the lower Chesapeake Bay, field surveys indicated that *A. monilatum* cyst distribution was extensive and persistent. Results suggest that *A. monilatum* has established itself in the sediments of the York River region and could continue to expand its range within the Bay over time. Data collected in this study could be used in future models of *A. monilatum* bloom dynamics that could be used to attempt to predict the timing, distribution, and severity of blooms. The role of hydrodynamic processes in *A. monilatum* resting cyst distribution should be investigated further. Additionally, adult *C. virginica* appear to consume *A. monilatum* cells, and can exhibit health impacts from exposure to *A. monilatum.* Effects of exposure can range from minor epithelial erosion of external tissues or delayed feeding to, at least in the laboratory, severe gill erosion and death. Further research is needed on the health impacts of natural *A. monilatum* blooms on all life stages of *C. virginica*. It is essential that regionally-emerging bloom species like *A. monilatum* continue to be monitored and investigated so that the shellfish aquaculture industry can be aware of, and prepared for, related potential HAB issues.

APPENDIX

Cyst Visual Quantification Methods

Validating qPCR results through comparison with another method would provide more confidence in the qPCR values and supply information that could lead to a better understanding of DNA content within *A. monilatum* cysts. Primulin staining, basic light microscopy, and FISH methods are all currently being explored by our lab as quantification comparison methods.

Sediment collection for primulin staining is essentially identical to that for qPCR analysis, with the added step of covering the sample tubes in foil to ensure they stay dark (Erdner *et al*. 2010). In the primulin staining technique, sediment samples are diluted with artificial seawater, sonicated, and sieved to isolate the size fraction of interest (20-100 μm). The sample is then treated with a series of chemicals: formaldehyde fixes the sample, methanol permeates the cyst wall, and primulin (a fluorescent dye) stains the cysts; samples are rinsed with DI water between each step. Primulin binds lipids (White *et al*. 1998) and chitin (Batt and Tortorello 2014). Using a FITC filter (460-500 em), 1 mL of sample is examined under the microscope and all stained cysts are identified and counted.

One issue we have experienced with applying the primulin method is that the microscope set-up utilizes a band-pass emission filter, which filters out autofluorescence from chlorophyll-*a*, making it difficult to distinguish phototrophic cysts from heterotrophic, or dead cysts. Traditionally, a longpass emission filter is employed to allow visualization of fluorescence from both chlorophyll-*a*, and the primulin stain at the same time (Caron 1983). There is also ample non-specific staining with the primulin, and empty cysts take up more stain than those that contain cellular material, leading to extreme difficulty in distinguishing and counting viable cysts. Previous studies have found that non-specific binding of primulin dye can lead to high background fluorescence in particle-laden samples (Kemp *et al*. 1993).

We have also compared the primulin method to the simpler method of visual counts with basic light microscopy. Under basic light microscopy cysts can be distinguished from other cell types and sediments when there is not an excessive amount of debris, however it is difficult to tell if the cysts are *A. monilatum* cysts. Basic light microscopy and primulin staining methods require the ability to visually distinguish *A. monilatum* cysts from other cells or particles. Unfortunately, cysts of *A. monilatum* share their appearance with many other endemic species' cysts; they are simple spheres of ~30-60 μm in diameter without spikes or horns.

As mentioned in the Discussion, FISH is also currently being explored as a cyst quantification method.

Step-by-step field and laboratory methods for collection and preparation of sediment cyst samples for quantification by qPCR, primulin, and FISH, follow.

LITERATURE CITED

Batt CA, Tortorello ML, eds. 2014. Encyclopedia of food microbiology. 2nd ed. Burlington (MA): Academic Press. p 692.

Caron DA. 1983. Technique for enumeration of heterotrophic and phototrophic nanoplankton, using epifluorescence microscopy, and comparison with other procedures. *Appl Environ Microbiol,* 46:491–498.

Erdner DL, Percy L, Keafer BA, Lewis J, Anderson DM. 2010. A quantitative real-time PCR assay for the identification and enumeration of *Alexandrium* cysts in marine sediments. *Deep Sea Res Part II Top Stud Oceanogr,* 57:279–287.

Kemp PF, Sherr BF, Sherr EB, Cole JJ, eds. 1993. Handbook of methods in aquatic microbial ecology. Boca Raton (FL): Lewis Publ. p 223.

White T, Bursten S, Federighi D, Lewis RA, Nudelman E. 1998. High-resolution separation and quantification of neutral lipid and phospholipid species in mammalian cells and sera by multi-one-dimensional thin-layer chromatography. *Anal Biochem,* 258:109–117.

ALEXANDRIUM MONILATUM CYST FIELD COLLECTION AND PROCESSING FOR QUANTIFICATION

Modified by Sarah Pease
with special thanks to Dave Kulis, Alexis Fischer, Don Anderson, and Theresa Hattenrath-Lehmann.

Adapted from:

Erdner DL, Percy L, Keafer BA, Lewis J, Anderson DM. 2010. A quantitative real-time PCR assay for the identification and enumeration of *Alexandrium* cysts in marine sediments. *Deep Sea Res Part II Top Stud Oceanogr,* 57:279–287.

Hattenrath-Lehmann TK, Zhen Y, Wallace RB, Tang YZ, Gobler CJ. 2016. Mapping the distribution of cysts from the toxic dinoflagellate *Cochlodinium polykrikoides* in bloom-prone estuaries by a novel fluorescence *in situ* hybridization assay. *Appl Environ Microbiol,* 82:1114–1125.

Original method by:

Yamaguchi M, Itakura S, Imai I, Ishida Y. 1995. A rapid and precise technique for enumeration of resting cysts of *Alexandrium* spp. (Dinophyceae) in natural sediments. *Phycologia,* 34:207–214.

Field sediment sampling:

1. Locate the site using GPS and deploy a grab to collect surface sediments.
2. Carefully scoop about three spoonfuls of the surface (top 1 cm) of the sediment sample (look for lighter-colored oxic sediments) into a clean, labeled, pre-weighed 250 mL wide-mouthed container (scoop an equivalent amount into a small Whirl-pak bag and store in cooler, these will be sent to the VIMS Analytical Services Laboratory for sediment grain size analysis).
3. Samples should be wrapped in foil and placed in a cooler prior to return to the laboratory.
4. Samples should be kept in the cool (3-4º C) and dark until processing. Process within 3 days!

The following portion of the protocol, including the PowerLyzer PowerSoil DNA Isolation kit (MO BIO, Carlsbad, CA) extraction, takes one person ~6 hours to complete for processing 23 samples and 1 blank.

Dry qPCR Method

1. Weigh sample bottles and remove sediment with a clean plastic spoon until the container weighs around 90 g.
2. Use a clean plastic spoon to homogenize the sediment sample in its sample container.
3. Tare an empty, clean 1.5 mL tube.
4. Fill the tube to the 1 mL mark, tap down to get air bubbles out. Weigh and record the sediment density value.
5. Weigh out 0.25 g of sediment onto a small tared piece of Parafilm, record actual mass.

6. Carefully scrape the entire sediment sample into the bead tube for the PowerLyzer PowerSoil DNA Isolation kit and proceed with the extraction process.

Slurry qPCR Method

1. Mix 20 ppt artificial sea water (ASW).
2. Re-weigh the sediment in the 250 mL container and record the weight.
3. Use a spreadsheet to subtract the sample container weight and calculate an amount of artificial seawater to add to dilute the sample to 4/5 sediment. (Divide sediment volume-calculated using sediment density- by 4 and add this volume of ASW using a 10 mL pipette.)
4. Close the sample container, wrap Kimwipe around cap to absorb any spillage, shake and vigorously vortex for 5 seconds and quickly pipette up and down 0.2 mL of slurry and transfer into a bead tube for the PowerLyzer PowerSoil DNA Isolation kit, pipette up and down to rinse out tip, and proceed with the extraction process.
5. Create a blank using 0.2 mL of ASW.

The following portion of the protocol takes one person ~5 hours to complete for processing 4 samples (this number could be slightly increased with a centrifuge that holds >4 15 mL tubes at a time, and with practice sieving).

Sediment Processing

(Adapted from Erdner et al. 2010 and Hattenrath-Lehmann et al. 2016.)

1. Add 15x as much filtered sea water (<0.2 µm) as ASW was added above (using a 100 mL graduated cylinder) to bring to a 1:5 ratio of sediment to FSW.
2. Mix well (pipette up and down with large pipettor with large bore tips) and remove 10 mL of sediment homogenate into designated 50 mL tube. **Prepare two 10 mL samples in separate tubes for each sediment sample, one for future counts and primulin staining (PRIM), and one for FISH staining (FISH).**
3. Bring volume to 40 mL of 50 mL tube with FSW, put tube in plastic beaker filled with ice for sonication. Rig a stand for the beaker while it is being sonified.
4. Sonicate 60 seconds at 20% (Branson 450 digital sonifier).
5. Sieve sequentially through large 100 µm and then thru a large 20 µm Nitex screen as follows: Copiously wash the material onto the 100 µm sieve with FSW (500 mL-1L) and save the filtrate in a beaker. Discard the material retained on the 100 µm sieve. Pour the contents of the beaker thru the 20 µm sieve and collect the material retained on 20 µm sieve, rinse down to corner w/FSW (take all water out! – can use paper towel to pull water through bottom). Use fingers to coax sediment out through Nitex. Wash with copious amounts of FSW. The more time and water used sieving will greatly reduce viewing difficulties under the scope.
6. Use FSW squirt bottle to wash material retained on 20 µm screens from back into 15 mL tube using a funnel to help collect. Use the "swirl & quickly pour" through a funnel technique. Fill to 14 mL, **DO NOT OVERFILL**! Keep on ice or in fridge (3-4° C).

Preservation and Counting

Take an aliquot of 8% PFA solution out of the freezer and place in a fume hood to defrost.

PRIM Tubes:

a. In the fume hood, add 0.40 mL of 37% formaldehyde to the 14 mL (1% final concentration). Vortex to homogenize. Store 1-2 hr in fridge (3-4° C).

The next section can be done at same time as the first section for the FISH Tubes methodology to save time.

---

b. Centrifuge tubes in Eppendorf 5702 Centrifuge (3000 x g for 10 min).
c. Carefully aspirate and discard formaldehyde as hazardous waste, without any loss of flocculent pellet.
d. Resuspend the pellet in 10 mL MilliQ water. Vortex until pellet is resuspended.
e. Centrifuge tubes in Eppendorf 5702 Centrifuge (3000 x g for 10 min).
f. Carefully aspirate and discard the water, without any loss of flocculent pellet.
g. Resuspend pellet in another 10 mL MilliQ water. Vortex to resuspend pellet and quickly remove 2 mL of sample and move to a clean 15 mL tube labeled for counting. Store these tubes for counting in the fridge (3-4° C).
h. Centrifuge tubes with remaining 8 mL sample in Eppendorf 5702 Centrifuge (3000 x g for 10 min).
i. Carefully aspirate and discard the water, without any loss of flocculent pellet.
j. Resuspend pellet in 10 mL cold methanol. Vortex until pellet is resuspended and refrigerate at -20° C for long term storage. *Note that 1/5 of the sediment has been removed—sample represents 1.6 cc sediment.

---

k. From the 2 mL sample reserved for counting, count >500 cells or whole slide in Sedgwick-Rafter counting chamber.
*Note that the 2 mL sample represents 0.4 cc sediment.

FISH Tubes:

a. Allow tubes to rest 1-2 hr in fridge (3-4° C) while PRIM tubes are fixing.
b. Centrifuge tubes in Eppendorf 5702 Centrifuge (3000 x g for 10 min).
c. Carefully aspirate and discard overlying water **down to 2 mL mark**.
d. Add 2 mL of cold 8% PFA solution, vortex and incubate in fridge (3-4° C) overnight (~13 hr).

The following portion of the protocol takes one person ~1 hour to complete for processing 4 samples (this number could be increased with a centrifuge that held >4 15 mL tubes at a time).

e. Centrifuge tubes in Eppendorf 5702 Centrifuge (**1500** x g for 10 min).
f. Carefully aspirate and discard PFA as hazardous waste, without any loss of flocculent pellet.
g. Resuspend the pellet in 4 mL 1xPBS. Vortex until pellet is resuspended.
h. Centrifuge tubes in Eppendorf 5702 Centrifuge (**1500** x g for 10 min).
i. Carefully aspirate and discard 1xPBS as hazardous waste, without any loss of flocculent pellet.
j. Add 1 mL of 1:1 1xPBS-absolute ethanol, vortex and quickly transfer the sample to a clean, labeled 2 mL microcentrifuge tube labeled for FISH. Store these tubes in a freezer (-20° C) until ready for further processing.

Primulin Staining

1. Centrifuge in Eppendorf 5702 Centrifuge (3000 x g for 10 min), aspirate and discard methanol.
2. Resuspend pellet in 10 mL MilliQ water. Vortex until pellet is resuspended.
3. Centrifuge in Eppendorf 5702 Centrifuge (3000 x g for 10 min), aspirate and discard water as methanol waste.
4. Add 2 mL primulin stock (primulin stock 2 mg/mL) to pellet, mix well using vortex, refrigerate in the dark for 1 hour.

   ---
5. Centrifuge (3000 x g for 10 min in Eppendorf 5702 Centrifuge) and remove supernatant, treat as primulin waste.
6. Resuspend in 10 mL MilliQ water. Vortex until pellet is resuspended.
7. Centrifuge in Eppendorf 5702 Centrifuge (3000 x g for 10 min), aspirate and discard supernatant.
8. Resuspend with MilliQ water. The final resuspension volume is subjective and dependent upon the size of the pellet. Generally, for pellets ~0.5 cc, resuspend to 5 mL and for pellets ≥0.5 cc resuspend to 10 mL. The goal is to dilute the sample enough to eliminate viewing issues where too much sediment is likely to obscure cysts while maintaining the lowest possible detection limit.

Counting

1. Count 1 mL in Sedgwick-Rafter counting chamber, using FITC filter (Zeiss Axioskop ex=450-490 em = 510LP) or chlorophyll filter (ex = 436 em = >510LPZeiss IM-35).

Notes:

- Once cysts are stained, primulin denatures, lasts only ~1 week –Read right away!
- Store stained samples in dark at 3-4° C; it is OK to have then off of ice at room temperature for ~24 hours if needed.

SOLUTIONS:

8% PFA in 1xPBS solution:

1. **In a fume hood:** weigh out 16 g of paraformaldehyde (PFA) into a clean weigh boat and set aside in the fume hood.
2. Set up a heating plate in the hood that has stirring capabilities. Put a magnetic stir bar and tape a thermometer into a wide-mouthed 500 mL Erlenmeyer flask.
3. Use a graduated cylinder to measure out 200 mL of 1xPBS and pour it into the Erlenmeyer.
4. Heat the 1xPBS to 60° C and add the 16 g of PFA while the stir bar is mixing (DO NOT LET THE SOLUTION GET ABOVE 65° C, PFA starts to denature at 70° C).
5. Add 1N NaOH dropwise until all of the PFA goes into solution (it took ~44 drops using a fine tip Pasteur pipette).
6. Allow the solution to cool to room temperature and adjust the pH to 7.5.
7. Use #2 filter paper and a funnel to gravity filter the solution into a clean glass container. The solution should be clear.
8. Aliquot the solution into small glass scintillation vials and store around -20° C for up to one month.

Primulin stock solution (2 mg/mL):

1. Weigh 100 mg primulin (MP Biomedicals: Cat#195454; ordered thru Fisher)
2. Add MilliQ water to achieve 50 mL final volume.
3. Precipitate or cloudy yellow solution will be formed, clear solution by filtering.

Primulin stock solution is good for at least several months if stored filtered, cold (3-4° C), and in the dark.

VITA

SARAH KRYSTAL DESAUTELS PEASE

Sarah K. D. Pease was born in Dover, New Hampshire (NH) on April 21, 1989 to Donna M. Desautels-Pease and Dave N. Pease. She graduated in 2007 from Oyster River High School in Durham, NH and went on to earn a B.S. in Biology with a minor in Environment from McGill University in Montréal, Québec, Canada in 2011. During and after her undergraduate degree, she worked for the NH Department of Environmental Services, and for NH Fish and Game. In 2013, Sarah entered the M.S. program at the College of William and Mary, School of Marine Science under the advising of Drs. Wolfgang K. Vogelbein and Kimberly S. Reece.